Pertanika Journal of

SCIENCE & TECHNOLOGY

JST

VOL. 32 (S3) 2024

A Special Issue Devoted to

Natural Polymers and Derivatives: Composition, Uses and Application

Guest Editors

Lee Chuan Li, Chin Kit Ling and Ainun Zuriyati Mohamed @ Asa'ari

PERTANIKA JOURNALS

A scientific journal published by Universiti Putra Malaysia Press

Pertanika Journal of Science & Technology
Pertanika Journal of Science & Technology

Pertanika Journal of Science & Technology

About the Journal

Overview

Pertanika Journal of Science & Technology (JST) is the official journal of Universiti Putra Malaysia published by UPM Press. It is an open-access online scientific journal which is free of charge. It publishes the scientific outputs. It neither accepts nor commissions third party content.

Recognized internationally as the leading peer-reviewed interdisciplinary journal devoted to the publication of original papers, it serves as a forum for practical approaches to improving quality in issues pertaining to science and engineering and its related fields.

JST is currently published 6 issues a year, periodically in January, March, April, July, August, and October. It is considered for publication of original articles according to its scope. The journal publishes in **English** and it is open to authors around the world regardless of the nationality.

The Journal is available world-wide.

Aims and scope

Pertanika Journal of Science and Technology aims to provide a forum for high quality research related to science and engineering research. Areas relevant to the scope of the journal include: bioinformatics, bioscience, biotechnology and bio-molecular sciences, chemistry, computer science, ecology, engineering, engineering design, environmental control and management, mathematics and statistics, medicine and health sciences, nanotechnology, physics, safety and emergency management, and related fields of study.

History

Pertanika was founded in 1978. A decision was made in 1992 to streamline *Pertanika* into three journals as Pertanika Journal of Tropical Agricultural Science, Pertanika Journal of Science & Technology, and Pertanika Journal of Social Sciences & Humanities to meet the need for specialised journals in areas of study aligned with the interdisciplinary strengths of the university.

After almost 28 years, as an interdisciplinary Journal of Science & Technology, the journal now focuses on research in science and engineering and its related fields.

Goal of *Pertanika*

Our goal is to bring the highest quality research to the widest possible audience.

Quality

We aim for excellence, sustained by a responsible and professional approach to journal publishing. Submissions are guaranteed to receive a decision within 14 weeks. The elapsed time from submission to publication for the articles averages 5-6 months.

Abstracting and indexing of *Pertanika*

The journal is indexed in SCOPUS (Elsevier), Clarivate-Emerging Sources Citation Index [ESCI (Web of Science)], BIOSIS, National Agricultural Science (NAL), Google Scholar, MyCite and ISC.

Future vision

We are continuously improving access to our journal archives, content, and research services. We have the drive to realise exciting new horizons that will benefit not only the academic community, but society itself.

Citing journal articles

The abbreviation for Pertanika Journal of Science & Technology is *Pertanika J. Sci. Technol.*

Publication policy

Pertanika policy prohibits an author from submitting the same manuscript for concurrent consideration by two or more publications. It prohibits as well publication of any manuscript that has already been published either in whole or substantial part elsewhere. It also does not permit publication of manuscript that has been published in full in Proceedings.

Code of Ethics

The *Pertanika* Journals and Universiti Putra Malaysia takes seriously the responsibility of all of its journal publications to reflect the highest in publication ethics. Thus all journals and journal editors are expected to abide by the Journal's codes of ethics. Refer to *Pertanika*'s **Code of Ethics** for full details, or visit the Journal's web link at http://www.pertanika.upm.edu.my/code_of_ethics.php

International Standard Serial Number (ISSN)

An ISSN is an 8-digit code used to identify periodicals such as journals of all kinds and on all media–print and electronic. All *Pertanika* journals have ISSN as well as an e-ISSN.

Pertanika Journal of Science & Technology: ISSN 0128-7680 (*Print*); ISSN 2231-8526 (*Online*).

Lag time

A decision on acceptance or rejection of a manuscript is reached in 3 to 4 months (average 14 weeks). The elapsed time from submission to publication for the articles averages 5-6 months.

Authorship

Authors are not permitted to add or remove any names from the authorship provided at the time of initial submission without the consent of the Journal's Chief Executive Editor.

Manuscript preparation

Refer to *Pertanika*'s **Instructions to Authors** through the official website.

Editorial process

Authors are notified with an acknowledgement containing a *Manuscript ID* on receipt of a manuscript, and upon the editorial decision regarding publication.

Pertanika follows a **double-blind peer-review** process. Manuscripts deemed suitable for publication are usually sent to reviewers. Authors are encouraged to suggest names of at least three potential reviewers at the time of submission of their manuscript to *Pertanika*, but the editors will make the final choice. The editors are not, however, bound by these suggestions.

Notification of the editorial decision is usually provided within ten to fourteen weeks from the receipt of manuscript. Publication of solicited manuscripts is not guaranteed. In most cases, manuscripts are accepted conditionally, pending an author's revision of the material.

The Journal's peer-review

In the peer-review process, three referees independently evaluate the scientific quality of the submitted manuscripts.

Peer reviewers are experts chosen by journal editors to provide written assessment of the **strengths** and **weaknesses** of written research, with the aim of improving the reporting of research and identifying the most appropriate and highest quality material for the journal.

Pertanika Journal of Science & Technology
Pertanika Journal of Science & Technology

Pertanika Journal of Science & Technology
Pertanika Journal of Science & Technology

Operating and review process

What happens to a manuscript once it is submitted to *Pertanika*? Typically, there are seven steps to the editorial review process:

1. The Journal's Chief Executive Editor (CEE) and the Editorial Board Members (EBMs) examine the paper to determine whether it is appropriate for the journal and should be reviewed. If not appropriate, the manuscript is rejected outright and the author is informed.

2. The CEE sends the article-identifying information having been removed, to 2 or 3 reviewers who are specialists in the subject matter represented by the article. The CEE requests them to complete the review within 3 weeks.

   Comments to authors are about the appropriateness and adequacy of the theoretical or conceptual framework, literature review, method, results and discussion, and conclusions. Reviewers often include suggestions for strengthening of the manuscript. Comments to the editor are in the nature of the significance of the work and its potential contribution to the research field.

3. The Editor-in-Chief (EiC) examines the review reports and decides whether to accept or reject the manuscript, invites the author(s) to revise and resubmit the manuscript, or seek additional review reports. Final acceptance or rejection rests with the CEE and EiC, who reserve the right to refuse any material for publication. In rare instances, the manuscript is accepted with almost no revision. Almost without exception, reviewers' comments (to the author) are forwarded to the author. If a revision is indicated, the editor provides guidelines to the authors for attending to the reviewers' suggestions and perhaps additional advice about revising the manuscript.

4. The authors decide whether and how to address the reviewers' comments and criticisms and the editor's concerns. The authors return a revised version of the paper to the CEE along with specific information describing how they have answered' the concerns of the reviewers and the editor, usually in a tabular form. The author(s) may also submit a rebuttal if there is a need especially when the authors disagree with certain comments provided by reviewer(s).

5. The CEE sends the revised paper out for re-review. Typically, at least 1 of the original reviewers will be asked to examine the article.

6. When the reviewers have completed their work, the EiC examines their comments and decides whether the paper is ready to be published, needs another round of revisions, or should be rejected. If the decision is to accept, the CEE is notified.

7. The CEE reserves the final right to accept or reject any material for publication, if the processing of a particular manuscript is deemed not to be in compliance with the S.O.P. of *Pertanika*. An acceptance letter is sent to all authors.

   The editorial office ensures that the manuscript adheres to the correct style (in-text citations, the reference list, and tables are typical areas of concern, clarity, and grammar). The authors are asked to respond to any minor queries by the editorial office. Following these corrections, page proofs are mailed to the corresponding authors for their final approval. At this point, **only essential changes are accepted**. Finally, the manuscript appears in the pages of the journal and is posted online.

Pertanika Journal of

SCIENCE & TECNOLOGY

A Special Issue Devoted to

Natural Polymers and Derivatives: Composition, Uses and Application

VOL. 32 (S3) 2024

(Special Issue)

Guest Editors

Lee Chuan Li, Chin Kit Ling and Ainun Zuriyati Mohamed @ Asa'ari

PERTANIKA JOURNALS

A scientific journal published by Universiti Putra Malaysia Press

PJST
Pertanika Journal of Science & Technology
AN INTERNATIONAL PEER-REVIEWED JOURNAL

EDITORIAL OFFICE
JOURNAL DIVISION
Putra Science Park
1st Floor, IDEA Tower II
UPM-MTDC Technology Centre
Universiti Putra Malaysia
43400 Serdang, Selangor Malaysia.

General Enquiry
Tel. No: +603 9769 1622 | 1616
E-mail:
executive_editor.pertanika@upm.edu.my
URL: www.journals-jd.upm.edu.my

PUBLISHER
UPM Press
Universiti Putra Malaysia
43400 UPM, Serdang, Selangor, Malaysia.
Tel: +603 9769 8851
E-mail: penerbit@putra.upm.edu.my
URL: http://penerbit.upm.edu.my

ABSTRACTING AND INDEXING OF PERTANIKA JOURNALS

The journal is indexed in SCOPUS (Elsevier), Clarivate-Emerging Sources Citation Index (ESCI), BIOSIS, National Agricultural Science (NAL), Google Scholar, MyCite, ISC. In addition, Pertanika JSSH is recipient of "CREAM" Award conferred by Ministry of Higher Education (MoHE), Malaysia.

Pertanika Journal of Science & Technology
Vol. 32 (S3) 2024

Contents

Natural Polymers and Derivatives: Composition, Uses and Application

Preface i
Lee Chuan Li, Chin Kit Ling and Ainun Zuriyati Mohamed @ Asa'ari

UV-absorption Capacity of Selected Crude and Functionalized Lignin for Use in Sunscreens 1
Jeanette O. Grande-Flores and Biljana M. Bujanovic

Preparation of Pulp, Microfibrillated Cellulose, and Paper Hand Sheets from Bakong (*Hanguana malayana* (Jack) Merr.) 15
Glenn Christian P. Acaso, Ramon A. Razal, Veronica P. Migo, Catalino G. Alfafara and Adela S. Torres

The Effects of Autohydrolysis Pretreatment on the Properties of OPT Pulps for the Production of Dissolving Pulp 27
Natra Joseph, Mohamad Haafiz Mohamad Kassim, Mazlan Ibrahim, Nurul Fazita Mohammad Rawi, Kumar Sudesh, Takamitsu Arai, Akihiko Kosugi and Leh Cheu Peng

The Effect of Spinning Parameters and Fiber Blending Ratio on the Physical Properties of Pineapple Leaf Fiber (PALF)-Cotton Yarns 41
Nurul Husna Zolkifflee, Mohd Nazrul Roslan, Juliana Abdul Halip, Khairu Kamarudin, Muhammad Farid Shaari and Asna Nabilah Aziz

Comprehensive Evaluation of Printing Process Parameters and Tensile Properties of Coconut Polypropylene Filament Composites in Additive Manufacturing 57
Noryani Muhammad, Mohd Aiman Jamaludin, Nuzaimah Mustafa, Yuzliza Yusuf, Mohd Adrinata Sharuzaman and Nurul Hanim Razak

Carrageenan-based Film Utilization for Eco-friendly Tea Bag 69
Yeni Pamita Sukmawati, Putri Alisya Oktavia Sarumaha, Nabila Fisa Sabrina, Reza Widyasaputra and Ida Bagus Banyuro Partha

Enhancing the Mechanical Strength and Thermal Stability of Polylactic Acid (PLA) with the Addition of Epoxidized Waste Cooking Oil (EWCO) 80
Nur Batrisyia Norhazlin, Nurul Hanim Razak, Anis Ainaa Omar, Mohd Hafidzal Mohd Hanafi and Asmah Mat Desa

Preface

With great pleasure, we introduce this Special Issue of the Pertanika Journal, dedicated to exploring the intricate realm of natural polymers and their derivatives. Within these pages lie a collection of papers stemming from the wealth of knowledge presented at the recent Wood and Biofibre International Conference (WOBIC 2023), which had the theme "Forest to Shelves: Roles in Mitigating Climate Change and Community Entrepreneurship."

Natural polymers derived from renewable resources, specifically plants, have garnered significant attention in recent years owing to their inherent biocompatibility, biodegradability, and low toxicity. These versatile materials offer a myriad of opportunities across various fields, from biomedical applications to green packaging solutions and beyond.

In this Special Issue, we delve into the composition, properties, and applications of natural polymers and their derivatives. From elucidating their chemical structures to exploring novel processing techniques and investigating their performance in diverse applications, each contribution sheds light on the remarkable potential of these sustainable materials.

The papers presented herein encompass a wide spectrum of topics, including extracting and modifying natural polymers, fabricating packaging material, developing advanced composite materials, and exploring their potential for pharmaceutical and biomedical applications. We aim to provide a comprehensive overview of the current state-of-the-art research in this rapidly evolving field through these diverse perspectives.

We extend our heartfelt gratitude to all authors who have contributed their work to this Special Issue, as well as to the reviewers for their invaluable feedback and insights. Furthermore, we thank the WOBIC 2023 organizers for providing a platform for exchanging ideas and fostering collaboration within the scientific community.

We hope this issue will catalyze further exploration and innovation in natural polymers and their derivatives. May the research presented here inspire future efforts to harness the full potential of these remarkable materials for the betterment of society and the environment.

Guest Editors

Lee Chuan Li (Dr.)
Chin Kit Ling (Dr.)
Ainun Zuriyati Mohamed @ Asa'ari (Dr.)

Pertanika J. Sci. & Technol. 32 (S3): 1 - 14 (2024)

PERTANIKA JOURNALS

SCIENCE & TECHNOLOGY

Journal homepage: http://www.pertanika.upm.edu.my/

UV-absorption Capacity of Selected Crude and Functionalized Lignin for Use in Sunscreens

Jeanette O. Grande-Flores[1, 2]* and Biljana M. Bujanovic[1, 3]

[1]*Department of Chemical Engineering, State University of New York College of Environmental Science and Forestry, Syracuse, 13210, New York*

[2]*Department of Forest Products and Paper Science, College of Forestry and Natural Resources, University of the Philippines Los Baños, College, Laguna, 4031, Philippines*

[3]*USDA-FS-Forest Products Laboratory, Madison, Wisconsin, 53726, USA*

ABSTRACT

The most commonly used commercial sunscreen agents are aromatic compounds oxybenzone and octinoxate, as they offer a wide range of protection in the UV spectrum. However, oxybenzone has the highest rate of skin irritation, while octinoxate has poor photostability. Oxybenzone is also a genotoxicant and skeletal endocrine disruptor to corals. Appropriate, less toxic and preferentially biorenewable alternatives should be recommended. Lignin, an abundant byproduct of pulp and biorefinery industries, is expected to be an effective replacement for oxybenzone and octinoxate due to its aromatic structure, which, in synergy with a wide variety of functional groups, produces the absorption of energy in the entire UV region. Additionally, lignin is a biocompatible polyphenolic with a strong radical quenching ability, i.e., anti-oxidizing potential. Therefore, it is a promising replacement for synthetic chemicals in cosmetics, sunscreen, and other applications. The UV absorption analysis of selected crude and functionalized lignin samples was conducted, and the results were compared to those of commercially used UV-absorption agents—oxybenzone and octinoxate. The results showed that the total absorption capacity of the lignin samples is lower by 6.4x and 16.3x compared to oxybenzone and octinoxate, respectively; however, it covers a wide absorption range in the UV spectrum. The lignin samples also showed good photostability and color stability, in contrast to the observed yellowing of octinoxate after 3 hours of exposure to sunlight. The UV spectra of some of the lignin samples indicate that their UV absorption capacity was enhanced by as much as 13.31% after exposure to sunlight.

Keywords: Absorbance spectra, bio-renewable sunscreen, hot water extraction, lignin, UV absorption capacity

ARTICLE INFO

Article history:
Received: 22 February 2024
Accepted: 30 May 2024
Published: 30 July 2024

DOI: https://doi.org/10.47836/pjst.32.S3.01

E-mail addresses:
jogrande@up.edu.ph (Jeanette O. Grande-Flores)
biljana.bujanovic@usda.gov / bbujanovic@esf.edu (Biljana M. Bujanovic)
*Corresponding author

ISSN: 0128-7680
e-ISSN: 2231-8526

INTRODUCTION

Lignin is the most abundant natural aromatic polymer and is the second most abundant polymer, next to cellulose. The Department of Energy targets a 30% replacement of fossil fuels with biofuels by 2030, which equates to 0.225 billion tons of lignin (Holladay et al., 2007). As a byproduct of biorefineries, Lignin is currently utilized mostly as feed for boilers for energy production. However, lignin has the potential to be developed into higher-value products, which will help increase the profitability of biorefineries (Dhiman et al., 2018). In these applications, the native structure of lignin is preferred over sulfur-containing and more condensed lignin from industrial operations. Mild processes like hot water extraction (HWE) are recommended to produce lignin with properties that can be altered for desired higher-value applications (Bujanovic et al., 2012).

Lignin possesses amphiphilic properties because of its abundance in hydrophilic groups (hydroxyl groups, carboxyl groups) and hydrophobic structural units (benzene rings, alkyl chains) (Zhang et al., 2019). Lignin is known to have UV-absorbing properties due to its phenolic units and thus has been integrated into different UV protection applications (Lee et al., 2019). Studies showed that lignin has a high antioxidant capacity with no cytotoxic effect over various concentrations (Gil-Chávez et al., 2019; Ugartondo et al., 2008). Lignin has antioxidant capacity due to its wide variety of functional groups (phenolic and aliphatic hydroxyls, carbonyls, carboxyls) as well as its phenylpropanoic structure. They interfere with sequential free radical reactions, reducing the risk of DNA and membrane damage (García et al., 2017; Randhir et al., 2004). Therefore, lignin can be used in sunscreen lotions and other cosmetics as a biocompatible and natural alternative to commercial sunscreen agents.

Although beneficial for vitamin D synthesis and immune development, ultraviolet radiation poses clinical acute and chronic effects on humans, which include erythema (sunburn), pigmentation, suppression of acquired immunity, photocarcinogenesis and photoaging. Thus, sunscreens were developed (Young et al., 2017). However, commercial sunscreen agents such as para-aminobenzoic acid (PABA) cause irritation, contact allergies, and skin staining. On the other hand, cinnamates like octinoxate need frequent reapplication due to their poor photostability. Additionally, benzophenones such as oxybenzone are good UV-absorbing agents; however, they also set the record for the highest rate of causing allergies (Sambandan & Ratner, 2010). The Hawaiian State Legislature recently banned sunscreens containing oxybenzone and/or octinoxate to preserve marine ecosystems. A study by Downs et al. (2015) showed that increasing concentration of oxybenzone increases the rate of coral bleaching and is a genotoxicant and skeletal endocrine disruptor to corals. Downs et al. (2015) concluded that "oxybenzone poses a hazard to coral reef conservation and threatens the resiliency of coral reefs to climate change." Thus, there is a need to develop a natural, non-toxic, and environmentally friendly alternative to this commercial sunscreen agent.

Studies about the feasibility of lignin in UV protection applications have been broadly explored. However, as far as researchers know, lignin's total UV absorption capacity has not yet been widely investigated. In this study, the selected lignin is pure lignin isolated through weak acid hydrolysis from a commercial facility, sugar maple and willow lignins recovered from HWE and functionalized willow lignins. The main objective of this study was to determine the total UV absorption capacity of the selected crude and functionalized lignin and compare it to oxybenzone and octinoxate. Specifically, this study sought to:

1. Determine the absorbance spectra of the lignin samples and the commercial sunscreen agents.
2. Investigate the color- and photostability of the lignin samples and compare them to the commercial sunscreen agents.
3. Determine the absorptivity coefficients of the lignin samples in a chosen solvent, DMSO, and
4. Investigate the potential of the lignin samples as broad-spectrum UV absorption agents.

MATERIALS AND METHODS

Materials/Reagents

Five lignin samples were collected: (1) pure lignin isolated through weak acid hydrolysis from a commercial facility (PL), (2) sugar maple lignin recovered from hot water extract (SMRecL), (3) willow lignin recovered from hot water extract (WRecL), (4) acetylated willow lignin (WAc), and (5) fatty acid esterified willow lignin (WFAE). Supplementary data can be obtained from the publisher to process each lignin sample. Commercial sunscreen agents for UV absorption, oxybenzone and octinoxate, were purchased from Sigma-Aldrich.

Preparation of Solutions

It was washed with a sulfuric acid solution of pH 5 to remove the impurities in the PL sample. A binary solvent system of 9:1 (v/v) acetone/water was used to dissolve all the lignin samples and the oxybenzone. Solutions of 0.4% wt/v were prepared for each set-up. The octinoxate is liquid at room temperature, while the rest are in powdered form. Each experimental set-up was prepared in triplicates.

Experimental Set-ups

300 μL of the solution was spread and air-dried on a pre-weighed glass slide. The lignin and the commercial UV-absorbance agents were set up in three environments: (1) unexposed,

(2) exposed to sunlight but covered with a *WRX* glass bottom, and (3) exposed directly to sunlight. The time of exposure was 3 hours (12:40H–15:40H).

The hour-by-hour UV index forecast of the USA area code of the study was taken from the US Environmental Protection Agency, and the temperatures were also noted (Table 1). The optical properties of the background used for the exposed samples are given in Table 2. The brightness and opacity were taken using the Technidyne Color Touch 2 Model ISO. The L, a*, and b* were measured using the TAPPI T 527 standard method.

Table 1
Hour-by-hour UV index forecast and temperature of the experimental set-up

Time	Temperature (^{0}F/°C)	UV-Index Forecast*
12:00H	63/17.2	3
13:00H	63/17.2	4
14:00H	65/18.3	3
15:00H	66/18.9	3
16:00H	65/18.3	1

Table 2
Optical properties of the background paper of the exposed samples

Brightness	Opacity	L*	a*	b*
92.092	99.462	98.22	-0.43	2.49

UV-Vis Spectrophotometry

The collected slides were allowed to equilibrate with the room temperature before it was weighed. The exact mass of the samples was noted by weighing them by difference.

The samples were dissolved in a known volume of dimethyl sulfoxide (DMSO). The lignin samples were diluted to 33x while the oxybenzone and the octinoxate were diluted to 11x31x (or 341x) to fit the accuracy range of the UV-Vis Spectrophotometer. Data on the total area under the curve within the UV range (200–400 nm) were gathered. Area under the curve for UVA (320–400 nm), UVB (280–320 nm), and UVC (200–280 nm) were also noted.

Determination of the Lignin Absorption Characteristics

The wavelength where the maximum absorption for each lignin in the UV range was determined using the UV-Vis Spectrophotometry. The five lignin samples were oven-dried for 12 hours. An amount of 0.0250 g of lignin was dissolved in DMSO and diluted to mark in a 25 mL flask. It was further diluted, as shown in Table 3. It was done in triplicates. The absorbance was recorded at the maximum wavelength, and the absorptivity was calculated using the slopes of the absorbance-concentration curve. The relationship between the absorption capacity and absorptivity was also determined.

RESULTS AND DISCUSSION

UV Absorbance Spectra

The absorbance of the lignin, functionalized lignin, and the commercial sunscreen agents were taken within the UV range. Lignin samples displayed maximum peak

Table 3
Stock solution dilution table

Lignin	Stock Solution Volume (µL)	DMSO (µL)	Concentration (mg/mL)
PL	240	2760	0.08
SMRecL	210	2790	0.07
WRecL	180	2820	0.06
WAc	150	2850	0.05
WFAE	120	2880	0.04

(λ_{max}) at 260-280 nm (Figure 1). λ_{max} is a characteristic absorption band of aromatic and polyphenolic structures (Lagesson et al., 2000). On the other hand, octinoxate has a relative peak at ~255 nm, which is attributed to benzene rings, but its λ_{max} is at 311nm, which is due to its anisole moiety (Hopkins et al., 2017; Kaflé, 2020; Sambandan & Ratner, 2011). Oxybenzone has peaks at ~260 nm due to the presence of aromatic rings and has λ_{max} at ~290 nm, which is attributed to phenols (Sambandan & Ratner, 2011). Figure 2 (a-g) show the UV absorption spectra of octinoxate and oxybenzone.

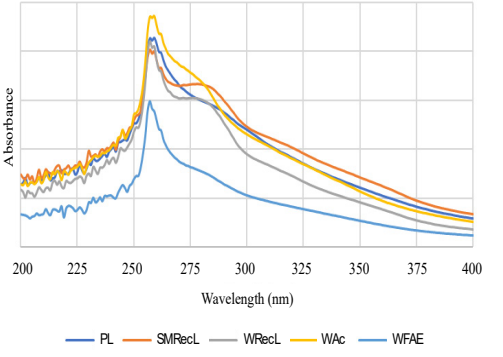

Figure 1. UV absorbance spectrum of unexposed lignin normalized to absorbance of 1 mg/mL of the substance

Radiation-enhanced UV Absorption Effect

The photostability of lignin is an indirect measure of its efficiency even after long exposure to UV radiation. Octinoxate is known to degrade after a certain period of exposure (Sambandan & Ratner, 2011), which is evident by the observed color change discussed in the succeeding subtopic. UV-Vis Spectrophotometry showed that its UV absorption capacity was reduced by 7.95% after 3 hours of exposure to sunlight. UV absorption spectra in Figure 2 not only

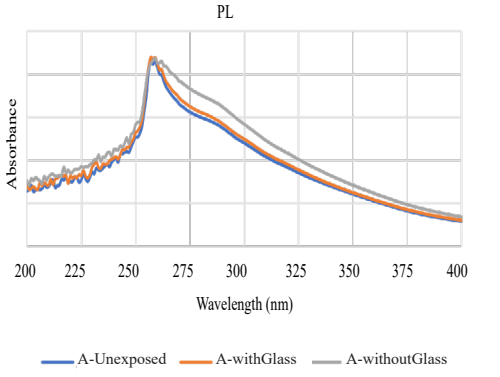

(a)

Figure 2. UV absorbance spectra of lignin derivatives and commercial sunscreen agents normalized to the absorbance of 1 mg/mL of the substance

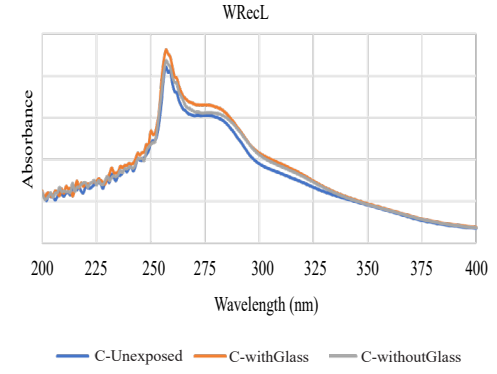

(b)

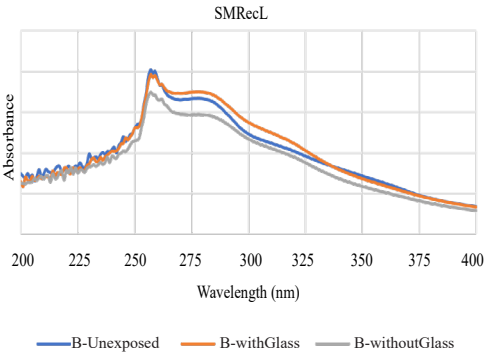

(c)

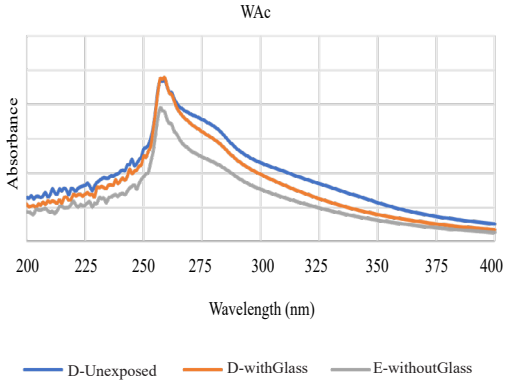

(d)

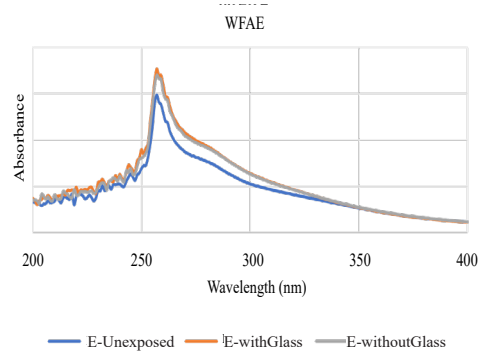

(e)

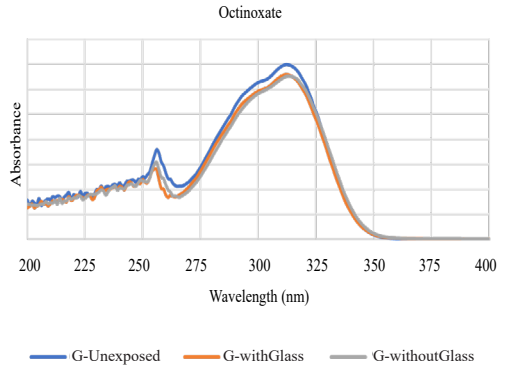

(f)

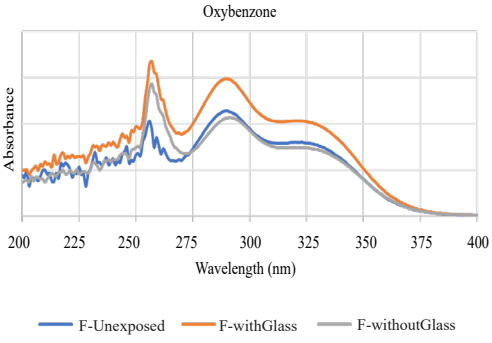

(g)

Figure 2. Continue

prove the photostability of lignin but also show that its UV absorbance increases, especially in the UVB region, after exposure to sunlight. For example, the UV absorbance capacity of PL and WFAE increased by 13.31% and 12.60%, respectively. It is true for almost all the samples of lignin except for WAc. The same results were obtained by Qian et al. (2015), who described this observation as “unexpected and promising." Although the exact mechanism is not yet understood, it may be attributed to lignin's free radical scavenging ability due to its wide variety of functional groups and phenylpropanoic units. Not many available studies have explored this phenomenon, thus opening more interesting scientific inquiries.

Among WRecL, WAc, and WFAE, unmodified willow lignin (WRecL) is the most photostable. WAc has a slight decrease in its absorption intensity after exposure to sunlight. The blocked hydroxyl and methoxyl groups are expected to enhance the aromatic rings' UV absorption capacity (Figure 3). This trend was also expected for the WFAE; however, ^{31}P-NMR of this sample shows that the amount of carboxylic acid groups is high in this esterified lignin. The carboxylic groups form a conjugated system with aromatic structures that stabilize the UV absorption capacity (Ovadias, 2019; Young et al., 2017).

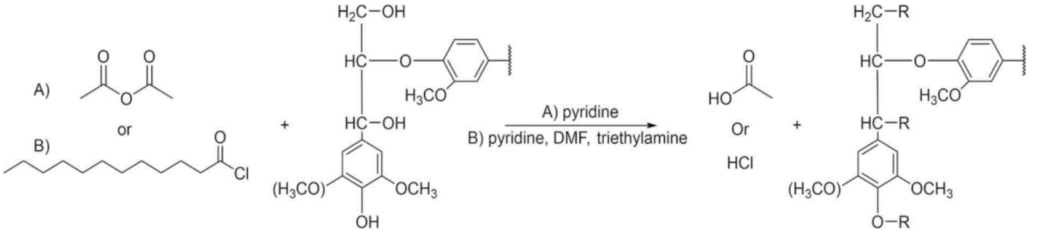

Figure 3. Proposed acylation of β-O-4 lignin structure by A) acetylation (C_2 addition) or B) acylation with lauroyl chloride (C_{12} addition)

Source: Nagardeolekar (2020)

Color stability is very important in marketing cosmetics and pharmaceutical products. Although lignin has a dark color that obstructs its usage in commercial products, a study by Zhang et al. (2019) showed that it can be whitened through fractionation and follow-up acetylation. Afterward, it can still be used effectively in sunscreen applications. Contrasting this potential of lignin, Figure 4 shows the yellowing of octinoxate after 3 hours of exposure to sunlight. Nanoparticle encapsulation improves the photostability of octinoxate (Perugini et al., 2002), yet it degrades upon exposure to sunlight and decreases its efficiency (Sambandan & Ratner, 2011).

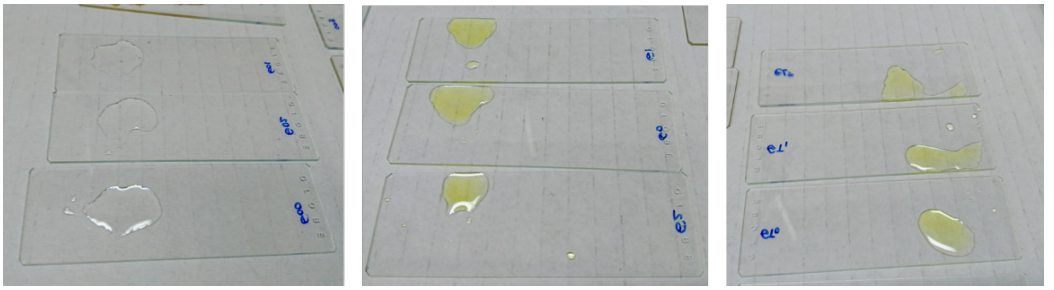

Figure 4. Yellowing of octinoxate upon exposure to sunlight. (Left to right: unexposed, exposed with glass cover, exposed directly to sunlight)

Absorption Characteristics

The absorbance and the concentration follow a linear relationship, as indicated by Beer-Lambert's Law). Absorption intensity can be expressed as absorbance according to Equation 1:

$$Absorption\ (A) = \log\frac{I_0}{I} = kcb = \varepsilon cb \qquad [1]$$

where k is a constant of solute, c is the solute concentration, b is the path length through the sample, and ε is a constant called absorptivity. The absorptivity coefficients for the lignin are presented in Table 4. PL and SMRecL have the highest absorptivity values among the lignin, while WFAE has the lowest. Therefore, PL and SMRecL will exhibit the highest absorbance ability, while WFAE will have the lowest given the same concentration. The linear relationship between the absorbance and the absorptivity can be extended to the total absorption capacity and the absorptivity. Figure 5 illustrates this relation.

Total UV Absorption Capacity

On average, the total absorption capacity of the lignin samples is lower by 6.4x and 16.3x compared to oxybenzone and octinoxate, respectively (Figure 6). Although this is the case, the direct linear relationship between the concentration and the total absorption capacity, as presented in Figure 5**,** proves that it can be compensated by increasing the lignin concentration. Increasing the lignin concentration in the sunscreen can also increase the total absorption capacity. It can also be used synergistically with other sunscreen agents to lower the amount of relatively unsafe ingredients. Zhang et al. (2019) found that blending 8% light-colored

Table 4
Absorption characteristics of the selected crude and functionalized lignin

Sample	Wavelength at Maximum Absorption (λ_{max}) [nm]	Absorptivity [$L*g^{-1}*cm^{-1}$]
PL	261	19.488
SMRecL	279	19.057
WRecL	278	16.292
WAc	268	16.078
WFAE	259	9.447

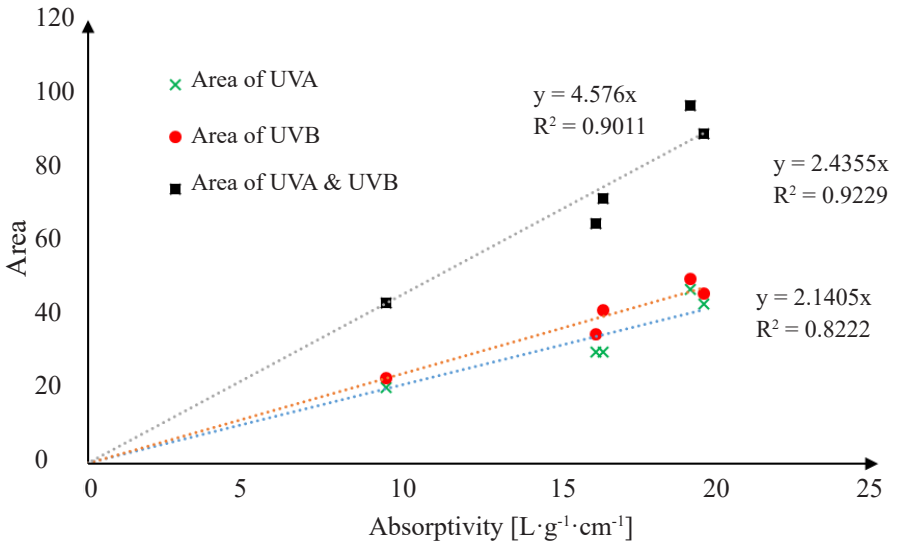

Figure 5. Relationship between absorption capacity and absorptivity

lignin with an SPF 15.3 lotion improved the SPF to 75.2. It proves lignin's potential in increasing sunscreens' UV absorption capacity.

The absorptivity coefficients and the total absorption capacities of the PL and SMRecL show no significant difference. No definite conclusion can be made since these lignin came from different species and processes. However, comparing the absorptivity coefficients and total absorption capacities of SMRecL and WRecL, WRecL showed a slightly lower capacity to absorb UV. The functionalized lignin shows a relatively lesser UV absorption capacity than the other. It may be due to the blocked hydroxyl and methoxyl groups that could have enhanced the UV absorption capacity of the aromatic rings.

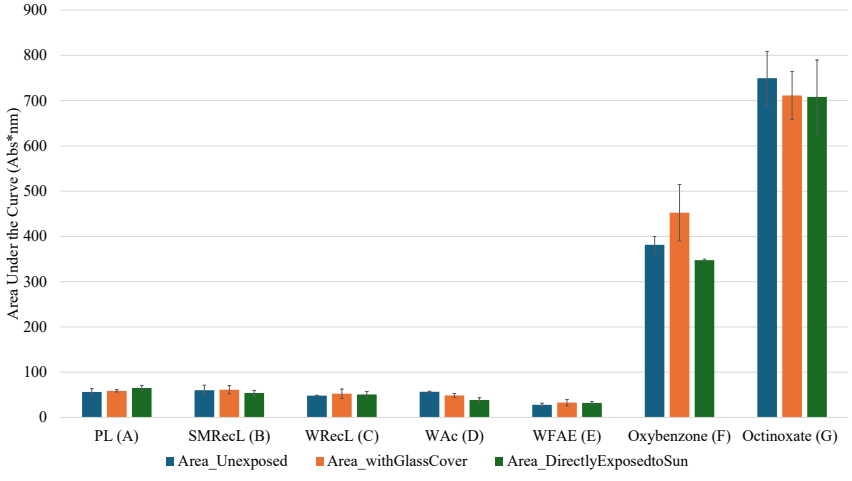

Figure 6. Total UV absorption capacity of lignin derivatives and commercial sunscreen agents normalized to a concentration of 0.1 mg/ 33 mL (33x dilution)

Broad-spectrum UV Absorption Capacity

One of the fundamental requirements for sunscreen is broad-spectrum coverage; that is, it covers most of the entire UV range, especially the UVA and UVB areas (Sambandan & Ratner, 2011). The absorption of the lignin and functionalized lignin samples were evaluated in the three UV regions. Results illustrated in Figure 7 show the potential of lignin in broad-spectrum sunscreen applications. Results showed that at a dilution of 33x, lignin and modified lignin absorbs up to more than 30 (absorbance unit-nm) in the UVA and UVB regions. These capacities can, of course, be intensified by increasing the concentration of lignin or by mixing it with other UV-absorbing agents.

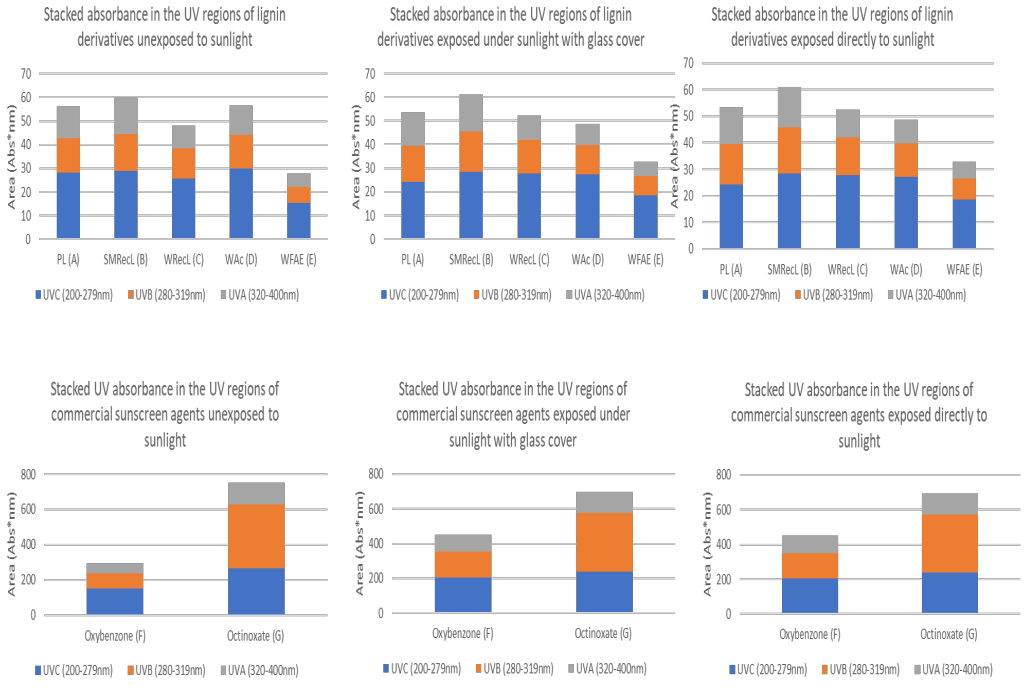

Figure 7. Stacked absorbance in the UV region of lignin and commercial sunscreen agents (normalized to a concentration of 0.1 mg/ 33 mL or 33x dilution)

CONCLUSION

UV absorption spectra of lignin and modified lignin samples were taken and were compared with commercial sunscreen agents—oxybenzone and octinoxate. Absorption peaks occurred at ~255–280 nm, reflecting the aromatic and polyphenol structures of the compounds. Unexpected results showed that most lignin samples displayed increased UV absorption capacity after sunlight exposure, which could be attributed to lignin's free radical scavenging ability. Lignin samples showed good color stability and photostability;

in contrast, yellowing of octinoxate was observed after 3 hours of sunlight exposure. Lignin has a lower UV absorption capacity compared to octinoxate and oxybenzone. However, it can be compensated by increasing its concentration or mixing it with other agents to synergistically increase its UV absorption capacity. Lignin also covers a good range of UVA and UVB regions and thus has a great prospect as an ingredient to natural broad-spectrum sunscreen lotions.

ACKNOWLEDGEMENTS

The authors acknowledge Kaiwen Yang from Beijing University of Chemical Technology, China and State University of New York College of Environmental Science and Forestry (BUCT-SUNY ESF), Syracuse, New York, United States of America (2020) for contributing to the relationship between absorption capacity and absorptivity. The authors also wish to acknowledge Pure Lignin Environmental Technology Ltd. in West Kelowna, British Columbia, Canada as well as Prajakta Dongre and Mathew Ovadias of SUNY ESF for providing the samples.

REFERENCES

Bujanovic, B. M., Goundalkar, M. J., & Amidon, T. E. (2012). Increasing the value of a biorefinery based on hot-water extraction: Lignin products. *Tappi Journal, 11*(1), 19–26. https://doi.org/10.32964/10.32964/tj11.1.19

Dhiman, G., Akhtar, N., Mukherjee G, & Mukherjee G. (2018) Valorization of lignin: Emerging technologies and limitations in biorefineries. In A. Kuila & V. Sharma (Eds.), *Principles and applications of fermentation technology* (pp 163-180). Wiley https://doi.org/10.1002/9781119460381.ch9

Dongre, P. (2018). Characterization and Utilization of Hot-Water Extracted Lignin for Formaldehyde-Free Resin Applications. [Unpublished doctoral dissertation]. State University of New York College of Environmental Science and Forestry.

Downs, C. A., Kramarsky-Winter, E., Segal, R., Fauth, J. E., Knutson, S., Bronstein, O., Ciner, F. R., Jeger, R., Lichtenfeld, Y., Woodley, C. M., Pennington, P. L., Cadenas, K., Kushmaro, A., & Loya, Y. (2015). Toxicopathological effects of the sunscreen UV filter, oxybenzone (benzophenone-3), on coral planulae and cultured primary cells and its environmental contamination in Hawaii and the U.S. Virgin Islands. *Archives of Environmental Contamination and Toxicology, 70*(2), 265–288. https://doi.org/10.1007/s00244-015-0227-7

García, A., Spigno, G., & Labidi, J. (2017). Antioxidant and biocide behaviour of lignin fractions from apple tree pruning residues. *Industrial Crops and Products, 104,* 242–252. https://doi.org/10.1016/j.indcrop.2017.04.063

Gil-Chávez, G. J., Padhi, S. S. P., Pereira, C. V., Guerreiro, J. N., Matias, A. A., & Smirnova, I. (2019). Cytotoxicity and biological capacity of sulfur-free lignins obtained in novel biorefining process. *International Journal of Biological Macromolecules, 136,* 697–703. https://doi.org/10.1016/j.ijbiomac.2019.06.021

Holladay, J. E., White, J. F., Bozell, J. J., & Johnson, D. K. (2007). *Top value-added chemicals from biomass - Volume II—Results of screening for potential candidates from biorefinery lignin.* https://doi.org/10.2172/921839

Hopkins, Z. R., Snowberger, S., & Blaney, L. (2017). Ozonation of the oxybenzone, octinoxate, and octocrylene UV-filters: Reaction kinetics, absorbance characteristics, and transformation products. *Journal of Hazardous Materials, 338,* 23–32. https://doi.org/10.1016/j.jhazmat.2017.05.016

Kaflé, B. P. (2020). Application of UV–VIS spectrophotometry for chemical analysis. In *Chemical Analysis and Material Characterization by Spectrophotometry* (pp. 79–145). Elsevier. https://doi.org/10.1016/b978-0-12-814866-2.00005-1

Lagesson, V., Lagesson-Andrasko, L., Andrasko, J., & Baco, F. (2000). Identification of compounds and specific functional groups in the wavelength region 168–330 nm using gas chromatography with UV detection. *Journal of Chromatography A, 867*(1–2), 187–206. https://doi.org/10.1016/s0021-9673(99)01123-1

Lee, S. C., Tran, T. M. T., Choi, J. W., & Won, K. (2019). Lignin for white natural sunscreens. *International Journal of Biological Macromolecules, 122,* 549–554. https://doi.org/10.1016/j.ijbiomac.2018.10.184

Nagardeolekar, A., Ovadias, M., Wang, K., & Bujanovic, B. (2020). Willow lignin recovered from hot-water extraction for the production of hydrogels and thermoplastic blends. *ChemSusChem, 13*(17), 4702–4721. https://doi.org/10.1002/cssc.202001259

Ovadias, M. (2019). *Lignin thermoplastic blends: Biorefinery willow lignin and poly (lactic acid).* [Unpublished master's thesis]. 119. State University of New York College of Environmental Science and Forestry.

Perugini, P., Simeoni, S., Scalia, S., Genta, I., Modena, T., Conti, B., & Pavanetto, F. (2002). Effect of nanoparticle encapsulation on the photostability of the sunscreen agent, 2-ethylhexyl-p-methoxycinnamate. *International Journal of Pharmaceutics, 246*(1–2), 37–45. https://doi.org/10.1016/s0378-5173(02)00356-3

Qian, Y., Qiu, X., & Zhu, S. (2015). Lignin: A nature-inspired sun blocker for broad-spectrum sunscreens. *Green Chemistry, 17*(1), 320–324. https://doi.org/10.1039/c4gc01333f

Randhir, R., Lin, Y., & Shetty, K. (2004). Stimulation of phenolics, antioxidant and antimicrobial activities in dark germinated mung bean sprouts in response to peptide and phytochemical elicitors. *Process Biochemistry, 39*(5), 637–646. https://doi.org/10.1016/s0032-9592(03)00197-3

Sambandan, D. R., & Ratner, D. (2011). Sunscreens: An overview and update. *Journal of the American Academy of Dermatology, 64*(4), 748–758. https://doi.org/10.1016/j.jaad.2010.01.005

Ugartondo, V., Mitjans, M., & Vinardell, M. P. (2008). Comparative antioxidant and cytotoxic effects of lignins from different sources. *Bioresource Technology, 99*(14), 6683–6687. https://doi.org/10.1016/j.biortech.2007.11.038

Young, A. R., Claveau, J., & Rossi, A. B. (2017). Ultraviolet radiation and the skin: Photobiology and sunscreen photoprotection. *Journal of the American Academy of Dermatology, 76*(3), S100–S109. https://doi.org/10.1016/j.jaad.2016.09.038

Zhang, H., Liu, X., Fu, S., & Chen, Y. (2019). High-value utilization of kraft lignin: Color reduction and evaluation as sunscreen ingredient. *International Journal of Biological Macromolecules, 133,* 86–92. https://doi.org/10.1016/j.ijbiomac.2019.04.092

SUPPLEMENTARY DATA

Extraction and Processing of the Lignin

Pure Lignin (PL) (Pure Lignin Environmental Technology Ltd, 2010)

The lignin was obtained from the #9 and #10 production line of Pure Lignin Environmental Technology Ltd processing of dry and green pines, respectively. The lignin is collected using gravity filtration. Five hundred grams of the lignin was washed with 500 mL of water (pH 6.63) and 0.30 ml of sulfuric acid (pH 2.05). The first of four-reverse osmosis (RO) water (250 mL, pH 6.65) washing was done when a thin film of the acid wash appeared on top of the lignin.

Sugar Maple Recovered Lignin (Dongre, 2018)

The sugar maple (*Acer saccharum*) chips were subjected to hot-water extraction (HWE) under 160°C for 2 hours. HWE was carried out in a Struthers-Wells 65 ft^3 stainless-lined batch digester. The water-bust biomass ratio was 4. The extract from HWE underwent ultrafiltration through a Hilco HM634-01 ceramic filter with a pore size of 0.01 µm. The retentate was recovered, and the pH was adjusted to 2 before centrifugation to collect the sugar maple fraction. It undergoes nanofiltration, and the permeation is acid hydrolyzed with concentrated sulfuric acid (1.5% by mass of extract) at 130°C for 45 min. The precipitate was recovered with dissolution in acetone/water (1:1) binary solvent and steam-stripped to remove the solvents.

Willow Recovered Lignin (WRecL) (Ovadias, 2019)

The hydrolysates of recovered willow (*Salix spp*., Family: Salicaceae; a blend of commercial cultivars with bark) were from the pilot plant biorefinery in PBE, SUNY-ESF. The pH of the hydrolysate was dropped to 2 using 20% H_2SO_4, and the lignin was precipitated and collected through centrifugation and vacuum filtration.

Acetylated Willow Lignin (WAc) (Ovadias, 2019)

WRecL was dissolved into 20 mL/g-lignin of pyridine and acetic anhydride (1:1 v/v). The solution was mixed on a stir plate for at least 24 hours and up to 72 hours. 300 mL ice-cold water per one gram of starting lignin was poured to precipitate the acetylated lignin. It was collected using vacuum filtration and again washed with ice-cold water to remove excess pyridine, acetic anhydride and acetic acid (a byproduct of the reaction). The acetylated lignin was dried overnight in a vacuum oven (40°C). When scaling this reaction up to 5 grams, 70 mL of pyridine and acetic anhydride was utilized (0.4:1 v/v) to reduce pyridine usage. Appendix Figure A1 shows the proposed reaction mechanism.

Willow Fatty Acid Esterified (WFAE) (Ovadias, 2019)

WRecL was acylated with lauroyl chloride, a chloride derivative of lauric acid, by dissolving into 30 mL of N, N-dimethylformamide per gram of lignin in the presence of

pyridine (5.5 mL) and triethylamine (1.5 mL). Once the solution was homogenized, 1 mmol-lauroyl chloride/mmol-OH was added to start the reaction. Constant stirring was employed for 2 hours at room temperature. The lignin acylated with lauroyl chloride was precipitated by pouring the solution into 600 mL of ice-cold 2% HCl per one gram of starting lignin. The mixture was vacuum-filtered with nylon filters to make it easier to recover the lignin laureate. The filter cake was then washed with ethanol and water (1:1 v/v) to remove excess solvent, unreacted lauroyl chloride, and unbound fatty acid, lauric acid. The lignin laurate was dried overnight in a vacuum oven (40°C).

Pertanika J. Sci. & Technol. 32 (S3): 15 - 25 (2024)

PERTANIKA JOURNALS

SCIENCE & TECHNOLOGY

Journal homepage: http://www.pertanika.upm.edu.my/

Preparation of Pulp, Microfibrillated Cellulose, and Paper Hand Sheets from Bakong (*Hanguana malayana* (Jack) Merr.)

Glenn Christian P. Acaso[1]*, Ramon A. Razal[1], Veronica P. Migo[2], Catalino G. Alfafara[2] and Adela S. Torres[3]

[1]Department of Forest Products and Paper Science, College of Forestry and Natural Resources, University of the Philippines Los Baños, College, 4031 Laguna, Philippines
[2]Department of Chemical Engineering, College of Engineering and Agro-Industrial Technology, University of the Philippines Los Baños, College, 4031 Laguna, Philippines
[3]Forest Products Research and Development Institute, Department of Science and Technology, College, 4031 Laguna, Philippines

ABSTRACT

Bakong (*Hanguana malayana* (Jack) Merr.) is a perennial herbaceous plant that grows abundantly in certain parts of the Philippines. This study investigates Bakong fibers' potential as a pulp source for papermaking. Furthermore, microfibrillated cellulose (MFC) produced from the fibers was used as an additive in the Bakong fiber-based hand sheets at 2%, 6%, and 10% w/w, and their effects on their strength properties were observed. The soda pulping method produced Bakong pulp with a total yield of 47.36%. Proximate chemical analysis showed that the method reduced the lignin content from 13.19% to 8.76%, and the resulting pulp was successfully formed into paper hand sheets. The strength properties of the hand sheets were tested, and the resulting burst index, tear index, tensile index, and folding endurance values were 5.98 kPa/m2·g, 6.41 mN·m2/g, 105.97 N·m/g, and 626 double folds, respectively. Aside from the tear index, the Bakong hand sheets' strength properties were much higher than that of locally produced commercial printing paper. The addition of MFC on the hand sheets negatively affected the burst and tensile index values of the Bakong hand sheets but significantly improved the tear index up to 6% w/w. These results show that the pulp produced from the Bakong fibers can potentially be used as an alternative source of pulp for papermaking, but further optimization of the pulping process is recommended to increase the yield, lower lignin content, and improve compatibility with the MFC.

Keywords: Microfibrillated cellulose, non-wood fibers, papermaking, pulping

ARTICLE INFO

Article history:
Received: 22 February 2024
Accepted: 30 May 2024
Published: 30 July 2024

DOI: https://doi.org/10.47836/pjst.32.S3.02

E-mail addresses:
gpacaso@up.edu.ph (Glenn Christian P. Acaso)
rarazal@up.edu.ph (Ramon A. Razal)
vpmigo@up.edu.ph (Veronica P. Migo)
cgalfafara@up.edu.ph (Catalino G. Alfafara)
adelatorres95@yahoo.com (Adela S. Torres)
*Corresponding author

ISSN: 0128-7680
e-ISSN: 2231-8526

INTRODUCTION

The pulp and paper industry has been growing rapidly globally, so there is a great demand for raw pulp and paper materials. Since wood resources are scarce, there is increased interest in utilizing non-woody raw materials for pulp and papermaking (El-Sayed et al., 2020). *Hanguana malayana* (Jack) Merr., commonly known as Bakong, is a perennial herbaceous plant native to Sri Lanka, Southeast Asia, and Palau. In the Philippines, Bakong can be found in Laguna de Cagayan in Santa Teresita, Cagayan. It is an invasive species in the lake area, and excessive amounts may even be detrimental to the ecosystem (Choe et al., 2023).

As a fibrous plant, previous studies investigated utilizing its stems and leaves to produce fibers ranging from 1.2 to 1.4 m long. It has since been popular in the area and is projected to become a great source of livelihood for the people. According to the Design Center of the Philippines (2022), these fibers can be used as components for handicrafts and furniture designs. Other studies investigated its antibacterial use as leaf extractives are effective against certain bacteria (Borela et al., 2021).

However, not much research has been done on this plant and its utilization for pulp and papermaking. Thus, the potential of Bakong as a non-wood cellulose source is investigated in this study. Proximate chemical analysis was first performed to determine the holocellulose, lignin, and ash content of the Bakong fibers. Due to its similarities with other non-wood fiber sources, soda pulping was the chosen method to produce Bakong pulp (Wunna et al., 2017). The pulp produced from Bakong was processed to form hand sheets, and their strength properties were evaluated.

Moreover, this study also explored the use of Bakong pulp to produce nanocellulose. Since nanocelluloses were observed to increase the mechanical and barrier properties of paper, the Bakong pulp was further processed into microfibrillated cellulose (MFC) for use as an additive in the papermaking process (Balea et al., 2020). Using a friction grinder, MFC was produced by disrupting the intermolecular hydrogen bonding between the cellulose molecules in the Bakong pulp (Kargarzadeh et al., 2017). The MFC produced was then added to the Bakong hand sheets to explore its effect on the strength properties. A study by Viana et al. (2018) showed that adding up to 10% nanofibrillated cellulose positively affected the mechanical properties of paper hand sheets. Another study by Hollertz et al. (2017) showed that adding 2% chemically modified cellulose micro- and nanofibrils improved tensile strength when used as a paper additive. Based on these, this study investigated adding 2%, 6% and 10% MFC by weight.

MATERIALS AND METHODS

Proximate Chemical Analysis

Bakong stem fibers were received from the Design Center of the Philippines in connection with the Laguna de Cagayan Handicrafts Association. The fibers were bleached and

decorticated in bundles approximately 1 m long. The fibers were washed with distilled water to remove dirt and other contaminants and then cut by hand to lengths of 50 mm. The composition of Bakong fibers was analyzed using the following methods: TAPPI T204 cm-07: Solvent extractives of Wood and Pulp, TAPPI T207 cm-08: water solubility of wood and pulp, TAPPI T211 om-02: Ash in wood, pulp, paper and paperboard, and TAPPI T222 om-02: Acid-insoluble lignin in wood and pulp. As a general baseline, the holocellulose content of the fibers was determined by difference.

Pulping and Handsheet Formation

In the study of Jimenez et al. (2005), the optimum pulping conditions for abaca, a non-wood plant with similar lignin content, were 170°C for 30 min, with 7.5% active alkali. Since the lignin content of the Bakong fibers is slightly higher, the pulping conditions were slightly modified. 600 g of air-dried 50 mm long Bakong fibers and 120 g NaOH in 4200 mL distilled water were cooked in a laboratory digester at 170°C for 2.5 h. The pulp was then washed with water until a neutral pH was achieved. The produced pulp was then passed through a disc refiner at 0.1 clearance, followed by beating using a Valley beater to achieve pulp freeness values of 250 Canadian Standard Freeness (CSF).

A standard 159 mm diameter sheet machine with a stirrer produced Bakong hand sheets based on the TAPPI Standard T205. A 30 g of Bakong pulp was diluted and disintegrated at 3000 rpm for 10 min. The slurry was then fed to a TAPPI hand sheet former cylinder to produce 80 g/m^2 hand sheets. The hand sheets were pressed for 10 min at 345 kPa and dried at 27°C for 24 h. The hand sheets were then conditioned in an atmosphere with a temperature of 23±1°C and 50±2% relative humidity before testing.

Preparation of Bakong Microfibrillated Cellulose (MFC)

Bakong pulp was first milled to 2 mm lengths to increase surface area for the bleaching process. Hypochlorite bleaching was performed using a modified method based on a previous study (Yuanita et al., 2015). The pulp was then soaked in 5.25% sodium hypochlorite solution at 10% w/v consistency for 30 min at room temperature. The bleached pulp was washed with distilled water until a neutral pH was achieved. The bleached pulp was soaked with distilled water at 1% w/v and subjected to a mechanical friction grinding process using the Masuko Supermasscolloider, model MKCA6-2. The grinder was operated at a speed of 1500 rpm, and the suspension was subjected to grinding for 15 passes. The grinder clearance was reduced every 1 to 2 passes until a clearance of -10 was reached at the 15th pass. The produced MFC was incorporated into the hand sheets at a 2%, 6% and 10% w/w ratio before formation.

A gravimetric test was performed to test for the retention of MFC in the hand sheets. Hand sheets were made from pulp with known oven-dry weights. Hand sheets with

additional MFC of known oven-dry weights were also prepared. The hand sheets were oven-dried at 105°C and weighed every hour until the weight variation was less than 0.01 g. Afterward, the weights of the hand sheets with and without MFC were compared.

Characterization of Produced Hand Sheets

Surface Morphology

A scanning electron microscope was used to capture high-magnification micrographs of the surface of the Bakong hand sheets. Due to their organic and non-conductive nature, the samples were ion-coated prior to viewing under the microscope.

Handsheet Testing

The grammage of the produced hand sheets was determined using ISO standard 534. The hand sheets were cut according to TAPPI T220 to test the mechanical properties. The hand sheets' burst index, tensile index, tear index, and folding endurance were tested according to ISO standards 2758, 1924-2, 1974, and 5626, respectively. Five replicates were done for each type of hand sheet produced. For comparison, commercial-grade paper was tested using the same methods. The data obtained were subjected to a one-way analysis of variance (ANOVA) at a 95% confidence level ($p \leq 0.05$) to check if the differences among the compared groups were statistically significant. It was followed by the Tukey-Kramer post hoc test to analyze the differences when significance was observed.

RESULTS AND DISCUSSIONS

Chemical Composition of Bakong Fibers

The Bakong fibers received were air-dried and brown. Milling was performed using a Wiley mill to reduce the size of the fibers to about 2 mm long. (Figure 1). A summary of the chemical composition of the Bakong fibers based on the oven-dry weight is shown in Table 1. The moisture content of the Bakong samples after air-drying for at least 24 h was found to be 13.12%. It was the basis for determining the chemicals needed for the succeeding proximate analysis and pulping.

Figure 1. Bakong fibers: (a) as received, (b) after milling, (c) after hand sheet formation

Table 1
Chemical composition of Bakong fibers

Chemical Components	Compositions (%)
Moisture Content	13.12 ± 0.45
Ash Content	7.09 ± 0.10
Cyclohexane-ethanol Extractives	2.25 ± 0.09
Hot Water Extractives	8.78 ± 0.20
Lignin Content	13.19 ± 1.16
Holocellulose Content (by difference)	68.69 ± 2.00

The fibers' ash content was 7.09%, which is typical of wheat straw species (Plazonic et al., 2016). It is considered relatively high and may be disadvantageous in pulp and papermaking as they could interfere with pulping and recovery of pulping chemicals. The cyclohexane-ethanol extractives and hot water extractives of the Bakong fibers were 2.25% and 8.78%, respectively. These values add up to 11.03%, much higher than wood's, typically containing 3 to 8% of total extractives and normally not exceeding 5% (Lehr, 2021). These negatively affect the pulping and bleaching processes, as they can react with the pulping liquor and block the diffusion of bleaching chemicals and lignin (Dai, 2001). It is suggested that additional pre-treatment methods be employed to lower the ash and extractive content of the fibers before they are used in pulping and papermaking.

The lignin content of the fibers was found to be 13.19%, which is generally lower than those of wood species. Additionally, the holocellulose content of the fibers was found to be 68.69%. It shows that Bakong is a promising source of pulp, having similar holocellulose content values compared to other fiber sources (Moral et al., 2017). Soda pulping was chosen since the raw material contains significantly lower lignin than wood sources. Moreover, Kraft pulping was not employed to minimize the use of sulfur-containing compounds, which are considered environmental pollutants.

Production of Bakong Pulp and Microfibrillated Cellulose

The soda pulping yield of the Bakong fibers is listed in Table 2. On average, the pulping method yielded 48.85% yield, with the resulting pulp having a lignin content of 8.76%. It is within the range of typical Kraft pulping yields, which is between 43 to 70% (Biermann, 1996). However, this value is much lower than that obtained by Jimenez et al. (2005) for abaca, which is 77.33% and has a lignin content of around 4.8%. Although the method produced pulp from the Bakong fibers with a reasonable yield and removed 70% of the lignin content of the original fibers, improvements can still be made to the process.

The pulp underwent refining and beating to further increase the fiber surface area and make it more suitable for papermaking. A beating time of 5 min, with a 5 kg load, was determined for the pulp to reach freeness values of around 250 CSF, which is typical for paper stock. Circular hand sheets were successfully produced after the beating process, as

Table 2
Soda pulping and refining yield of Bakong fibers

Process	Yield(%)
Soda Pulping, Beating, and Refining	47.36 ± 2.89
Pulp Bleaching	66.47 ± 3.10
Friction Grinding (Masuko Supermasscolloider)	87.53 ± 0.056
Overall MFC yield	27.5 ± 2.98

shown in Figure 1, with minimal losses. The overall yield after beating was determined to be 47.36%, showing that Bakong can be a good non-wood alternative source of pulp for papermaking.

To produce MFC, the Bakong pulp was bleached to reduce lignin content to as low as 1.42%. After friction grinding using a Masuko Supermasscolloider, the resulting product is a white suspension with a gel-like consistency. The bleaching and friction grinding yields are summarized in Table 2. An overall yield of 27.55% was obtained, and this value may be attributed to the low yields after pulp bleaching. It suggests that the bleaching process degraded the celluloses and hemicelluloses in the fibers, and further optimization of the process is recommended.

The MFC was incorporated into the hand sheets by adding the suspension into the pulp before formation. MFC retention was determined to be 94.4%. Thus, the method used successfully incorporated the MFC into the hand sheets.

Microscopy of the MFC and Hand Sheets

The formed hand sheets were observed under a scanning electron microscope. The pulped Bakong fibers were randomly oriented within the hand sheet. The fibers had diameters of 20 μm and lengths greater than 2 mm, as shown in Figure 2. Destruction of natural fiber bundles during the bleaching and friction grinding process resulted in fibrillation. In a previous study, alkali and oxidative bleaching of fibers reduced fiber diameters from 75–90 μm to 5–6 μm (Yuanita et al., 2015). In this study, while milder bleaching conditions were

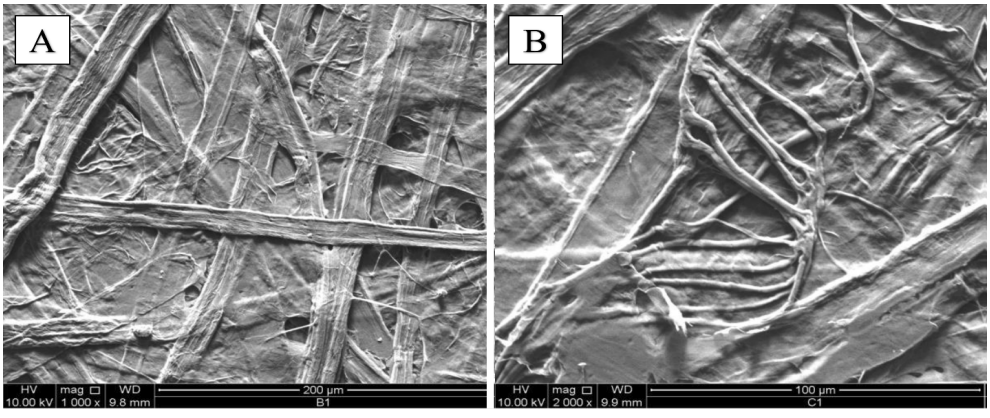

Figure 2. SEM images of the hand sheet (a) without MFC and (b) with MFC

used, friction grinding was employed to further fibrillate the Bakong fibers. Under SEM, the fiber diameters were reduced to about 3 μm. The hand sheets with additional MFC showed the presence of these separate smaller fibers on the surface, which were presumed to be MFC adhered to the pulp fibers.

Bakong Pulp Handsheet Properties

Hand sheets were produced from the Bakong pulp with grammage values of 80 $g \cdot m^{-2}$. A summary of the strength properties of the produced hand sheets is shown in Table 3. Commercial printing paper produced locally (labeled "C") was also tested using the same methods and shown for comparison. The values listed for the commercial printing paper were for the machine direction, which are normally higher than those for cross direction. The effect on the strength properties of adding MFC to the Bakong pulp during hand sheet formation was also tested. Figures 3–6 show the burst index, tear index, tensile index and folding endurance, respectively.

Table 3
Mechanical properties of hand sheets produced from Bakong pulp compared to commercial printing paper

Mechanical Properties	Bakong Hand Sheets Prepared in This Study	Commercial Printing Paper
Burst Index ($kPa \cdot m^{-2} \cdot g^{-1}$)	5.98 ± 0.23	3.01 ± 0.13
Tear Index ($mN \cdot m^{2} \cdot g^{-1}$)	6.41 ± 0.55	7.53 ± 0.18
Tensile Index ($N \cdot m \cdot g^{-1}$)	105.97 ± 3.97	52.56 ± 2.19
Folding Endurance (double folds)	626 ± 189	41 ± 8.29

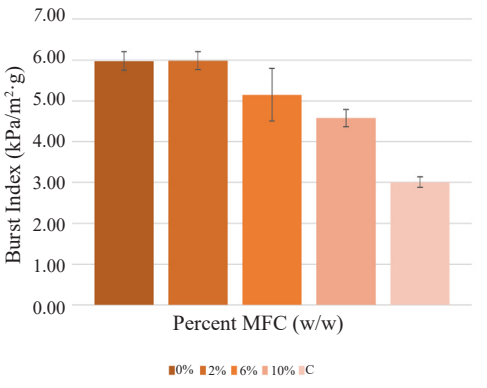

Figure 3. Burst index of the produced hand sheets

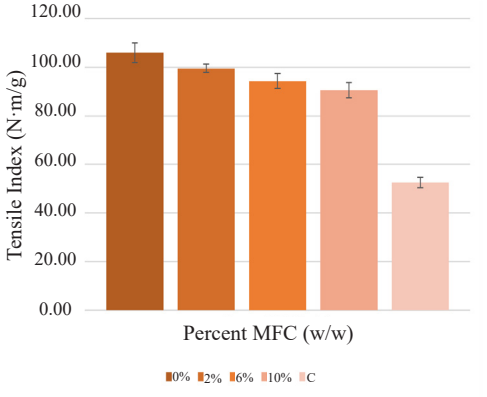

Figure 4. Tensile index of the produced hand sheets

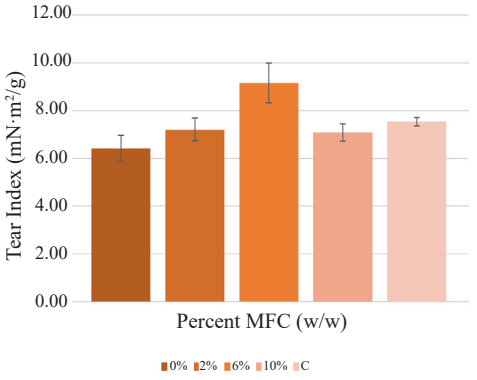

Figure 5. Tear index of the produced hand sheets

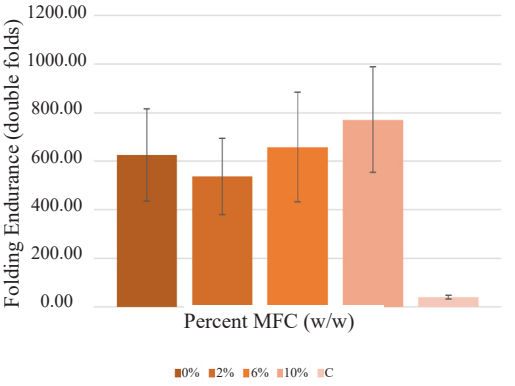

Figure 6. Folding endurance of the produced hand sheets

The burst and tensile indices of the hand sheets were tested as general indicators of their strength characteristics (PITA Raw Materials Working Group, 2005). It was observed that the hand sheets produced from the Bakong pulp had significantly greater burst and tensile strength than that of commercially produced printing paper. It could be attributed to the long fibers' strong inter-fiber bonding. It shows that the pulp suits withstanding strains associated with the papermaking process and end-use.

However, with the addition of MFC, the burst index and tensile index values decreased noticeably. A similar case was found in the study of Viana et al. (2018), wherein no significant improvement in the mechanical property of newsprint was observed with the addition of nanofibrillated cellulose. Since the Bakong pulp fibers still contained a significant amount of lignin, adding MFC may have been less compatible with the fibrous elements and did not promote inter-fiber bonding.

A different trend was observed when testing the tear index of the formed hand sheets. Although tear resistance also depends on the degree of bonding between the fibers, it mostly depends on the fiber elements' resistance, like the wall's length and thickness (Viana et al., 2018). The addition of up to 6% MFC reinforced the thickness of the fiber walls by bonding with the surface. Further increasing this to 10% resulted in weaker inter-fiber bonding, ultimately negatively affecting the tear index. Since the tear index of Bakong hand sheets was much lower than that of commercial printing paper, they may not be suitable for wrapping or packaging applications. However, the tear resistance was improved significantly with the addition of 6% MFC. Although the other mechanical properties decreased with the addition of MFC, at a level of 6% by weight, all the mechanical properties of the MFC-reinforced Bakong hand sheets were still higher than those of commercial printing paper.

Lastly, the folding endurance of the fibers was tested. The test gives extremely variable results. Using one-way ANOVA, no significant property differences were observed between the untreated hand sheets and those reinforced with MFC (p-value > 0.05). However, the folding endurance of the Bakong hand sheets was much higher than that of printing paper. Thus, Bakong pulp can be an additive for specialty papers requiring high folding endurance, such as currency bank paper. Along with Abaca, Salago and other fibers, it can contribute to the country's goal of producing banknotes using 100% locally sourced fibers. (Fernandez, 2018).

CONCLUSION

Pulp, microfibrillated cellulose, and paper hand sheets were produced from Bakong (*Hanguana malayana* (Jack) Merr.) fibers. Soda pulping at 170°C and 7.5% active alkali effectively isolated the individual plant fibers. However, additional pre-treatment methods are recommended for commercial pulping purposes due to the plant material's high ash content. The pulping yields were high, but the pulp still had a considerably high lignin content, so optimization of the process is needed. Bleaching conditions using 5.25% sodium hypochlorite were effective in further lignin removal, which was necessary for producing microfibrillated cellulose (MFC) and using friction grinding. MFC yields were 87.53%. Scanning electron microscopy supported that microfibrillation occurred and that the MFC had fiber widths of 3 μm. The MFC produced was successfully incorporated into the hand sheets made from Bakong pulp. The MFC was added at 2, 6, and 10% w/w, and it was observed that the burst and tensile indices of the pulp slightly decreased with increasing MFC loading. However, the tear index was greatly improved, and compared to commercial printing paper, the MFC-reinforced Bakong pulp had desirable properties at 6% w/w loading. Bakong pulp is a suitable candidate for use as an alternative to wood pulp in papermaking. Moreover, MFC from Bakong pulp may be used as an additive to commercial pulp to improve its tear resistance, but this requires further study. Overall, the Bakong fibers showed promise as a source of pulp for both microcellulose production and papermaking. The MFC yields were relatively high, and the hand sheets had good mechanical properties.

ACKNOWLEDGEMENTS

The author acknowledges the University of the Philippines Los Baños (UPLB) and the Department of Science and Technology - Forest Products Research and Development Institute (DOST-FPRDI), Philippines for providing the facilities for experiments and testing. The author also acknowledges the Design Center of the Philippines for providing the Bakong fiber samples used in this study.

REFERENCES

Balea, A., Fuente, E. Monte, M. C., Merayo, N., Campano, C., Negro, C., & Blanco, A. (2020). Industrial application of nanocelluloses in papermaking: A review of challenges, technical solutions, and market perspectives. *Molecules*, *25*(3), 526. https://doi.org/10.3390/molecules25030526

Biermann, C. J. (1996). *Handbook of pulping and papermaking* (2nd ed.). Academic Press.

Borela, V. T., Urbano, J. A., Tayag, A. J., & Teresa, M. G. (2021). Antibacterial property of *Hanguana malayana* (Bakong) crude leaf ethanolic extract against *Staphylococcus aureus*. *International Journal Papier Advance and Scientific Review*, *2*(1), 1-5. https://doi.org/10.47667/ijpasr.v2i1.25

Choe, J. Y., Yusof, K. M. K. K., & Rohani, S. (2023). A raw data on the physico-chemical water parameters and sedimentation rates of two different aquatic macrophytes in Tasik Berombak, Malaysia. *Data in Brief*, *49*, 109397. https://doi.org/10.1016/j.dib.2023.109397

Dai, Q. (2001). *Influence of extractives on the bleachability of batch extended delignified Kraft pulps*. [Unpublished doctoral dissertation]. North Carolina University.

Design Center of the Philippines (2022). *Bakong*. Philippine Department of Trade and Industry. https://bakong.carrd.co/

El-Sayed E. S. A., El-Sakhawy, M., & El-Sakhawy, M. A. (2020). Non-wood fibers as raw material for pulp and paper industry. *Nordic Pulp & Paper Research Journal*, *35*(2), 215-230. https://doi.org/10.1515/npprj-2019-0064

Fernandez, R. (2018, August 13). DOST finds abaca, other fibers viable for banknotes. *The Philippine Star*. https://www.philstar.com/headlines/2018/08/13/1842083/dost-finds-abaca-other-fibers-viable-banknotes

Hollertz, R., Duran, V. L., Larsson, P. A., & Wagberg, L. (2017). Chemically modified cellulose micro- and nanofibrils as paper-strength additives. *Cellulose*, *24*, 3883-3899. https://doi.org/10.1007/s10570-017-1387-6

Jimenez, L., Ramos, E., Rodriguez, A., De La Torre, M. J., & Ferrer, J. L. (2005). Optimization of pulping conditions of abaca: An alternative raw material for producing cellulose pulp. *Bioresource Technology*, *96*, 977-983. https://doi.org/10.1016/j.biortech.2004.09.016

Kargarzadeh, H., Ioelovich, M., Ahmad, I., Thomas, S., & Dufresne, A. (2017). Methods for extraction of nanocellulose from various sources. In H. Kargarzadeh, I. Ahmad, S. Thomas & A. Dufresne (Eds.), *Handbook of nanocellulose and cellulose nanocomposites* (pp. 1-49). Wiley-VCH.

Lehr, M., Miltner, M., & Friedl, A. (2021). Removal of wood extractives as pulp (pre-) treatment: A technological review. *SN Applied Sciences*, *3,* 886. https://doi.org/10.1007/s42452-021-04873-1

Moral, A., Aguado, R., Tijero, A., Tarres, Q., Delgado-Aguilar, M., & Mutje, P. (2017). High-yield pulp from *Brassica napus* to manufacture packaging paper. *BioResources*, *12*(2), 2792-2804. https://doi.org/10.15376/biores.12.2.2792-2804

PITA Raw Materials Working Group (2005). *PITA guide to commonly used test methods for paper and board*. The Paper Industry Technical Association.

Plazonic, I., Barbaric-Mikocevic, Z., & Antonovic, A. (2016). Chemical composition of straw as an alternative material to wood raw material in fibre isolation. *Drvna Industrija*, *67*(2), 119-125. https://doi.org/10.5552/drind.2016.1446

Viana, L., Potulski, D., Muniz, G., Andrade, A., & Silva, E. (2018). Nanofibrillated cellulose as an additive for recycled paper. *Cerne*, *24*(2), 140-148. https://doi.org/10.1590/01047760201824022518

Wunna, K., Nakasaki, K., Auresenia, J. L., Abella, L. C., & Gaspillo, P. D. (2017). Effect of alkali pretreatment on removal of lignin from sugarcane bagasse. *Chemical Engineering Transactions*, 56, 1831-1836. https://doi.org/10.3303/CET1756306

Yuanita, E., Pratama, J. N., Mustafa, J. H., & Chalid, M. (2015). Multistages preparation for microfibrillated celluloses on Arenga Pinnata "ijuk" fiber. *Procedia Chemistry*, 16, 608-615. https://doi.org/10.1016/j.proche.2015.12.099

Pertanika J. Sci. & Technol. 32 (S3): 27 - 39 (2024)

PERTANIKA JOURNALS

SCIENCE & TECHNOLOGY

Journal homepage: http://www.pertanika.upm.edu.my/

The Effects of Autohydrolysis Pretreatment on the Properties of OPT Pulps for the Production of Dissolving Pulp

Natra Joseph[1], Mohamad Haafiz Mohamad Kassim[1], Mazlan Ibrahim[1], Nurul Fazita Mohammad Rawi[1], Kumar Sudesh[2], Takamitsu Arai[3], Akihiko Kosugi[3] and Leh Cheu Peng[1*]

[1]Division of Bioresource Technology, School of Industrial Technology, Universiti Sains Malaysia, 11800, USM, Penang, Malaysia

[2]School of Biological Sciences, Universiti Sains Malaysia, 11800, USM, Penang, Malaysia

[3]Japan International Research Center for Agricultural Sciences (JIRCAS), 1-1 Owashi, Tsukuba 305-8686, Ibaraki, Japan

ABSTRACT

This preliminary study investigated an environmentally friendly method for fabricating cellulose-rich dissolving pulp from Oil Palm (*Elaeis guineensis*) Trunk (VBOPT) fibre. This method encompassed an autohydrolysis pretreatment followed by soda pulping procedures. The impact of autohydrolysis pretreatment on the separation of lignocellulosic components was scrutinised to facilitate the production of chemical cellulose. Autohydrolysis was performed on VBOPT fibre for 60 min at temperatures ranging from 140°C to 160°C, maintaining a solid-to-liquid ratio of 1:8. The yield of the prehydrolysed OPT varied between 73.5% and 91.5%. The chemical composition of the prehydrolysed VBOPT fibre comprised 70.6–80.0% holocellulose, 63.7–87.1% α-cellulose, 7.4–10.9% ß-cellulose, 5.5–25.4% γ-cellulose, and 21.5–26.6% lignin. The prehydrolysed OPT was subsequently subjected to alkaline pulping under fixed conditions: a temperature of 160°C, a treatment time of 60 min, a chemical charge of 25%, and a solid-to-liquid ratio of 1:6. The resultant pulp exhibited properties such as a screening yield of 41.5–46.4%, a kappa number of 4.5–9.6, and α, β, and γ cellulose content of 89.4– 98.1%, 1.5–5.3%, and 0.4–6.9%, respectively. Based on the chemical composition of the OPT biomass before and after pretreatment, as well as post-alkaline cooking, the autohydrolysis pretreatment

ARTICLE INFO

Article history:
Received: 22 February 2024
Accepted: 30 May 2024
Published: 30 July 2024

DOI: https://doi.org/10.47836/pjst.32.S3.03

E-mail addresses:
jsnatra@gmail.com / jsnatra@student.usm.my (Natra Joseph)
mhaafiz@usm.my (Mohamad Haafiz Mohamad Kassim)
maz@usm.my (Mazlan Ibrahim)
fazita@usm.my (Nurul Fazita Mohammad Rawi)
ksudesh@usm.my (Sudesh Kumar)
tkarai@affrc.go.jp (Takamitsu Arai)
akosugi@affrc.go.jp (Akihiko Kosugi)
cpleh@usm.my (Leh Cheu Peng)
*Corresponding author

ISSN: 0128-7680
e-ISSN: 2231-8526

was determined to significantly influence the resultant pulp. A more comprehensive understanding of the interdependence of autohydrolysis and pulping processes can be achieved by executing an optimisation study focusing on key parameters of autohydrolysis and pulping, including temperature, treatment duration, and chemical charge.

Keywords: Autohydrolysis, dissolving pulp, non-wood biomass, oil palm trunk, soda pulping

INTRODUCTION

Dissolving grade pulp is a cellulose-rich pulp normally known as dissolving pulp or chemical cellulose. Distinct from papermaking grade pulp, dissolving pulp possesses a higher level of cellulose purity with α-cellulose content of 90–98%, relatively low hemicellulose (<5%), less than 1% lignin and less than 0.1% ash content (Andrade & Colodette, 2014; Biermann, 1996). Dissolving pulp is commonly used by dissolving it in certain chemical solutions or undergoing chemical modification to produce regenerated cellulose (such as viscose rayon, cellophane, cellulose hydrogel) and cellulose derivatives including cellulose esters (e.g. cellulose acetates and cellulose nitrates) and cellulose ethers (e.g. methylcellulose, carboxymethyl- and ethyl-cellulose) and other cellulose-based products such nano- and micro-crystalline cellulose) (Chen et al., 2016; Miao et al., 2014; Sixta et al., 2013).

In recent years, there has been a significant increase in the production of dissolving pulp, driven by strong market demand growth. The dissolving pulp production in 2020 was 8.86 million tons. It is expected to grow at a compound annual growth rate (CAGR) of 6.22% from 2020 to 2027, about 73% higher than papermaking pulp (CAGR of 3.6%). The rapid growth of dissolving pulp in the global market causes the demand for its primary sources, conventional pulp wood (both hardwoods and softwoods) and cotton linter, to rise, as well as their market price.

On the other hand, in the bioeconomy era, it is anticipated that the utilisation of dissolving pulp will experience a significant increase due to its prominence as a sustainable and renewable resource, primed to replace petroleum-based resources in the production of various commodities, chemicals and energy. Efforts are ongoing to explore new alternative sources for producing dissolving pulp to undertake the expected expanding demand (Batalha et al., 2012). Numerous potential non-wood biomass, including from agricultural residues (e.g. empty fruit bunch (EFB), plant stalks, tobacco and corn, sugarcane bagasse and grain straw, rice, and wheat), naturally growing plant (e.g. bamboo and dhaincha) and industrial crops (e.g. jute, and kenaf) have been subjected to investigation (Andrade & Colodette, 2014; Batalha et al., 2012; Behin & Zeyghami, 2009; Chen et al., 2016; Huang et al., 2019; Jahan et al., 2007; Sarkar et al., 2021; Wan Rosli et al., 2003). The production of dissolving pulp made from bamboo has already been successfully commercialised.

Among all the vegetable oil productions, palm oil contributes to the biggest world market, accounting for 35.7% (79.5 million tonnes) of the total global vegetable oil production (217.5 million tonnes). Malaysia is one of the largest palm oil producers in the world, standing as the second-largest oil palm producer (19 million tonnes), following Indonesia (47 million tonnes), with a harvested area covering approximately 5.65 million hectares. Based on Market Analysis Report (2024), the global palm oil market will be increased at a CAGR of 5.5% from 2024 to 2030. It indicated that the byproduct or processing waste from the oil palm industry would increase significantly (Ishak et al., 2021), which includes oil palm trunk (OPT), oil palm fronds (OPF), empty fruit bunches (EFB), and mesocarp fibres. Bukhari et al. (2018) reported that the oil palm industry generates about 85 million tons of lignocellulosic biomass residues annually from plantation and milling activities.

In general, oil palm fruits can be harvested after three years post-planting and reach maximum yield in the 12^{th}–13^{th} year of their 25-year lifespan (Abdullah & Sulaiman, 2013). When the oil palm trees reach the unproductive stage, replantation becomes necessary. It is estimated that 74.5 tonnes of OPT per hectare (on a dry-weight basis) will be generated in replantation areas. Based on an annual replantation rate of 5% of the current plantation areas, about 21 million tonnes of felled OPT would be available (Bukhari et al., 2018). Under the common practice, felled OPT is left within the plantation area for natural decomposition. However, this method of decomposing takes about five to six years to fully decompose the felled OPT, posing challenges to replanting activities and attracting insect pests, which may inhibit the growth of new trees. Besides, open burning is a ban imposed by the Malaysian Government in 1998 (A1102 Act/Environment Quality Act 2001) due to environmental pollution issues (ASEAN, 2003); thus, burning of felled OPT within the plantation should not be a viable option for managing this biomass waste. Thus, the prudent approach to handle this massive biomass is to convert it into value-added products.

A previous study reported that OPT comprises 62% vascular bundles; the remaining percentage is parenchyma. Chemical composition analysis of the vascular bundles revealed that they consist of 56.91% cellulose, 25.47% hemicellulose, 11.91% lignin and 15.33% extractive (Lamaming et al., 2015). Given its high cellulose content, comparable to bamboo, vascular bundles of OPT present great potential as an alternative source for producing dissolving cellulose.

The conventional methods for producing dissolving pulp from pulpwood include the acid sulphite pulping process and the prehydrolysis kraft pulping process. However, both processes raise environmental concerns due to the emission of sulphur-containing compounds, such as sulphur dioxide (SO_2), which can lead to acid rain formation. Considering this concern, adopting sulphur-free pulping should be a priority, particularly when utilising non-wood biomass for dissolving pulp production. Different from

papermaking pulp production, the attainment of high-purity α-cellulose is critical in producing dissolving pulp, where non-cellulose impurities, besides lignin, hemicellulose (γ-cellulose), and even degraded cellulose (β-cellulose), can significantly impose negative impacts on its application. Owing to the amorphous nature and low degree of polymerisation (200–300) of branched hemicellulose, acidic pretreatment before alkaline pulping can effectively eliminate it.

This study evaluates the feasibility of utilising vascular bundles of OPT to produce dissolving pulp. Moreover, environmentally sustainable processes are implemented to ensure commercial viability, incorporating non-toxic chemicals and diminishing chemical consumption. Therefore, water hydrolysis, also known as autohydrolysis, is adopted in conjunction with soda-pulping. Since autohydrolysis is a process solely utilising water at elevated temperatures to treat the biomass to remove hemicellulose through the catalytic effect of the self-generated organic acids, it enhances sustainability. As a preliminary investigation, this study aims to examine the effects of autohydrolysis pretreatment parameters on subsequent soda pulp properties. Hence, the result of this study is expected to provide fundamental insight into autohydrolysis pretreatment towards OPT, of the potential to maximise yields and α-cellulose content and minimise kappa number and ash content in the resultant pulp.

MATERIALS AND METHODS

Materials

Kluang Pilot Plant, Johor, Malaysia, provided the oil palm trunk (OPT) vascular bundles (VBOPT). The raw OPT, collected from a palm oil plantation, underwent an OPT fibre extraction process, which included chipping, screw pressing, drying, and vascular bundles-parenchyma separation processes. To enhance the purity of the vascular bundle used in this study, the VBOPT received was further sieved to remove the residual parenchyma portion.

Experimental

Autohydrolysis Pretreatment

All autohydrolysis experiments utilised a stationary, 4-litre stainless-steel digester produced by NAC Autoclave Co. Ltd., Japan. The digester was equipped with a computer-controlled thermocouple and did not have external circulation mixing. The autohydrolysis was conducted by inserting 350 g (on a dry weight basis) of VBOPT into the digester vessel, and water was added at a liquor-to-material ratio of 8:1. The reaction temperature was maintained within a required range of 140–160°C for 60 min. Upon completing the autohydrolysis process, the autohydrolysed VBOPT was rinsed in a stainless-steel mesh filter, spin-dried, kept in a sealed plastic bag, and subsequently stored in a refrigerator at

4°C for future use. The spent liquor was collected for pH assessment, and the yield was calculated based on the oven-dried fibre.

Soda Pulping

The soda pulping of prehydrolysed VBOPT was carried out in the same digester described earlier (autohydrolysis). An amount of 200 g (on a dry weight basis) of prehydrolysed VBOPT was cooked at a constant liquor-to-fibre ratio of 6:1 and a time-to-maximum temperature of 90 min, time-at-temperature of 60 min for a reaction temperature of 160°C using 25% alkali charge based on the dry weight of prehydrolysed VBOPT. After the pulping process, the resulting pulps and spent liquor were collected. The spent liquor was tested for pH, and the obtained pulp was disintegrated with a tri-blade mixer for 1 min at a pulp consistency of 2.0%. Subsequently, the pulps were screened using Somerville Screener with a flat-plate screen with a slit width of 0.15 mm. The yield was quantified based on dry weight basis.

Chemical Composition Analysis

The air-dried untreated and prehydrolysed VBOPTs were prepared by grinding into small particles using a RETSCH cutting mill SM100 and sieving into a range of size of (0.595–0.25 mm) by passing through a 35–60 mesh pore size. The chemical compositions of the untreated VBOPT and parenchyma cell (in powder form), prehydrolysed VBOPT, and prehydrolysed-soda pulp were examined according to standard test methods as follows: The extractive-free untreated VBOPT was prepared following the TAPPI 24 cm - 97 method with slight modifications, wherein ethanol-toluene served as the solvent for the extraction. However, this procedure was not applied to the prehydrolysed VBOPT because, during the autohydrolysis pretreatment, most of the organic compounds soluble in organic solvent could have degraded and been removed at elevated temperatures. Applying an organic solvent to biomass would likely result in higher extractive content than the original biomass, as the lignocellulosic composition, which experienced structural changes, may also dissolve in the solvent.

Thus, this procedure could yield faulty results for chemical composition analyses. The lignin content of untreated and prehydrolysed VBOPT was determined following TAPPI 222 om-02—Acid Insoluble Lignin, while the kappa number of prehydrolysed-soda pulp was evaluated according to TAPPI-236—Kappa Number of Pulp. The cellulosic contents viz. holocellulose, α-cellulose, β-cellulose, and γ-cellulose were examined using methods described by Wise et al. (1946) and the Japanese Standard Method JIS 8101 methods, respectively. All analyses were performed in triplicate, and results were presented in mean with standard deviation. Equations 1–9 correspond to the calculation in Tables 2 and 3. The flowchart with the process condition of this research work is shown in Figure 1.

For untreated biomass:

$$(\alpha, \beta, \gamma)\ Cellulose_{UTB\ basis}\ of\ UTB\ (\%) = (\alpha, \beta, \gamma)_{UTB,}\ (\%) \times Holocellulose_{UTB},\ (\%)/100 \quad \text{Eq. 1}$$

For pretreated biomass:

$$Holocellulose_{UTB\ basis}\ (\%) = Holocellulose_{PTB}(\%) \times (Yield_{PTB},\ \%/100) \quad \text{Eq. 2}$$

$$(\alpha, \beta, \gamma)\ Cellulose_{PTB\ basis}\ (\%) = (\alpha, \beta, \gamma)_{PTB,}\ (\%) \times Holocellulose_{PTB},\ (\%)/100 \quad \text{Eq. 3}$$

$$(\alpha, \beta, \gamma)\ Cellulose_{UTB\ basis}\ (\%) = (\alpha, \beta, \gamma)_{PTB,}\ (\%) \times Yield_{PTB},\ (\%)/100 \quad \text{Eq. 4}$$

$$Klason\ lignin\ _{UTB\ basis}\ (\%) = Klason\ lignin_{PTB,}\ (\%) \times (Yield_{PTB},\ (\%)/100) \quad \text{Eq. 5}$$

Reduction of γ cellulose content, (%)

$$= \frac{[\gamma\ Cellulose_{UTB\ basis}\ of\ UTB(\%) - \gamma\ Cellulose_{UTB\ basis}\ of\ PTB\ (\%)]}{[\gamma Cellulose_{UTB\ basis}\ of\ UTB\ (\%) \times 100]} \quad \text{Eq. 6}$$

Reduction of Klason Lignin, (%)

$$= \frac{[Klason\ lignin_{UTB\ basis}\ of\ UTB, (\%) - Klason\ lignin_{UTB\ basis}\ of\ PTB, (\%)]}{[Klason\ lignin_{UTB\ basis}\ of\ UTB\ (\%) \times 100]} \quad \text{Eq. 7}$$

For autohydrolysed-soda pulp:

$$(\alpha, \beta, \gamma)\ Cellulose_{PTB\ basis}\ (\%) = (\alpha, \beta, \gamma)_{PTSP}\ (\%) \times Screen\ Yield,\ (\%)/100 \quad \text{Eq. 8}$$

$$(\alpha, \beta, \gamma)\ Cellulose_{UTB\ basis}\ (\%) = (\alpha, \beta, \gamma)_{PTSP}\ (\%) \times Screen\ Yield_{UTB}\ (\%)/100 \quad \text{Eq. 9}$$

UTB = Untreated biomass
PTB = Pretreated biomass
UTB basis = Based on untreated biomass
PTB basis = Based on pretreated biomass
PTSP = Pretreated biomass-soda pulp

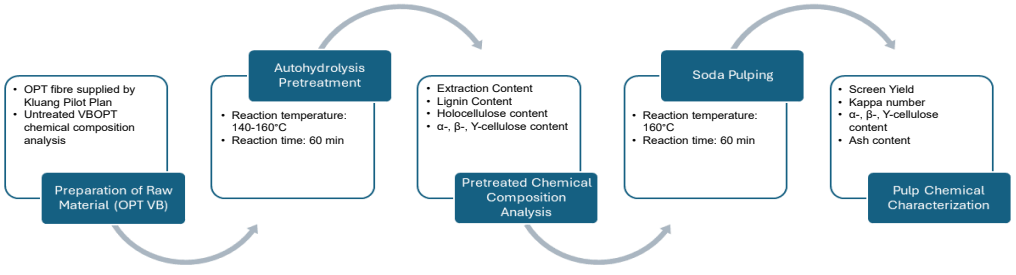

Figure 1. The flowchart with process condition of the research work

RESULTS AND DISCUSSIONS

Chemical Composition Analyses of Oil Palm Trunk

In contrast to wood, OPT, as a non-wood biomass, appears in two distinct fractions after milling: the hard woody vascular bundles particles and the powder-like parenchyma cells,

including a minor portion of other softer tissue components. Figure 2 shows the vascular bundles and residual parenchyma cells separated from the raw sample of vascular bundles received from the factory. The chemical compositions of these two factions are presented in Table 1. The results reveal that the vascular bundle faction contains lower percentages of extractive (4.1%) and lignin (19.3%) contents but higher holocellulose content (79.4%) compared to parenchyma cells, which exhibits percentages of 6.4%, 23.2% and 76.5%, respectively.

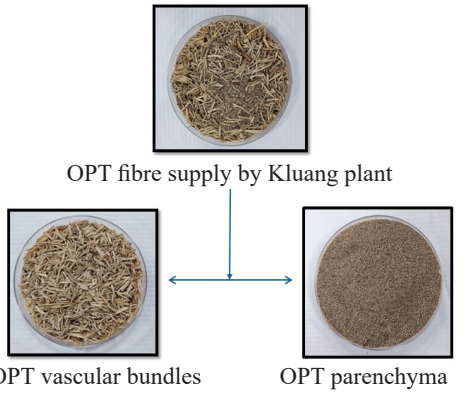

Figure 2. OPT Vascular bundles and parenchyma cells separated from OPT fibre supplied by Kluang Pilot Plant

Moreover, one can see that the vascular bundles show a higher cellulose content (a total of α-cellulose and β-cellulose) (60.0%) and lower hemicellulose content (γ-cellulose) (40.0%) in comparison to the parenchyma cells (48.8% and 51.2%, respectively). The findings suggested that the vascular bundles of OPT (VBPOT) demonstrated high potential as raw material for dissolving pulp production. The segregation of residual parenchyma cells from the VBOPT could improve the pulping efficiency because parenchyma cells will require higher pulping chemicals and result in lower pulp yield. Parenchyma cells exhibit a high affinity to absorb chemicals and are easily degraded due to their size and thin cell wall structure (Paul & Kasiviswanathan, 1998).

Table 1
Chemical composition of OPT fibre (vascular bundles and parenchyma)

Chemical composition	Vascular bundles	Parenchyma
Extractives*, %	4.1±0.4	6.4±1.0
Holocellulose§	82.7±0.9	81.7±1.0
Holocellulose*, %	79.4	76.5
α- Cellulose#, %	54.8±0.5	45.0±0.2
β- Cellulose#, %	5.2±0.3	3.8±0.8
γ- Cellulose#, %	40.0±0.3	51.2±0.9
Lignin content §, %	20.1±0.2	24.8±0.4
Lignin content*, %	19.3	23.2

§ Percentage calculated based on extractive-free biomass
* Percentage calculated based on original biomass
# Percentage calculated based on holocellulose

Effect of Autohydrolysis Pretreatment on VBOPT

The effects of autohydrolysis at varying temperatures on the properties of VBOPT are detailed in Table 2. Autohydrolysis is an effective pretreatment of biomass utilising only water at elevated temperatures to hydrolyse and remove hemicellulose. Notably, the pH of the spent liquor decreased from 3.84 to 3.42 (equivalent to about 0.0013 M to 0.0085 M of acetic acid) as temperature increased from 140ºC to 160ºC. During autohydrolysis, biomass is heated to an elevated temperature (140ºC and higher) within a closed system to achieve high pressure. Under this condition, water produces hydronium ion (H_3O^+), which penetrates the biomass, causing the degradation of the susceptible component—primarily amorphous hemicellulose. As a result, its principal functional group—acetyl group, undergoes hydrolysis and releases acetic acid (Carvalheiro et al., 2016).

A minor quantity of formic acid is also formed from carbohydrate-degradation products in biomass (Chen, 2015). The release of these organic acids catalyses further hemicellulose hydrolysis, resulting in the liberation of more organic acids, including simple sugars. Hence, the drop in pH of spent liquor can be attributed to the generation of more acid (Alén, 2015), while an increase in temperatures promoted greater acetic acid release.

Table 2
Chemical composition of prehydrolysed vascular bundles of OPT

Chemical composition	Prehydrolysed VBOPT		
	140°C	150°C	160°C
Spent liquor pH	3.8±0.1	3.7±0.0	3.4±0.0
Solid yield, %	91.5±1.5	82.7±1.0	73.5±1.3
Extractives, %	-	-	-
Holocellulose, %			
PTB basis	80.0±0.5	77.6±1.0	70.6±1.3
UTB basis	73.2	64.2	51.9
α- Cellulose, %			
Based on holocellulose	63.7±1.0	71.5±0.5	87.1±0.7
PTB basis	51.0	55.4	61.5
UTB basis	46.6	45.9	45.2
β- Cellulose, %			
Based on holocellulose	10.9±0.5	8.4±0.6	7.4±0.5
PTB basis	8.7	6.5	5.2
UTB basis	8.0	5.4	3.8
γ- Cellulose, %			
Based on holocellulose	25.4±0.5	20.1±1.5	5.5±0.7
PTB basis	20.3	15.6	3.9
UTB basis	18.6	12.9	2.9
Reduction	43.8	61.0	91.2
Klason lignin, %			
PTB basis	21.5±1.5	23.6±0.3	26.6±0.5
UTB basis	19.7	19.5	19.6

PTB basis: calculated based on pretreated vascular bundles, UTB basis: calculated based on untreated vascular bundles

The declining trend in the solid yield with the increased autohydrolysis temperature implies that more components in VBOPT were degraded and dissolved. Although based on the holocellulose content, it is obvious that the loss of biomass is mainly attributed to the carbohydrate component. The substantial decrease of γ-cellulose content (hemicellulose) in the holocellulose from 40.0% (or 33.1% based on original biomass) to 25.4% (18.6%), 20.1% (12.9%) and 5.5% (2.9%) when the autohydrolysis temperature were 140ºC, 150ºC and 160ºC, respectively (Nguyen & Trinh, 2022; Peng et al., 2019).

It is very interesting to see that by subjecting the VBOPT to a temperature of 160°C for 60 min, the reduction of hemicellulose was achieved up to 91.2% (Table 2), followed by 61.0% under 150ºC and 43.8% under 140ºC. By correlating the decline in pH of spent liquor to the efficiency of hemicellulose removal, it is agreeable that by determining the pH of the autohydrolysis spent liquor, one can anticipate the efficiency of hemicellulose elimination.

Since the percentages of other types of cellulose (α- & β-celluloses) are interdependent with γ-cellulose, the reduction in the latter will increase the percentage of α-cellulose. The implication of simple autohydrolysis as pretreatment of VBOPT prior to the soda pulping process, even at 140ºC, possesses a significant effect on increasing the cellulose content (63.7%), with the highest achieved under 160ºC (87.1%).

One more attractive point to highlight is the increase of lignin content from 21.5% to 26.6% (based on prehydrolysed VBOPT) when the autohydrolysis temperature increased from 140ºC to 160ºC. The increase of lignin content in the prehydroylsed VBOPT is mainly due to the loss of holocellulose content, which is more prominent in the delignification reaction. As demonstrated in Table 2, when the lignin content is quantified based on untreated original biomass, the lignin contents were in the range of 19.5–19.7%, which is slightly lower than the VBOPT's lignin content counted based on extractive-free biomass (20.1%).

The finding agrees with a recent review conducted by Lu et al. (2021); it was discovered that only a minimal amount of lignin was removed from the biomass after undergoing autohydrolysis pretreatment. According to previous researchers, lignin undergoes fluidisation within the temperature range of approximately 120–200°C. During high-temperature pre-treatments, the fluidised lignin coalesces into smaller particles, separating from the cellulose and moving from the native cell wall to the bulk liquid phase. As the coalesced lignin solidifies upon cooling, it re-deposits on the surface of the biomass. This results in a biomass with an enriched surface lignin. It is important to note that this process does not remove lignin from the biomass but instead re-allocates it (Donohoe et al., 2008; Kristensen et al., 2008; Takada et al., 2019).

Effect of Autohydrolysis Pretreatment on Pulp Properties

The three prehydrolysed VBOPTs (PVB) treated under varying autohydrolysis temperatures and untreated VBOPT (UVB) were cooked using a soda pulping process to produce pulp. Based on the data obtained (Table 3), prehydrolysed-soda pulping, even the one treated at 140ºC produced pulp (PVB140) approaching dissolving properties with 89.4% α-cellulose and 5.3% of γ-cellulose compared to the pulp produced without undergoing prehydrolysis (87.2% and 12.1%, respectively). The significant effects of autohydrolysis were clearly shown by PVB160 (prehydrolysis under 160ºC), where its α-cellulose content was 98.1% while γ-cellulose was less than 0.5%.

On the other hand, all the kappa numbers of pulp produced from prehydrolysed VBOPT were below 10.0. It indicated that prehydrolysed lignin was more easily degraded by the subsequent soda pulping process. It might be due to the hydrolysis of biomass increasing the hydroxyl group in lignin and thus enhancing the delignification during the alkaline pulping process. Nevertheless, since the prehydrolysis process will enhance the dissolution of the biomass during the pulping process due to the removal of the remaining hemicelluloses and lignin, yield losses are attributed to it. The calculated pulp yield is based on the untreated original biomass shown in Table 3. The dissolving pulp produced from VBOPT is 30.5–35.4, within the range of the dissolving pulp yield produced from pulpwood. These analyses show that the autohydrolysis-soda process was beneficial to the pulping of VBOPT. However, extensive investigation is needed to determine the optimum autohydrolysis-soda pulping condition.

Table 3
Characteristics of untreated OPT-soda pulp and prehydrolysed VBOPT-soda pulp

Soda Pulping Condition	160°C, 60 min, 25% of NaOH			
Pulp Properties	UVB	PVB		
		140°C PVB140	150°C PVB150	160°C PVB160
Screen yield, %	32.0±0.7	46.4±0.9	42.8±0.4	41.5±1.5
Yield based on UTB, %	32.0	42.5	35.4	30.5
α-Cellulose, %	87.2±0.2	89.4±1.1	90.8±0.2	98.1±0.5
β-Cellulose, %	0.8±0.2	5.3±1.0	2.4±0.8	1.5±0.1
γ-Cellulose, %	12.1±0.8	5.3±0.7	6.9±0.5	0.4±1.1
Kappa number	12.0±0.6	9.6±1.3	6.4±0.7	4.5±0.1

UVB: untreated vascular bundles, PVB: pretreated vascular bundles

In this study, the autohydrolysis-soda process shows excellent potential for utilising the vascular bundles of the oil palm trunk to produce dissolving pulp. Autohydrolysis pretreatment at an elevated temperature of 160°C eliminated hemicellulose from the

biomass. Therefore, the subsequent soda pulping can produce dissolving grade pulp with very high α-cellulose content and low hemicellulose and lignin content. Statistical analysis and optimisation of the process conditions should be conducted to further understand the interactive effects of the autohydrolysis and soda pulping process parameters.

ACKNOWLEDGEMENT

Sincere gratitude for the support the Science and Technology Research Partnership for Sustainable Development (SATREPS) provided in collaboration with Universiti Sains Malaysia (203/PTEKIND/67811002) for this project. SATREPS is a Japanese government program that promotes international joint research. It is structured as a collaboration between the Japan Science and Technology Agency (JST) and the Japan International Cooperation Agency (JICA).

REFERENCES

Abdullah, N., & Sulaiman, F. (2013). The oil palm wastes in Malaysia. In M. D. Matovic (Ed.), *Biomass now: Sustainable growth and use* (pp. 75-100). InTech. https://doi.org/10.5772/55302

Alén, R. (2015). Pulp mills and wood-based biorefineries. In A. Pandey, R. Hofer, M. Taherzadeh, K. M. Nampoothiri & C. Larroche (Eds.), *Industrial biorefineries and white biotechnology* (pp 91-126). Elsevier. https://doi.org/10.1016/B978-0-444-63453-5.00003-3

Andrade, M. F., & Colodette, J. L. (2014). Dissolving pulp production from sugar cane bagasse. *Industrial Crops and Products*, *52*, 58–64. https://doi.org/10.1016/j.indcrop.2013.09.041

ASEAN. (2003). *Guidelines for the implementation of the ASEAN Policy on Zero Burning.* ASEAN Secretariat. https://asean.org/wp-content/uploads/2003/08/Guidelines-for-the-Implementation-of-the-asean-policy-on-zero-burning.pdf

Batalha, L. A. R., Colodette, J. L., Gomide, J. L., Barbosa, L. C. A., Maltha, C. R. A., & Gomes, F. J. B. (2012). Dissolving pulp production from bamboo. *BioResources*, *7*(1), 640–651. https://doi.org/10.15376/biores.7.1.0640-0651

Behin, J., & Zeyghami, M. (2009). *Dissolving pulp from corn stalk residue and wastewater of Merox unit*. *Chemical Engineering Journal*, *152*, 26–35. https://doi.org/10.1016/j.cej.2009.03.024

Biermann, C. J. (1996). *Handbook of Pulping and Papermaking* (2nd ed.). Elsevier Science Publishing.

Bukhari, N. A., Loh, S. K., Bakar, N. A., & Jahim, J. M. (2018). Lignocellulose-derived sugar from oil palm biomass. *Palm Oil Eng. Bull*, *126*, 25-36.

Carvalheiro, F., Duarte, L. C., Gírio, F., & Moniz, P. (2016). Hydrothermal/liquid hot water pretreatment (autohydrolysis): A multipurpose process for biomass upgrading. In S. I. Mussatto (Ed.), *Biomass fractionation technologies for a lignocellulosic feedstock based biorefinery* (pp. 315-348). Elsevier Science Publishing. https://doi.org/10.1016/B978-0-12-802323-5.00014-1

Chen, H. (2015). *Lignocellulose Biorefinery Engineering*: Principles and applications. Elsevier Science Publishing. https://doi.org/10.1016/B978-0-08-100135-6.00003-X

Chen, C., Duan, C., Li, J., Liu, Y., Ma, X., Zheng, L., Stavik, J., & Ni, Y. (2016). Cellulose (dissolving pulp) manufacturing processes and properties: A mini-review. *BioResources*, *11*(2), 5553–5564. https://doi.org/10.15376/biores.11.2.Chen

Donohoe, B. S., Decker, S. R., Tucker, M. P., Himmel, M. E., & Vinzant, T. B. (2008). Visualizing lignin coalescence and migration through maize cell walls following thermochemical pretreatment. *Biotechnology and Bioengineering, 101*(5), 913–925. https://doi.org/10.1002/bit.21959

Huang, C., Sun, R., Chang, H. M., Yong, Q., Jameel, H., & Phillips, R. (2019). Production of dissolving grade pulp from tobacco stalk through SO2-ethanol-water fractionation, alkaline extraction, and bleaching processes. *BioResources*, *14*(3), 5544-5558. https://doi.org/10.15376/biores.14.3.5544-5558

Ishak, M. T. B., Hashim, N. I. B., Hashim, F. R. B., Ibrahim, R. B., & Abd Rahman, R. (2021). Study the properties of mixed kenaf and Empty Fruit Bunch (EFB) oil palm fibre insulation paper. In *2021 3rd International Conference on High Voltage Engineering and Power Systems (ICHVEPS).* (pp. 318-322). IEEE. https://doi.org/10.1109/ichveps53178.2021.9600938.

Jahan, M. S., Chowdhury, D. N., & Islam, M. K. (2007). Pulping of dhaincha (*Sesbania aculeata*). *Cellulose Chemistry & Technology*, *41*(7), 413.

Kristensen, J. B., Thygesen, L. G., Felby, C., Jørgensen, H., & Elder, T. (2008). Cell-wall structural changes in wheat straw pretreated for bioethanol production. *Biotechnology for Biofuels, 1*, 1-9. https://doi.org/10.1186/1754-6834-1-5

Lamaming, J., Hashim, R., Sulaiman, O., Leh, C. P., Sugimoto, T., & Nordin, N. A. (2015). Cellulose nanocrystals isolated from oil palm trunk. *Carbohydrate Polymers*, *127*, 202–208. https://doi.org/10.1016/j.carbpol.2015.03.043

Lu, Y., He, Q., Fan, G., Cheng, Q., & Song, G. (2021). Extraction and modification of hemicellulose from lignocellulosic biomass: A review. *Green Processing and Synthesis*, *10*(1), 779-804.

Miao, Q., Chen, L., Huang, L., Tian, C., Zheng, L., & Ni, Y. (2014). A process for enhancing the accessibility and reactivity of hardwood kraft-based dissolving pulp for viscose rayon production by cellulase treatment. *Bioresource Technology*, *154*, 109–113. https://doi.org/10.1016/j.biortech.2013.12.040

Nguyen, A. Q., & Trinh, L. T. P. (2022). Thermochemical conversion of cellulose and hemicellulose. In N. P. Nghiem, T. H. Kim, & C. G. Yoo (Eds.), Biomass utilization: Conversion strategies (pp. 107–131). Springer International Publishing. https://doi.org/10.1007/978-3-031-05835-6_6

Paul, S. K., & Kasiviswanathan, K. S. (1998). Influence of pith on bagasse pulp, paper and black liquor properties. *IPPTA, 10*(3), 1-8.

Peng, X., Du, F., & Zhong, L. (2019). Synthesis, characterization, and applications of hemicelluloses based eco-friendly polymer composites. In Inamuddin, S. Thomas, R. K. Mishra and A. M. Asiri (Eds.), *Sustainable polymer composites and nanocomposites* (pp. 1267-1322). Springer. https://doi.org/10.1007/978-3-030-05399-4_43

Sarkar, A. M., Nayeem, J., Rahaman, M. M., & Jahan, M. S. (2021). Dissolving pulp from non-wood plants by prehydrolysis potassium hydroxide process. *Cellulose Chemistry and Technology*, *55*(1), 2. https://doi.org/10.35812/cellulosechemtechnol.2021.55.12

Sixta, H., Iakovlev, M., Testova, L., Roselli, A., Hummel, M., Borrega, M., van Heiningen, A., Froschauer, C., & Schottenberger, H. (2013). Novel concepts of dissolving pulp production. *Cellulose*, *20*(4), 1547–1561. https://doi.org/10.1007/s10570-013-9943-1

Takada, M., Chandra, R. P., & Saddler, J. N. (2019). The influence of lignin migration and relocation during steam pretreatment on the enzymatic hydrolysis of softwood and corn stover biomass substrates. *Biotechnology and Bioengineering, 116*(11), 2864–2873. https://doi.org/10.1002/bit.27137

Wan Rosli, W. D., Leh, C. P., Zainuddin, Z., & Tanaka, R. (2003). Optimisation of soda pulping variables for preparation of dissolving pulps from oil palm fibre. *Holzforschung*, *57*(1), 106–113. https://doi.org/10.1515/HF.2003.017

Wise, L. E., Murphy, M., & Adieco, A. A. (1946). Chlorite holocellulose, its fractionation and bearing on summative wood analysis and on studies on the hemicelluloses. *Paper Trade Journal, 122*(2), 35-43.

Pertanika J. Sci. & Technol. 32 (S3): 41 - 55 (2024)

PERTANIKA JOURNALS

SCIENCE & TECHNOLOGY

Journal homepage: http://www.pertanika.upm.edu.my/

The Effect of Spinning Parameters and Fiber Blending Ratio on the Physical Properties of Pineapple Leaf Fiber (PALF)-Cotton Yarns

Nurul Husna Zolkifflee[1], Mohd Nazrul Roslan[1]*, Juliana Abdul Halip[1,2], Khairu Kamarudin[1], Muhammad Farid Shaari[1] and Asna Nabilah Aziz[3]

[1]Faculty of Engineering Technology, Universiti Tun Hussein Onn Malaysia, Hab Pendidikan Tinggi Pagoh KM 1, Jalan Panchor, 84600 Panchor, Johor, Malaysia

[2]Institute of Tropical Forestry and Forest Products (INTROP), Universiti Putra Malaysia, 43400 UPM Serdang, Selangor, Malaysia

[3]Nature Renascent, No 1, Lot 387, Lorong Limau, Kg Sinaran Baru, 81300 Skudai, Johor, Malaysia

ABSTRACT

Pineapple leaf fiber (PALF) is known as pineapple residue and has potential as a textile material. Typical yarn manufacturing adopts ring spinning technique, yet it is challenging for course fibers, including PALF. PALF has been used in clothing and paper production using textile thread. It has the highest modulus among leaf fibers, comparable to synthetic fibers such as aramid and glass, and possesses the greatest tensile strength among leaf fibers. PALF has high fineness index makes it ideal for industrial yarn and woven fabric applications. Using natural fibers offers benefits such as being environmentally friendly, cost-effective, and lightweight yet sturdy. This study evaluates the physical properties of PALF-cotton yarn at three twist speeds, two total drafts, and three PALF-cotton blending ratios. The methodology of this study involves carding, drawing, and ring spinning of the PALF-cotton fibers. The process starts with cutting and opening PALF before blending it with cotton fiber using a carding machine. The finding shows that the average diameter and fineness values range from 205 μm to 458 μm and 31.2 to 67.0 tex, respectively. The study also reported that twist speed, total draft, and blending ratio affect the diameter and fineness of the yarns. In contrast, the increment of twist speed and total draft decreases the fineness and diameter of PALF-cotton yarns. Pineapple leaf fiber (PALF) shows great potential in the apparel industry. Three regression models were presented to predict the future ring-spinning process, and pineapple waste can be repurposed into valuable products, reducing overall waste.

Keywords: Cotton, diameter, fineness, PALF spinning

ARTICLE INFO

Article history:
Received: 22 February 2024
Accepted: 30 May 2024
Published: 30 July 2024

DOI: https://doi.org/10.47836/pjst.32.S3.04

E-mail addresses:
nurulhsnazlkfflee@gmail.com (Nurul Husna Zolkifflee)
nazrul@uthm.edu.my (Mohd Nazrul Roslan)
julianaah@uthm.edu.my (Juliana Abdul Halip)
khairu@uthm.edu.my (Khairu Kamarudin)
mdfarid@uthm.edu.my (Muhammad Farid Shaari)
asnanabihahaziz@gmail.com (Asna Nabihah Aziz)
*Corresponding author

ISSN: 0128-7680
e-ISSN: 2231-8526

INTRODUCTION

Pineapple, or Ananas comosus, belongs to the Bromeliaceae family and is one of the most popular crops planted in Malaysia (Bakar et al., 2021). Because of its enormous potential to generate income for farmers and governments, it is classified as an essential fruit (Md Ali, 2021). After Sarawak and Selangor, the state of Johor produces the most pineapples in the most significant and excellent plantation area on the peatland in Malaysia (DOA, 2021). Malaysia was placed 22nd among the top pineapple-producing countries on a worldwide scale. Pineapple waste can be used for energy generation, biofuels, and biogas. It can potentially be a source of bromelain, bioactive compounds, and cellulose nanocrystal feedstock. Pineapple waste can also be used as a bio-adsorbent to remove dyes and heavy metals. The high sugar content in different parts of the pineapple can be used as feedstocks for biofuels (Casabar et al., 2019). Nonetheless, Malaysia's economy is essential for food security, job stability, and income, particularly in small companies (Md Ali, 2021). According to the Pineapple Annual Report 2018 (MPIB, 2018), Malaysia's pineapple-based sector can help grow the socio-economy of agricultural entrepreneurs, thus helping to increase national income. By 2020, the country's demand will have increased to 3.8% due to encouraging trends in the growth rate of pineapple output over the previous ten years (Md Ali, 2021).

The rising consumer demand for pineapple has led to a substantial increase in production, resulting in the generation of a significant quantity of waste (Ali et al., 2020). During the transportation, storage, and processing of pineapples, over 80% of their components, including their crown, peels, leaves, core, and stems, are disposed of as waste (Das et al., 2022). As one of Southeast Asia's leading agricultural commodity producers, Malaysia produces 335,488 tons of pineapple, 67,098 tons of leaves, and 137,550 tons of peel wastes (Ali Hamzah et al., 2021). These wastes contain significant moisture levels, sugar, albumins, lipids, and vitamins susceptible to microbial degradation, adding to environmental issues (Rico et al., 2020). In most cases, after harvesting, pineapple residue often remains relatively unexploited and is usually disposed of or burnt in an open field. However, this method is ineffective and contributes to air pollution (Jehan et al., 2017; Omar et al., 2023). Pineapple is grown mainly for its fruit, and after harvest, the leaves remain unused, a waste of natural resources that must be explored due to the lack of fiber-specific technologies and the producers' ignorance of the various uses of the fibers, which provide additional income (Leão et al., 2015).

The demand for pineapple has increased, leading to significant waste (Ali et al., 2020) generation during transportation, storage, and processing (Das et al., 2022). Malaysia produces large amounts of pineapple waste, usually disposed of or burnt, contributing to environmental issues (Ali Hamzah et al., 2021). Pineapple residue is often unexploited, and the leaves are unused. This waste contains significant moisture levels, sugar, albumins, lipids, and vitamins, making it susceptible to microbial degradation (Rico et al., 2020).

The lack of fiber-specific technologies and producers' ignorance of the various uses of the fibers add to the problem (Leão et al., 2015).

Pineapple leaf fiber (PALF) is obtained from pineapple leaves by scraping, rotting, or decortication and used for essential purposes without additional cost (Padzil et al., 2020). PALF is white, creamy, and lustrous fiber (Dey, 2018). Various investigations show that the content of the PALF is mainly composed of cellulose, hemicellulose, lignin, wax, pectin, inorganic, and so on, with 56 to 82% of the cellulose content (Casabar et al., 2019). Compared with other natural fibers, PALF has excellent mechanical properties (Dey, 2018). The PALF has a wide range of modulus selection, varying from 34.5 to 82.51 GN/m2. Its tensile strength ranges from 413 to 1627 MN/m2, and its elongation at breaking ranges from 0.8 to 1.6%. Due to its high mechanical strength, PALF is a great material that can be used as an abrasive (BUKU PALF). Due to its high cellulose content, it has a high specific strength, rigidity, and hydrophilic characteristics. The PALF is characterized by a high average fracture strength and a low linear density, resulting in a high fiber spin capacity and a high-quality yarn (Ismoilov et al., 2019). No spinning system has been designated for the PALF (Niles et al., 2017). PALF can be turned into yarns through fiber spinning systems, such as jute spinning, semi-worsted, and flax. It can be achieved through binary or multi-blending techniques (Yusof et al., 2014). Despite the production of PALF yarns, they are still not as fine and uniform as cotton yarns in terms of properties (Ismoilov et al., 2019).

Several techniques have been developed for spinning yarn, including ring spinning, rotor spinning, and air-jet spinning. Ring spinning, which has been used since the 1770s, is the conventional method for producing yarn (Goyal & Nayak, 2019). The ring-spinning method is highly versatile and commonly used to produce yarns of excellent strength. The amount of energy used during the process depends on various factors such as fiber type, twist level (with higher twist requiring more energy), and yarn count (with finer yarns needing more energy) (Goyal & Nayak, 2019). Spinning PALF can be done manually or using machines. Initially, the long fibers were tied by hand and employed to create ropes and carpets to avoid spinning. But with the help of machines, fiber can be spun to produce better-quality textiles. However, there is currently no uniform method for spinning PALF due to its limited production and availability in the market (Jalil et al., 2021a). A technique of drafting and twisting is utilized to create yarn through spinning. The coarse sliver size is refined through the drafting system before it is spun into yarn.

PALF is generally bigger in terms of diameter than other textile fibers, namely jute fiber. Due to its big diameter, PALF produces a low percentage of quality ratios (Jalil et al., 2021b). However, this fiber could be increasingly consumed in the jute industry due to its larger diameter and lower cost than jute. Jalil et al. (2021b) reported that a high-strength fiber does not necessarily produce superior yarn unless it produces small-diameter yarn. Therefore, although the diameter of the PALF fiber is larger than jute, the spinning system and twist will affect the yarn's diameter (Jalil et al., 2021a). The diameter of the

yarn decreased with increasing twist level, and compact yarns had lower diameters than regular ring yarns (Basal & Oxenham, 2006). Thus, researchers are currently focused on developing competent yarn-forming methods and controlling parameters of connected machinery to broaden textile product diversity (Jalil et al., 2021a). As a result, improving the characteristics of fibers and yarn products, spinning and weaving productivity, and marginal capital investment may motivate entrepreneurs if this technology's development message reaches people worldwide.

Due to its bigger diameter, PALF is rarely used to form woven yarn, and mixing them with finer fibers such as cotton can provide a higher fiber count per area (Jalil et al., 2021a). Previous research has produced a blended fiber from the blending ratio of cotton: PALF 90:10 and 80:20 (Jalil et al., 2021a), and other researchers produced a blended fiber with 50% PALF and 50% cotton (Ismoilov et al., 2019). Previous research has shown that blending jute with cotton fiber is a helpful way to expand the use of jute and produce more valuable products. Jute fibers have several benefits, including a shiny golden appearance, high strength, and favorable properties. Thus, blending methods can be utilized to improve the quality of jute and develop a new range of fabrics made from jute that have a rising demand in both local and international markets (Ullah et al.,2016). According to their research, fabric made of a blend of yarn and cotton has characteristics similar to those of cotton fabric. It could reduce the need for imported cotton fiber (Ullah et al., 2016). Although PALF may not be suitable for clothing, it is possible to use thicker yarns made from this fiber to create various conventional and advanced textile products (Jalil et al., 2021a).

Therefore, this study aims to evaluate the effect of twist, draft, and blending ratio on the physical properties of PALF-cotton yarn. PALF fiber has a larger diameter than jute fiber, which affects the yarn's diameter (Jalil et al., 2021b). Researchers are focused on developing competent yarn-forming methods and controlling machinery parameters to create a variety of textile products (Jalil et al., 2021a). Blending PALF with cotton can produce a higher fiber count per area. Fabric made of a blend of yarn and cotton has characteristics similar to those of cotton fabric, which could reduce the need for imported cotton fiber (Ullah et al., 2016). This study aims to evaluate the effect of twist, draft, and blending ratio on the physical properties of PALF-cotton yarn.

MATERIALS AND METHODS

Materials Preparation

In this study, pineapple leaf fiber (PALF) was provided by the Malaysian Pineapple Industry Board (MPIB) in Pontian, Johor. The cotton fibers were also procured from Shijiazhuang Bibante Trading Co, China. The cotton fiber properties were studied as a benchmark for

the blended fiber. The average staple length of the textile cotton fibers used in this study was 34.5 mm, while the effective diameter was 16.58 μm.

Sample Preparation

Once the pineapple fruit is harvested between 146 and 152 days from the first day of flowering, the leaves are carefully detached from the trunk. The process of extracting PALF is executed manually through a meticulous decoration technique involving scraping and preparations. PALF fibers were cut into 3 to 4 cm long staple lengths, and PALF-cotton yarns' 1 meter in length, morphology, and physical properties were evaluated.

Prior to the spinning process, the PALF was manually cut into 3 to 4 cm in length to ease the fiber blending and spinning process. There are three majors: producing yarn opening, carding, drawing, and ring spinning. At the beginning of the process, cotton fibers underwent a carding machine to ease the condition of the fibers. Then, the feeding apron with PALF-cotton fibers was put into a carding machine according to the specified ratios. This study prepared the PALF and cotton fibers in three ratios: 30% PALF + 70% cotton, 40% PALF + 60% cotton, and 50% PALF + 50% cotton. Next, PALF and cotton fibers began the blending process using the carding machine. The formation of a sliver was also carried out through the carding machine. The quality of the yarn produced heavily relies upon the formation of slivers, which involves the removal of short fibers. Later, the carded sliver produced from the carding machine was the input for the ring spinning machine. The last process of manufacturing PALF cotton involves the ring-spinning process. Figure 1 illustrates the steps involved in the preparation of yarn. In this study, three levels of twisting speed (800 tpm, 850 tpm, and 900 tpm) and two levels of drafting (8 and 10 total drafts) were adjusted in the control panel of the ring spinning machine. Figure 2 depicts the sample preparation flowchart for this study. The study consists of five stages: preparation of pineapple fiber, blending of PALF-cotton fiber, preparation of PALF-cotton sliver, production of PALF-cotton yarn, and analysis of PALF-cotton yarn.

Eighteen samples of PALF-cotton yarn with three different blending ratios, three twisting speed levels, and two total draft levels were used to produce the yarn. Table 1 presents the parameters of the research studies on the PALF-cotton ratios, the studies' designation, the number of ratios, levels of twisting speed, and the number of total drafts. Besides, the ring frame speed (rpm) was kept constant at 5600 rpm in the ring spinning machine. The Spinning Technology Laboratory, located at the Faculty of Engineering Technology in Universiti Tun Hussein Onn Malaysia, housed the carding and ring spinning machines.

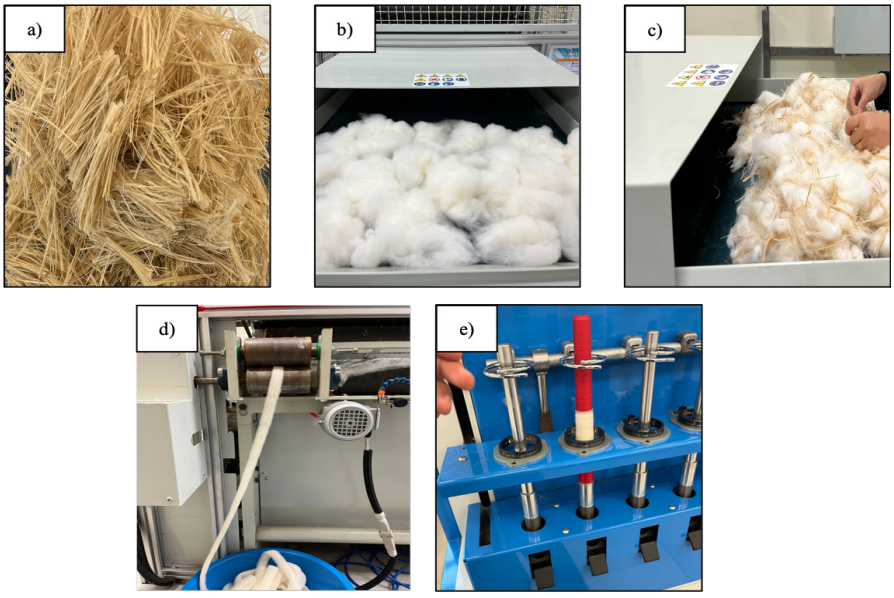

Figure 1. Sample preparation process of (a) PALF fiber; (b) opening cotton fiber; (c) feeding apron where PALF-cotton fiber was placed; (d) sliver development from the carding machine; (e) yarns production

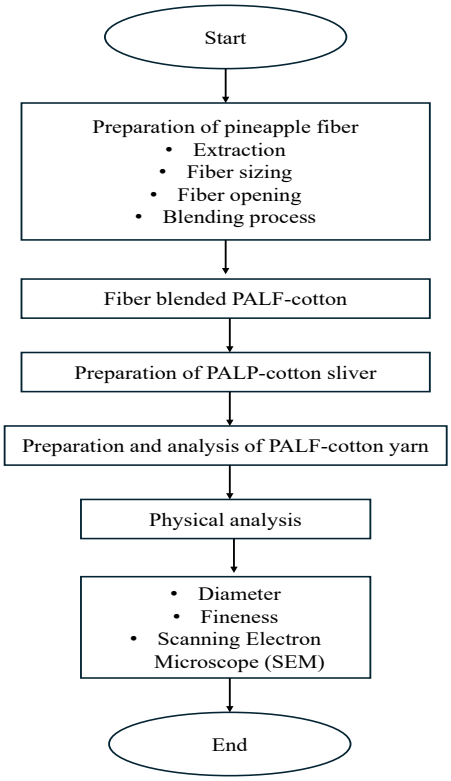

Figure 2 Sample preparation flowchart

Table 1
Parameters of PALF-cotton yarn

Designation	Ratios (%)	Twisting speed (tpm)	Total draft
30A	30/70	800	8
30B		850	
30C		900	
30D	30/70	800	10
30E		850	
30F		900	
40A	40/60	800	8
40B		850	
40C		900	
40D	40/60	800	10
40E		850	
40F		900	
50A	50/50	800	8
50B		850	
50C		900	
50D	50/50	800	10
50E		850	
50F		900	

Analysis of Variance (ANOVA)

An investigation was carried out to analyze the thickness and quality of PALF-cotton yarn, utilizing the general linear model (GLM) of analysis of variance (ANOVA) with the help of MINITAB 19 Software. The ANOVA identified the most prominent group that significantly impacted the outcome. If the p-value is less than 0.5, there are differences between the averages at a 0.05 significance level. Besides, the experimental data was fitted by the quadratic regression model. Equation 1 describes the relationship between the independent variables and the response variable:

$$Y_i = \beta_0 + \beta X_i + \varepsilon_i \quad (1)$$

Where Y_i is the c value of the dependent or response variable, β_0 and β_1 are the coefficients of the regression line (also known as the slope (β_1)) and intercept (β_0), X_i is the i-th independent or predictor variable, and ε_i is the prediction error, or "noise" or "residual." The regression model was carried out for the future yarn qualities based on the spinning parameters or yarn properties.

Yarn Diameter

Advanced Microscopy (Model Olympus U-MSSP4), located at the Material Science Laboratory, Faculty of Engineering Technology, UTHM, was used to measure the yarn diameter. To measure the diameter, the lens's magnification was set to 5x. A total of 90 yarn were measured, and 10 mm long yarn samples were made. The average diameter was determined by measuring it five times along the length of PALF-cotton yarn. Under a high-magnification microscope, the diameter of representative sampling fibers can be measured using the standard method test procedure adopted by ASTM D2130-90 (ASTM International, 2008).

Yarn Fineness

The measurement of yarn fineness using the standard gravimetric method, which involves cutting and weighing the yarn, was based on ASTM D 1907 (ASTM, 1989). In total, 90 yarns were measured, each cut to a length of 1 meter, and weighed five times to obtain the average yarn weight. The entire process was repeated five times to arrive at an average fineness for the yarn. The materials were precisely weighed to within 0.001 g using a calibrated balance after being divided into 10 cm pieces. The determination of yarn fineness was done using Equation 2. This mathematical formula computes the mass of the yarn per unit length in tex, where tex is the measure of yarn mass in grams per 1000 meters of length. A higher tex value indicates that the yarn is coarser, and its fineness is inversely proportional to this value (Equation 2).

$$\text{Yarn finess } \left(\frac{\text{mass}}{\text{length}}\right) \text{X } 100 \quad (2)$$

Scanning Electron Microscope (SEM) Analysis

The morphology and structure of PALF-cotton surfaces were observed by using Scanning Electron Microscopy device model no: JEOL JSM-6380LA MP-19500014, located at Material Science Laboratory, Faculty of Mechanical and Manufacturing (FKMP), Universiti Tun Hussein Onn Malaysia (UTHM). Platinum coating of a few thick nanometers coated the PALF-cotton yarn surfaces. The SEM analysis was carried out to identify the comparison imperfection of yarn subjected to the different spinning parameters.

RESULTS AND DISCUSSION

Yarn Physical Properties

Table 2 displays the ANOVA table for PALF-cotton at different spinning parameters and blending ratios subjected to diameter and fineness properties. Table 2 shows that twist speed, total draft, and blending ratio significantly affected the diameter of the yarn. Additionally, both spinning parameters and blending ratios significantly affected the fineness, with *p*-values indicated lower than 0.05.

Table2
ANOVA results for diameter and fineness

Source	DF	*F*-value	*P*-value	Significant level
1. Diameter				
Twist Speed	2	48.82	0.000	***
Draft	1	42.14	0.000	***
Blending Ratio	2	54.11	0.000	***
2. Fineness				
Twist Speed	2	23.21	0.000	***
Draft	1	47.72	0.000	***
Blending Ratio	2	35.03	0.000	***

Note:
*** Significantly different at $p<0.001$

In this study, all three parameters, namely twisting speed $\chi 1$ and total draft $\chi 2$, were chosen as the potential influences, and Yi were dependent variables calculated by the proposed model. The quadratic regression models that have been fitted and their significance are presented in Table 3. The β-coefficient for different yarn quality parameters. The calculation of beta coefficients involves standardization of variables, which means subtracting their means and dividing by their standard deviations. This analysis is performed to arrive at the values of beta coefficients. The coefficient of determination shows the

percentage of response variable variability the model explains. Examining standardized variables, after dividing them by their means and standard deviations, leads to estimations known as beta coefficients. Standardizing coefficients is necessary when variables are measured in different units to evaluate how well independent variables influence the response variable in fitted models.

Table 3
Response fineness equations of PALF-cotton yarn on the ratio

Ratio (%)	Response fineness equation
30:70	$506.4 – 0.5100\ x_1 – 42.33\ x_2 + 0.04833\ x½$
40:60	$1031.9 – 01.1600\ x_1 – 87.81\ x_2 + 0.10.333\ x½$
50:50	$261.7 – 0.1283\ x_1 – 8.01\ x_2 + 0.0042\ x½$

Figure 3 illustrates the average diameter of the PALF-cotton yarn. The blending ratio apparently shows the most significant effect on the average diameter. Generally, the increment of the PALF ratio increased the average diameter, especially at 50% of PALF yarn. From observation, the increment of the PALF ratio initially slightly decreases the average diameter of PALF-cotton yarn with 40% of PALF presence in the yarn. However, the average diameter increases significantly when the yarn ratio increases to 50%. Moreover, the increment of twist speed and total draft decreases the average diameter of PALF-cotton yarns, especially at 40% and 50% of PALF presence.

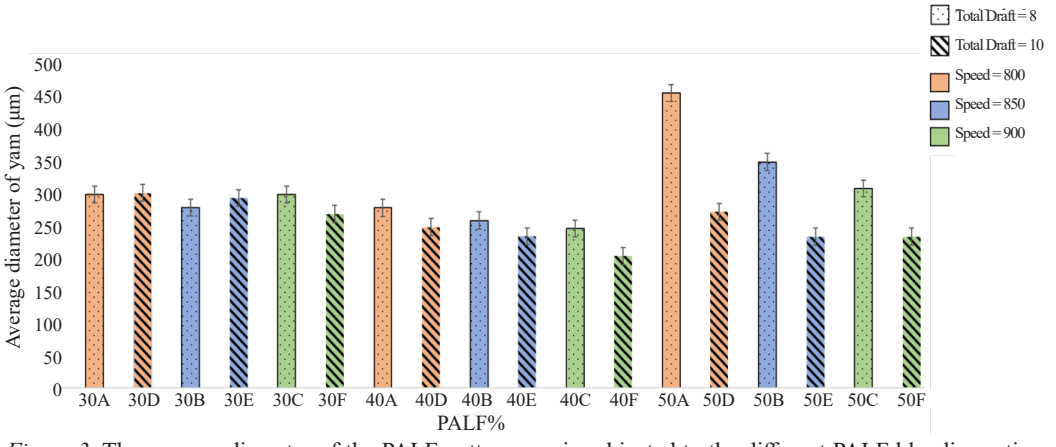

Figure 3. The average diameter of the PALF-cotton yarn is subjected to the different PALF blending ratios, twisting speeds, and total draft

Yarns 50A (50% PALF + 50% cotton, 800 twist speed, and 8 drafts) and 40F (40% PALF + 60% cotton, 900 twist speed, and 10 drafts) exhibit the highest and the lowest average diameter at values of 458 µm and 205 µm, respectively. Yarn 50A has the highest

diameter yarn due to the high amount of PALF fibers compared to others. These findings are tallied by Jalil et al. (2021a) due to a higher diameter, which could be affected by less fine. Hence, its coarseness and brittle nature cause the yarn to become loose and not interlocked with each other yarn in the blending ratio of 50% PALF + 50% cotton. Furthermore, from the previous study, yarn produced from 100% PALF has a larger diameter relative to other textile fibers, and due to this larger diameter, PALF will produce poor quality ratios (Jalil et al., 2021a). In a nutshell, 100% PALF fiber is not recommended to be spun alone to produce a better quality of yarn (Jalil et al., 2021b). On the other hand, twisting speed, draft and blending ratio had a significant effect on the diameter response, with p-values indicating lower than 0.05.

However, yarn 40F is smaller than those with 30% of PALF. It has been predicted that different ratios of cotton fiber in the PALF-cotton yarn 40F have a lower ratio of cotton (Jalil et al., 2021a). This study also revealed that higher twist speed (900 twist speed) and total draft (10) contribute to the smaller yarn diameter to produce high-quality yarn. These findings are similar to a study by Basal and Oxenham (2006), where the high speed and high total draft contributed to greater diameter or yarn.

Figure 4 illustrates the fineness of the PALF-cotton yarn subjected to the different twist speeds, total draft, and PALF ratio. Generally, the twist speed, total draft, and blending ratio affect the fineness of the yarn. The increment of twist speed and total draft decreases the fineness of PALF-cotton yarns, and the trend was exhibited in the yarn comprising 40% and 50% PALF. In the fineness study, the increment of the PALF blending ratio affects the fineness of the yarn.

The highest fineness value is given by yarn 30A (30% PALF + 70% cotton, 800 twist speed, and 8 drafts), followed by 40A (40% PALF + 60% cotton, 800 twist speed, and 8 drafts) and 50A (50% PALF + 50% cotton, 800 twist speed, and 8 drafts), with the values of 67.0 tex, 66.7 tex, and 66.4 tex, respectively. It indicated that at 800 twist speed and 8 drafts, it was able to spin the yarn and produce at similar fineness, regardless of the blending ratio of PALF. Meanwhile, the lowest values are given by 50F (31.2 tex), followed by 40C (31.4 tex) and 50E (31.8 tex). Low fineness is one of the good qualities of yarn. As reported by Jalil, low fineness resulted in excellent-quality yarn (Jalil et al., 2021b).

Next, since the text is proportional to the fineness of the yarn, a greater tex value indicates coarser yarn, and a lower tax value indicates finer yarn (Anuwar et al., 2022). Besides that, yarn fineness decreases as the twisting speed decreases because the adjustment of spinning parameters in twisting speed will control the input into the top front roller at the ring spinning machine. Based on previous research, blending more fine cotton fibers with PALF helps to enhance spinnability (Jalil et al., 2021a).

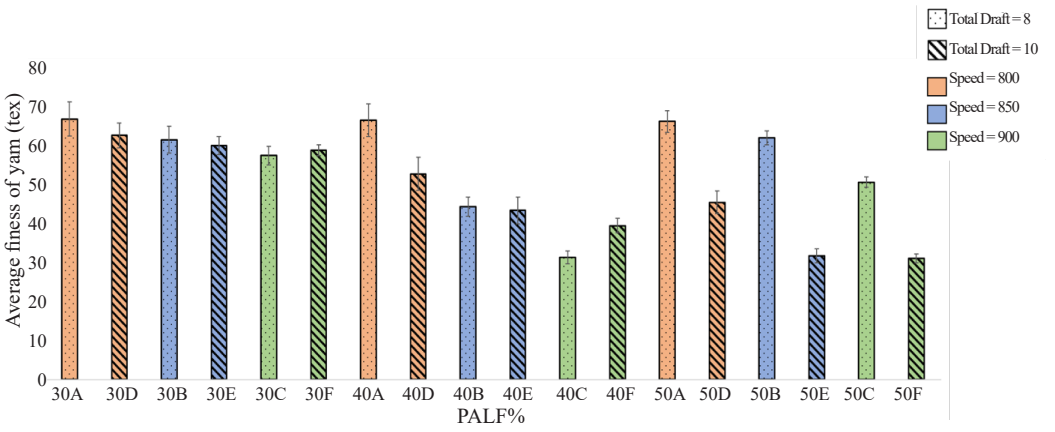

Figure 4. The fineness of the PALF-cotton yarn is subjected to the different PALF blending ratios, twisting speeds, and total draft

Morphology Analysis

The SEM image analysis was taken with 70x magnification. The yarn's structure micrographs can be seen in Table 4, which compares the surface morphologies subjected to different blending ratios, twisting speeds, and total draft. The SEM aims to analyze the morphology of PALF yarn. Surface Morphology in Table 4 shows the difference in morphology by increasing and decreasing the ratio of PALF + cotton, total draft, and twisting speed. A Visual inspection in Table 4 showed that 40% PALF + 60% cotton was found with an increased twisting speed of 800, 850, and 900 tpm, and total drafts 8 and 10; hence, will reveal a uniformity increase in the PALF-cotton yarn. Next, the structure of the yarn becomes significantly looser by decreasing the twisting speed, and the twisting speed increases the tighter structure.

According to the previous researcher, increasing the twisting level and adjusting the spinning systems will be significant by reducing yarn hairiness and improving the quality of yarn spinning (Basal & Oxenham, 2006). At the same time, the 50% PALF + 50% cotton total draft 10 revealed that the yarn size is smaller than draft 8. Thus, it had a tighter yarn structure. As a result, a looser structure of 50% PALF + 50% cotton was detected at 850 and 800 twisting speeds. Thus, from the previously obtained, the physical properties of constituent fibers and the yarn structure play important roles in yarn properties (Jalil et al., 2015). This study also revealed that 30% PALF + 70% cotton yarn by decreasing the PALF ratios and increasing the cotton fiber ratio size of the yarn affected the size of PALF-cotton yarn. As reported by Tursunbayevich et al. (2021), when yarns spun in a different spinning system are twisted, the strength of the yarns increases (Tursunbayevich et al., 2021).

Table 4
Surface morphology of PALF-cotton yarn

	30% PALF + 70% cotton		
	800 tpm	850 tpm	900 tpm
8 drafts	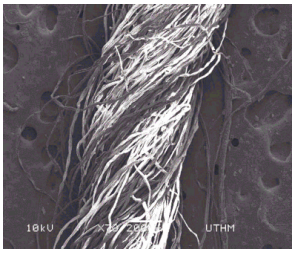	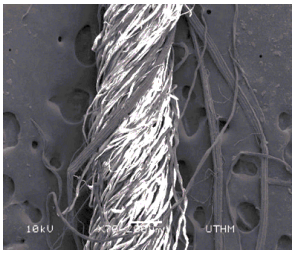	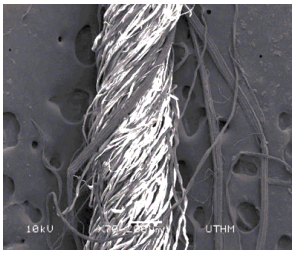
10 drafts	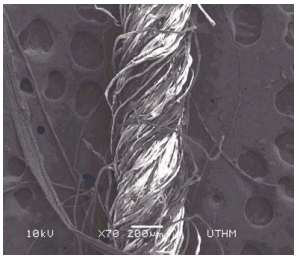	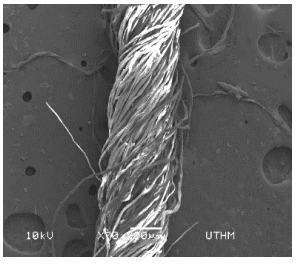	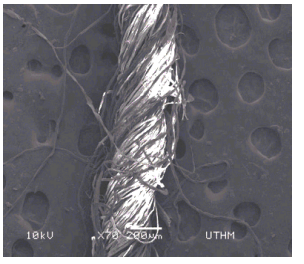
	40% PALF + 60% cotton		
8 drafts	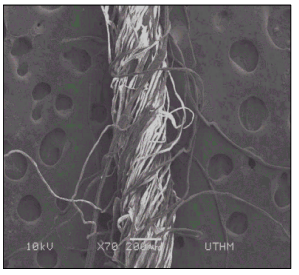	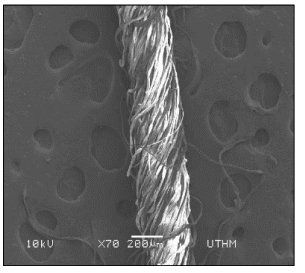	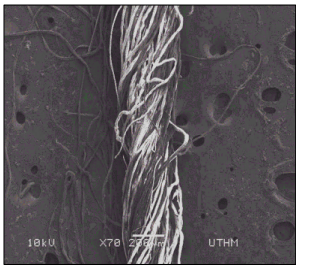
10 drafts	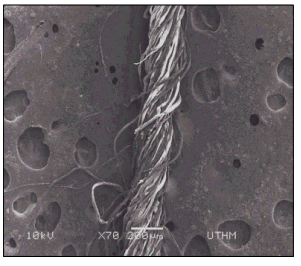	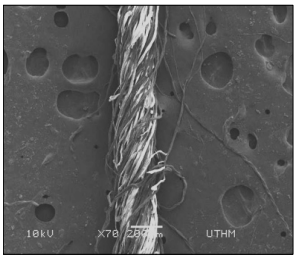	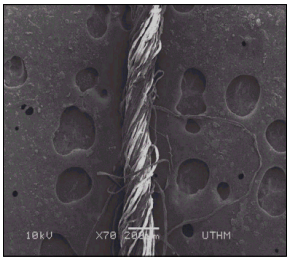

Table 4 *(Continue)*

	50% PALF + 50% cotton		
	800 tpm	850 tpm	900 tpm
8 drafts	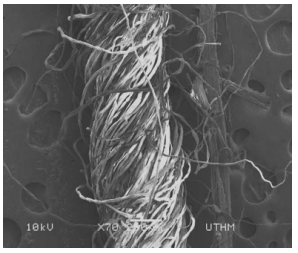	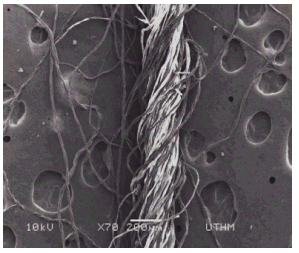	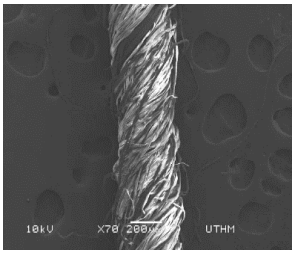
10 drafts	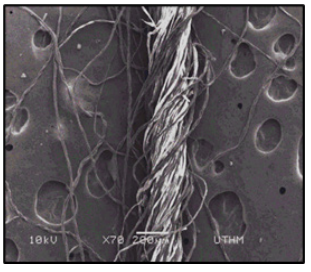	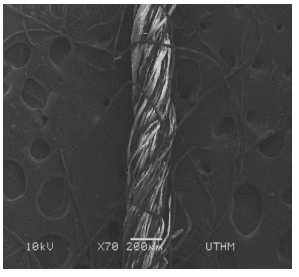	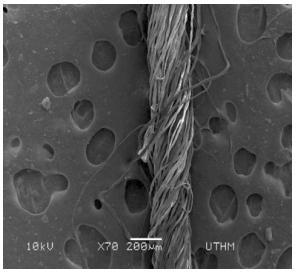

CONCLUSION

In conclusion, the diameter and fineness of PALF-cotton yarns were successfully evaluated. It was discovered that the different twist speeds and draft adjusting during the ring spinning process influenced the diameter and fineness of the yarns. PALF-cotton yarn developed by blending ratio of 50% PALF + 50% cotton achieved the best structure in terms of the fineness and compact structure of the yarn. Spinning parameters of 850 twist speeds and 10 total drafts are recommended to produce PALF-cotton yarn. Further preparation on raw PALF fiber can be undertaken, especially in the treatment process, to enhance PALF fiber characteristics and achieve a better quality of yarn. Generally, PALF processing and manufacturing could produce zero waste in Malaysia with the contribution of the textile industry. The blended yarn has great potential for producing fancy clothing items. The study concluded that the findings could directly impact the PALF and cotton industry. Implementing the suggested method could yield better-quality yarns and fabrics. It would improve the usage of PALF, which is environmentally friendly and biodegradable. Through efficient modification, PALF can be a source of garment manufacturing that is helpful to the industry and community.

ACKNOWLEDGEMENT

Universiti Tun Hussein Onn Malaysia supported this research through Industry Grant Vot M140, MHN Ventures Sdn Bhd, and Postgraduate research Grant (GPPS) Vote H729.

REFERENCES

Ali, M. M., Hashim, N., Abd Aziz, S., & Lasekan, O. (2020). Pineapple (*Ananas comosus*): A comprehensive review of nutritional values, volatile compounds, health benefits, and potential food products. *Food Research International*, *37*. https://doi.org/10.1016/j.foodres.2020.109675

Ali Hamzah, A. F., Hamzah, M. H., Che Man, H., Jamali, N. S., Siajam, S. I., & Ismail, M. H. (2021). Recent updates on the conversion of pineapple waste (Ananas comosus) to value-added products, future perspectives and challenges. *Agronomy*, *11*(11). https://doi.org/10.3390/agronomy11112221

Anuwar, A. A. N., Rashid, A. H. A., Jikan, S. S., Roslan, M. N., Tahir, A. A. H. M., Zolkifflee, N. H., & Razal, F. A. M. (2022). The effect of alkaline treatment on the schizostachyum grande fibre for textile applications. *International Journal of Integrated Engineering, 14*(8), 37–49. https://doi.org/10.30880/ijie.2022.14.08.006

ASTM. (1989). Standard Test Method for Linear Density of Yarn (Yarn Number) by the Skein Method. ASTM Designation: D1907-89, ASTM Standard on Textile Materials*, 7*(1), 1-15.

ASTM International. (2008). Standard test method for diameter of wool and other animal fibers by micro projection. ASTM Designation: D2130, ASTM Standard on Textile Materials, *7*(1), 1-15.

Bakar, B. A., Baharom, S. N. A., Rani, R. A., Ahmad, M. T., Zubir, M. N., Sayuti, A. F. A., Nordin, M. N., Bookeri, M. A. M., & Muslimin, J. (2021). A review of mechanization and automation in Malaysia's pineapple production. *Advances in Agricultural and Food Research Journal, 4*(2). https://doi.org/10.36877/aafrj.a0000206

Basal, G., & Oxenham, W. (2006). Comparison of properties and structures of compact and conventional spun yarns. *Textile Research Journal*, *76*(7), 567–575. https://doi.org/10.1177/0040517506065591

Casabar, J. T., Unpaprom, Y., & Ramaraj, R. (2019). Fermentation of pineapple fruit peel wastes for bioethanol production. *Biomass Conversion and Biorefinery*, *9*(4), 761–765. https://doi.org/10.1007/s13399-019-00436-y

Das, A., Islam, A., & Info, A. (2022). 272 International Journal for Modern Trends in Science and Technology as per UGC guidelines, an electronic bar code is provided to secure your paper. *International Journal for Modern Trends in Science and Technology*, *8*(05), 272–278. https://doi.org/10.46501/IJMTST0805039

Department of Agriculture (DOA). 2021. *Booklet statistik tanaman: Sub-sektor tanaman makanan*. Department of Agriculture Malaysia.

Dey, S. K. (2018). Future prospect for sustainable luxury textiles from pineapple leaf fibre - an agro waste. *Latest Trends in Textile and Fashion Designing*, *1*(2). https://doi.org/10.32474/lttfd.2018.01.000108

Goyal, A., & Nayak, R. (2019). Sustainability in yarn manufacturing. In R. Nayak (Ed.), *Sustainable technologies for fashion and textiles* (pp. 33-55). Elsevier. https://doi.org/10.1016/B978-0-08-102867-4.00002-5

Ismoilov, K., Chauhan, S., Yang, M., & Heng, Q. (2019). Spinning system for pineapple leaf fiber via cotton spinning system by solo and binary blending and identifying yarn properties. *Journal of Textile Science and Technology*, *5*(4), 86-91. https://doi.org/10.4236/jtst.2019.54008

Jalil, M. A., Moniruzzaman, M., Parvez, M. S., Siddika, A., Gafur, M. A., Repon, M. R., & Hossain, M. T. (2021a). A novel approach for pineapple leaf fiber processing as an ultimate fiber using existing machines. *Heliyon*, *7*(8). https://doi.org/10.1016/j.heliyon.2021.e07861

Jalil, M. A., Parvez, M. S., Siddika, A., & Rahman, M. M. (2021b). Characterization and spinning performance of pineapple leaf fibers: An economic and sustainable approach for Bangladesh. *Journal of Natural Fibers*, *18*(8), 1128–1139. https://doi.org/10.1080/15440478.2019.1687066

Jalil, M. A., Sinha, R. C., Mahabubuzzaman, A. K. M., Milon Hossain, M., & Idris, M. A. (2015). Study on physical and structural properties of jute-palf blended yarn spun by apron draft spinning. *Research Journal of Textile and Apparel*, *19*(3), 9–15. https://doi.org/10.1108/RJTA-19-03-2015-B002

Jehan, O. S., Sanusi, S. N. A., Sukor, M. Z., Noraini, M., Buddin, M. M. H. S., & Hamid, K. H. K. (2017). Biogas production from pineapple core - A preliminary study. *AIP Conference Proceedings*, *1885*. https://doi.org/10.1063/1.5002440

Leão, A. L., Cherian, B. M., Narine, S., Souza, S. F., Sain, M., & Thomas, S. (2015). The use of pineapple leaf fibers (PALFs) as reinforcements in composites. *Biofiber Reinforcements in Composite Materials*, 211–235. https://doi.org/10.1533/9781782421276.2.211

Md Ali, A. (2021). Industri nanas: Peranan dan cabaran dalam penjanaan ekonomi Malaysia [The pineapple industry: Role and challenges in generating the Malaysian economy]. *Journal of Economics and Sustainability*, *3*(2), 1–15. https://doi.org/10.32890/jes2021.3.2.1

MPIB. (2018). *Lembaga Perindustrian Nanas Malaysia*. Penerbitan - Lembaga Perindustrian Nanas Malaysia. https://www.mpib.gov.my/penerbitan/

Niles, S. N., Dias, W. P. P., & Perera, T. K. M. (2007). A vision-based method for analyzing yarn evenness. *International Journal of Scientific & Technology Research, 6*, 254-256.

Omar, S., Shafie, S. M., Hami, N., Othman, Z., & Hariths Numan Djaohari, A. (2023). Environmental analysis of power generation from pineapple waste. *Journal of Advanced Research in Fluid Mechanics and Thermal Sciences*, *105*(2), 88–98. https://doi.org/10.37934/arfmts.105.2.8898

Padzil, F. N. M., Ainun, Z. M. A., Abu Kassim, N., Lee, S. H., Lee, C. H., Ariffin, H., & Zainudin, E. S. (2020). Chemical, physical, and biological treatments of pineapple leaf fibres. *Pineapple Leaf Fibers: Processing, Properties and Applications*, 73-90. https://doi.org/10.1007/978-981-15-1416-6_5

Rico, X., Gullón, B., Alonso, J. L., & Yáñez, R. (2020). Recovery of high value-added compounds from pineapple, melon, watermelon, and pumpkin processing by-products: An overview. *Food Research International*, *132,* 109086. https://doi.org/10.1016/j.foodres.2020.109086

Tursunbayevich, Y. A., Lolashbayevich, M. S., Ahmadjanovich, K. S., Raufovna, A. S., & Raxmanbergan kizi, M. K. (2021). Investigation of influence of a new twist intensifier on the properties of the twisted yarn. *Turkish Journal of Computer and Mathematics Education*, *12*(5), 1943-1949. https://doi.org/10.17762/turcomat.v12i5.2275

Ullah, A. A., Foisal, A., & Nahar, N., (2016). Study on the characteristics of jute-cotton blended fabrics. *SEU Journal of Science and Engineering, 10*(2), 12-16.

Yusof, Y., Yahya, S. A., & Adam, A. (2014). A new approach for PALF productions and spinning system: The role of surface treatments. *Journal of Advanced Agricultural Technologies*, *1*(2). https://doi.org/10.12720/joaat.1.2.161-164

Pertanika J. Sci. & Technol. 32 (S3): 57 - 68 (2024)

PERTANIKA JOURNALS

SCIENCE & TECHNOLOGY

Journal homepage: http://www.pertanika.upm.edu.my/

Comprehensive Evaluation of Printing Process Parameters and Tensile Properties of Coconut Polypropylene Filament Composites in Additive Manufacturing

Noryani Muhammad[1,2]*, Mohd Aiman Jamaludin[3], Nuzaimah Mustafa[4], Yuzliza Yusuf[4], Mohd Adrinata Sharuzaman[1,2] and Nurul Hanim Razak[1, 2]

[1]Fakulti Teknologi dan Kejuruteraan Mekanikal, Universiti Teknikal Malaysia Melaka, Hang Tuah Jaya, 76100 Durian Tunggal, Melaka, Malaysia
[2]Centre for Advenced Research on Energy, Universiti Teknikal Malaysia Melaka, Hang Tuah Jaya, 76100 Durian Tunggal, Melaka, Malaysia
[3]Quality Department, HTM Hengtech Industry Sdn Bhd, 40470 Shah Alam, Selangor, Malaysia
[4]Fakulti Teknologi dan Kejuruteraan Industri Pembuatan, Universiti Teknikal Malaysia Melaka, Hang Tuah Jaya, 76100 Durian Tunggal, Melaka, Malaysia

ABSTRACT

The printing process parameters are important in producing coconut polypropylene (CcPP) products by filament composite in the additive manufacturing industry. Fused deposition modeling techniques in 3D printing applications have considered multiple parameters to meet good finishing parts. This study uses comprehensive measurements to identify the best printing parameter for evaluating the composite properties. Complete deposition, unwrapping, good finishing, and adequate heat are the qualitative printing process parameters used to finalize the optimum nozzle and bed temperature of the CcPP filament composite. The range between 50°C to 80°C and 225°C to 245°C for bed and nozzle temperatures were used to achieve a well surface and successful production. After multiple trials of printing the CcPP filament composite, the optimal bed and nozzle temperatures were found to be 80°C and 230°C, respectively. Two types of infill density were used to analyze the effect on the tensile properties of CcPP filament composite. The result showed that 50% infill density was higher for both 1% and 5% fiber loading than 25% infill density for tensile strength with 15.65 and 22.87 MPa compared to 12.93 and 16.59 MPa. The same pattern as the score of Young's moduli of 50% infill density was

ARTICLE INFO

Article history:
Received: 22 February 2024
Accepted: 30 May 2024
Published: 30 July 2024

DOI: https://doi.org/10.47836/pjst.32.S3.05

E-mail addresses:
noryani@utem.edu.my (Noryani Muhammad)
aimanjamal.htm@gmail.com (Mohd Aiman Jamaludin)
nuzaimah@utem.edu.my (Nuzaimah Mustafa)
yusliza@utem.edu.my (Yusliza Yusuf)
adrinata@utem.edu.my (Mohd Adrinata Shaharuzaman)
nurulhanim@utem.edu.my (Nurul Hanim Razak)
* Corresponding author

ISSN: 0128-7680
e-ISSN: 2231-8526

higher than 25% infill density for 1% and 5% fiber loadings with 479.52 and 641.23 MPa compared to 400.17 and 493 MPa. Qualitative and quantitative measurements of printing process parameters and properties help reduce the time and cost and benefit 3D printer users in the industry.

Keywords: Coconut/ PP composite, printing parameter, qualitative and quantitative analysis, tensile testing

INTRODUCTION

Fused Deposition Modelling (FDM) is one of the 3D printing methods that classified additive manufacturing techniques that have been gaining popularity in recent research, both academic and industry. The industry of additive manufacturing techniques is becoming increasingly popular due to their numerous advantages, including the ability to create a wide variety of complex shapes and structures while properly managing materials. FDM technology in manufacturing serves the same purpose as injection molding, primarily used for mass customization on productions. Moreover, the FDM technique can produce various personalized products and end parts that reduce production costs and make each product unique (Kristiawan et al., 2021).

Furthermore, no costs are incurred in the creation of precisely designed products. There are massive materials used in the 3D printing industry. Common materials in the FDM technique are thermoplastic polymers such as poly-lactic acid (PLA), polypropylene (PP), polyethylene (PE), and polystyrene (PS). The filament's thermo-plasticity, which influences the filament's capacity to form bonds between layers during the printing process and solidify at room temperature after printing, is a crucial task since FDM structures are constructed from layers of thin filament. Many processing parameters influence the mechanical characteristics of the printed object, such as layer thickness, width, and filament orientation (Le Duigou et al., 2020). Creating the filament's substance has proven difficult due to the complicated FDM process. The material's properties can influence the printing parameters, such as the nozzle's temperatures and the printer's bed. Extrusion consistency, good adhesion and good finishing are the other factors to be considered during the printing process for a high-quality printed part.

A recent study introduced the capability of natural fiber-reinforced composite to reduce the use of synthetic materials in the industry, which can benefit the user and the manufacturer (Mastura et al., 2022). The performance of two natural fibers (hemp and flax) with four synthetic materials (aramid, boron, carbon and glass) was compared using Young's modulus score; a significant difference was shown between these materials using hypothesis testing. The maximum score of Young's moduli for synthetic and natural fiber, which are aramid and flax, is 424.8 GPa and 57.3 GPa, respectively. Hybridization of these two materials can overcome the limitation of both natural and synthetic fibers.

Natural fiber-reinforced composite is made up of two materials: natural fiber and polymer matrix. Multiple benefits to both user and manufacturer include environmental friendliness, health and safety. Natural fibers such as cotton, wool and bamboo can offer comfort and aesthetic elements compared to synthetic materials. The manufacturer can also benefit from the cost-effectiveness of using local natural fiber, resulting in lower transportation costs. The industry can support regulation compliance, such as environmental regulation and sustainability standards. The combination of different ratios of the materials also influences the filament composite's mechanical, physical, and thermal performance (Radzi et al., 2017). Recently, this composite has demonstrated a good agreement with better physical, mechanical, chemical, and environmental properties than single fiber or polymer (Hamid et al., 2022; Ilyas et al., 2022; Muhammad et al., 2022).

Numerous studies have reported composite materials' ability to replace metal-based materials in many industries, such as automotive, food packaging, marine, aircraft, and medical (Alsubari et al., 2021; Hawary et al., 2023). In the application of 3D printing, the FDM technique is interesting for the industry in employing the filament composite. The printing process becomes more crucial to the design engineers when setting up the printing process parameters of the filament composite. Different filament composites have different characteristics based on combining two types of materials (Jumaidin et al., 2017). The crystallinity, flowability and thermal properties of the filament composite are very important to make sure the filament composite is printable. The filament composite's unique characteristics make the 3D printing process difficult. There are huge printing process parameters that should be considered during the printing process of filament composite, such as layer thickness, printing speed, nozzle and bed temperature, filling pattern, infill density, and build orientation (Alafaghani et al., 2021; Muthe et al., 2022). Identifying the printing process parameters before printing the filament composite is important.

The performance of the printed composite is affected by the printing process parameters setting during the printing process. The composite's tensile, flexural, and impact properties differ significantly based on the printing process parameters set up (Jeon et al., 2020). There is a relationship between the mechanical properties of printed parts using FDM and the process parameters for PLA and ABS polymers (Ahn & Wright, 2002; Hanon et al., 2021). A hybrid polypropylene composite with jute and coir also performs differently in tensile, flexural, impact, and hardness (Beg & Hasan, 2020). Filament composite in 3D printer technology offers many advantages, especially sustainability and environmental friendliness, supporting the fourth industrial revolution. The challenges and considerations during the printing process are critical in addressing the material selection properties and identifying the correct printing process parameters.

Qualitative measurements are essential to finalize a particular filament composite to achieve an excellent finishing printed part with an optimum time, cost, and minimum waste

materials. Based on the literature, minimal studies mentioned the qualitative measurements of printing process parameters such as complete deposition, unwarping, good finishing, and adequate heat for nozzle and bed temperature. This present study focuses on the best combination of nozzle and bed temperatures using qualitative assessments to produce good finishing during printing. The current study also contributes to the 3D printing industry by addressing the effect of infill density on the tensile properties of coconut polypropylene (CcPP) filament composite. Quantitative measurements, such as infill density, were used to analyze the overall performance of the mechanical properties of the composite.

MATERIALS AND METHODS

Preparation of CcPP Filaments Composite

Coconut fibers (coir) were collected from small- and medium-sized companies in food manufacturing in Melaka, Malaysia. The coconut fibers were processed to a smaller mesh size using a DF-15 hammer mill grinder (Pulveriser, Shenzhen, China) and further sieved to obtain an average fiber size of 125–300 μm. Recycled PP polymer was obtained as 2 mm pellets from a plastic industry at Ayer Keroh, Melaka. The fiber coconut fiber was dried in an oven at 70°C for 24 hours before extrusion. Different coconut fiber loadings of 1%, 3%, and 5% were mixed with PP and extruded using a single extruder from the Composite Laboratory, Universiti Teknikal Malaysia Melaka (UTeM). In this extrusion process, a temperature of 165°C and 300 RPM speed were used to produce the requirement diameter of filament composite, less than 1.75 mm. The filament was stored in a desiccator to maintain quality before printing.

Preparation of 3D Printed Sample

Ender-3 3D printer (Creality, Shenzhen, China) with a nozzle diameter of 0.8 mm was used to print the composite filament of CcPP. In this study, the best two printing parameters, nozzle temperature and bed temperature, were examined in relation to the printability of CcPP filaments from three different percentages of fiber loading (1%, 3%, and 5%). These three fiber loadings were used to select the best nozzle and bed temperature for the sample printing process. Nozzle temperatures were set at 225°C to 245°C and bed temperatures of 50°C and 80°C. Other printing parameters were fixed, as shown in Table 1. Wall line count, horizontal expansions, and top and bottom thickness

Table 1
Printing parameter settings

Parameters	Settings
Layer Height (mm)	0.2
Wall Thickness (mm)	1.6
Nozzle Temperature (°C)	225, 230, 235, 240 and 245
Bed Temperature (°C)	50 and 80
Printing Speed (mm/s)	70
Print Cooling	No
Build Plate Adhesion Type	Brim
Infill Pattern	Triangle

were defaulted for PP material. The printed samples were designed using SolidWorks 2016 CAD and Ultimaker Cura 4.10 software.

In the first stage, the temperature of the printing nozzle and print bed with the best printability results for the CcPP filaments with different fiber loadings (1%, 3%, and 5%) were identified and selected for further evaluation based on the qualitative evaluation. In the second stage, 3D printed specimens were produced using the selected temperature of the nozzle and print bed with the best printability results to evaluate the effects of infill densities (25% and 50%) and fiber loadings (1%, 3%, and 5%) on the tensile properties.

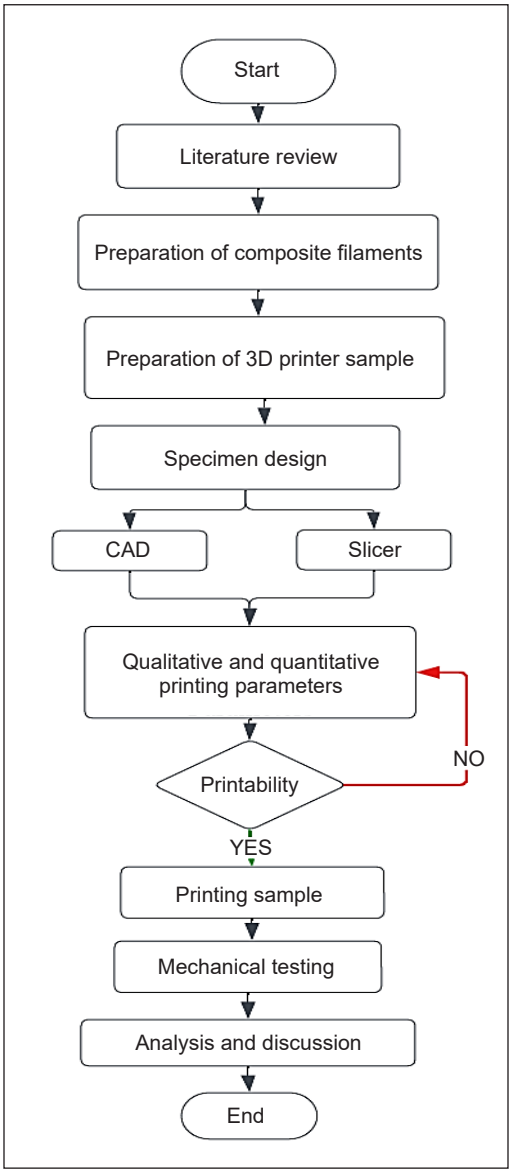

Figure 1. The process flow to identify the printability of filament composite using qualitative and quantitative measurements

Evaluation of the Printability

Figure 1 depicts the process flow chart to identify the printability of CcPP filament composite using qualitative and quantitative measurements. Four qualitative measurements were used to identify the printability of the filament composite: complete deposition, unwarping, good finishing, and adequate heat. Yes (/) and No (X) were used to complete the assessments of these four elements while printing each sample. Complete deposition means the sample was successful and uniformly laid down the material layer by layer, with no gaps and defects. Unwarping means no uneven cooling or contraction deformation of the printed sample, which retains its intended shape. Moreover, good finishing refers to achieving a smooth and aesthetically pleasing surface. Adequate heat in this study means two appropriate types of temperatures: bed and nozzle temperatures during the printing process. Correct temperature influences material flow, adhesion, and overall print quality. It is very important to prevent nozzle clogging,

unwarping, and poor layer adhesion. The quantitative printing process parameters involved infill density, which were 25 and 50%.

Evaluation of Tensile Properties

The tensile test samples were printed in accordance with ASTM D638, type IV. Tensile properties are measured to analyze the effect of infill density and fiber loading on the printed composite. A minimum of 50% of the grip section of the dumbbell-shaped specimen was clamped to the universal testing machines, then pulled by an amount of 10 kN of load with the speed of 10 mm/min to break the middle section of the specimen. The average, standard deviation and bar chart were used to analyze the tensile properties in this study.

RESULTS AND DISCUSSION

Qualitative and Quantitative Measurements of Printability for CcPP Filament Composite

The temperature of the nozzle and print bed is crucial in 3D printing process applications; the successful printing of filaments composite depends on the printing process parameters. The qualitative measurements were used to identify the ideal temperature for the printing nozzle and bed to print with CcPP filaments composite of different fiber loadings (1%, 3%, and 5%). Appropriate temperature settings are critical for melting the filament composite to ensure adhesion to the print bed. Specific temperature ranges are required for different filament composites to achieve optimal flow and bonding (Kristiawan et al., 2021). These issues are crucial to overcome the limitations in 3D printing applications, such as clogging, weak layer adhesion, warping, and surface defects (Ali et al., 2023; Jeon et al., 2020). Figure 2 (a) shows a printed sample with incomplete layer adhesion, (b) early warping, and (c) heavy warping. It is very important to identify the correct bed and nozzle temperature to print the sample. Bed temperature helps ensure the first print layer adheres properly to the building part. Warmer bed temperature can improve the adhesion of the filament to build a platform, reducing the chances of detachment or warping while printing the sample.

Temperature is critical in 3D printing as different materials have different melting temperatures. Jeon et al. (2020) reported significant differences in the samples printed with different nozzle and bed temperatures for four printing materials (PLA, lay-wood, ABS,

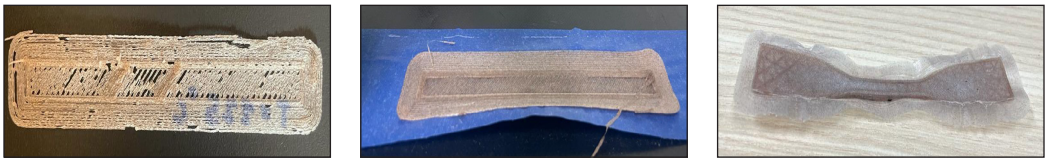

(a) (b) (c)

Figure 2. Incomplete layer thickness: (a) early warping; (b) heavy warping; and (c) CcPP filament composite

and nylon). Multiple printing trials of the samples were implemented between the range of nozzle and bed temperature to finalize the best combination. Table 2 shows the qualitative and quantitative measurements of printability for the CcPP filament composite in this study. The four qualitative measurements used in this study were complete deposition, unwarping, good finishing, and adequate heat for nozzle and bed temperatures.

Table 2
Qualitative and quantitative measurements of printability for CcPP filament composite

Temperature		Measurements of Printability			
Nozzle (°C)	Bed (°C)	Complete Deposition	Unwarping	Good Finishing	Adequate Heat (Nozzle and Bed)
225	50	X	X	X	X
230	50	/	X	X	X
230	80	/	/	/	/
235	80	/	/	X	X
240	80	/	/	X	X
245	80	/	X	X	X

Figures 3 (a) and (b) show the sample quality from the nozzle temperature of 245°C and 230°C, respectively. The sample from the nozzle temperature of 245°C had an unsatisfactory outcome with a poor surface finish and rough texture in Figure 3(a). High temperatures can rapidly melt CcPP filament composite, resulting in uneven flow and deposition (Khan & Mishra, 2020). Figure 3(b) shows better finishing on the sample's surface with a nozzle temperature of 230°C and bed temperature of 80°C. Additionally, there was no early warping, and the smooth printing process was finished with a complete sample for the tensile testing standard. After multiple trials with maximum observation during the printing process on the qualitative measurements, the best combination of bed and nozzle temperature to produce good surface finishing was identified with the printing setting as follows: 230°C for the nozzle temperature and 80°C for the bed temperature.

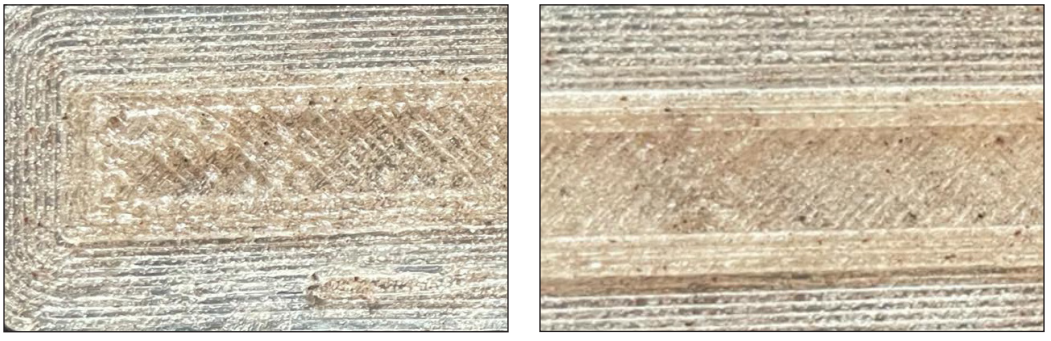

(a) (b)

Figure 3. The printing quality of CcPP filaments composite: (a) 245°C; and (b) 230°C

The selected nozzle and bed temperatures were used to print tensile testing samples with different fiber loading and infill density. Three samples were printed for each testing combination (fiber loading x infill density), with 18 printed tensile testing samples.

The infill density is another parameter affecting the printing sample's quality (Samykano et al., 2019). Figures 4 (a) and (b) show the CcPP filament composites with 25% and 50% infill density, respectively. The 25% infill density sample was lighter than the 50% infill density because less material was used to fill the sample's interior compared to the 50% infill density. Higher empty spaces were observed on printed samples with 25% infill density (Figure 4a) compared to 50% infill density (Figure 4b). Higher infill densities can provide greater strength and durability, but it will lead to higher time and material consumption. Previous studies on bamboo-filled PLA-based material showed a significant effect of infill density on the tensile strength and fatigue properties (Müller et al., 2022). Mechanical behavior is affected by the infill density and the infill pattern, as Tanveer et al. (2022) mentioned.

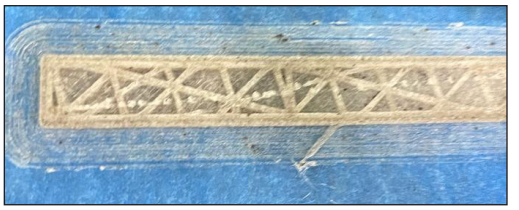

(a)

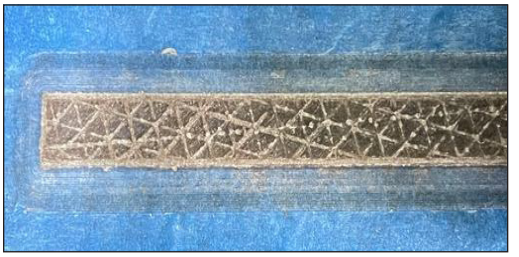

(b)

Figure 4. The printed sample from CcPP filaments composite with: (a) 25%; and (b) 50% infill densities

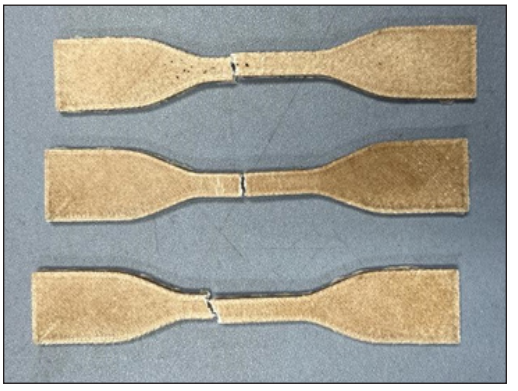

Figure 5. The tensile test samples

The effect of infill density on the tensile properties was further analyzed in this study. A previous study by Müller et al. (2022) proved that infill density significantly affects the tensile strength and fatigue properties of low-cycle stress bamboo-filled PLA-based materials in FDM 3D printing applications. Figure 5 shows the successful samples for tensile testing of the CcPP filament composite.

Tensile Properties of CcPP Filament Composite

Figures 6 and 7 present the tensile strength and tensile modulus of the CcPP composite. The highest tensile strength for 25% infill density was produced by 3% fiber loading with 17.23 MPa, while for 50% infill density, samples with 5% fiber loading had the highest

tensile strength of 22.87 MPa. This finding is equivalent to the tensile modulus shown in Figure 7. The tensile modulus increased with increments in the percentage of fiber loading. The highest tensile modulus of 641.23 MPa was contributed by 50% infill density with 3% fiber loading. Among the samples with 25% infill density, 5% fiber loading had the highest tensile modulus of 493 MPa. A higher infill density provides more material to resist deformation, resulting in a stiffer overall structure. The solid internal structure improves the load-bearing capacity of the printed object, leading to a higher modulus of elasticity (Płatek et al., 2020). Various factors affect the properties of the composite; for 3D printed parts, printing process parameters can be a factor that contributes to inconsistent output. Measuring the relationship between the printing process parameters is important to avoid relevance output (Attoye et al., 2019; Hanon et al., 2021). A previous study on the effect of infill density on tensile mechanical properties of 3D printed carbon-fiber nylon composite found that 50% infill density with a triangle pattern produced a higher tensile property

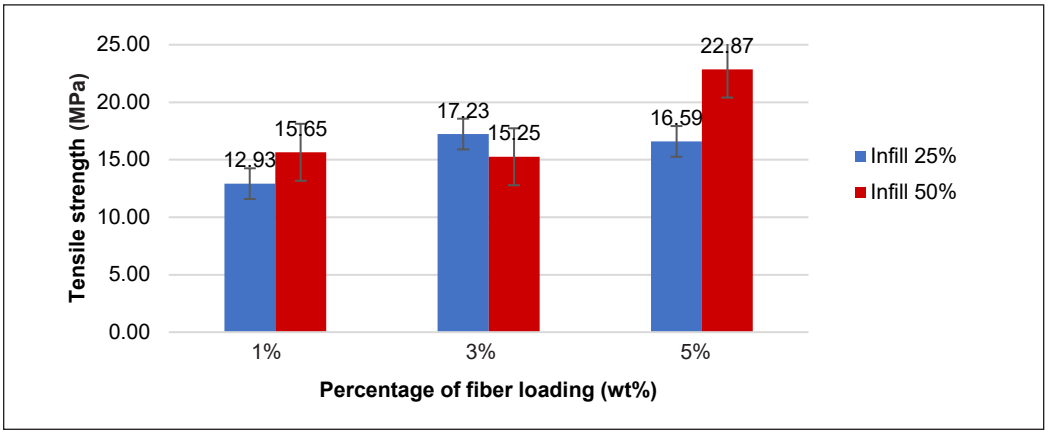

Figure 6. The Tensile Strength of CcPP for 25 and 50% infill densities

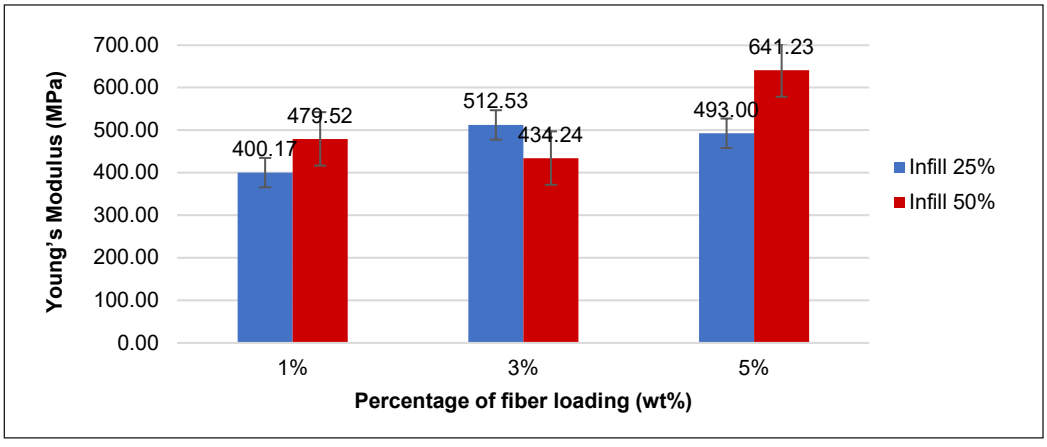

Figure 7. The Young's Modulus of CcPP for 25 and 50% infill densities

compared to 30 and 100% infill densities (Ali et al., 2023). The review of Tanveer et al. (2022) mentioned that appropriate infill density highly depends on the type of application for the printed part. Furthermore, a large number of printed parts can be replicated to increase accuracy during the data collection and analysis. The demand for natural fiber composite in 3D printing is increasing yearly. The development of bio-composite filament in the 3D industry needs a good understanding of material and technology (Birosz et al., 2022; Lalegani & Mohd Ariffin., 2020).

CONCLUSION

This study's first stage presents the best nozzle and bed temperature on the CcPP filament composite printability. Complete deposition, unwarping, good finishing, and adequate heat for the nozzle and bed temperature were the qualitative measurements used to assess the 3D printability of the CcPP filament composite. The result revealed that the highest printability ratings of CcPP filament composite were obtained with the printing nozzle temperature of 230 °C and bed temperature of 80 °C. Two infill densities (25% and 50%) with three different fiber loadings of filament composite (1%, 3%, and 5%) were used to analyze the effect on the tensile properties of the filament composite in the second stage of this study. The highest tensile strength of 22.87 MPa and Young's Modulus of 641.23 MPa were obtained from composite printed with 50% infill density and 5% fiber loading. The lowest tensile strength of 12.93 MPa and Young's Modulus of 400.17 MPa were obtained from composite printed with 25% infill density and 1% fiber loading. Moreover, at 1% and 3% fiber loadings, the effect of infill density on tensile strength and modulus was not significant; however, the effect of infill density on tensile strength and modulus became significantly different at 5% fiber loading. Further study on the physical and other mechanical properties, such as flexural testing, impact testing, and surface roughness, should be conducted to analyze the CcPP filament composite's performance further. The findings of the interconnection between the printing process parameters and mechanical properties can assist the design engineer in optimizing the usability of the material.

ACKNOWLEDGEMENT

The study is funded by the Ministry of Higher Education (MOHE), Malaysia, through the Fundamental Research Grant Scheme (FRGS), No: FRGS/1/2022/STG06/UTEM/02/1. The authors thank Universiti Teknikal Malaysia Melaka (UTeM) for all the support.

REFERENCES

Ahn, S., & Wright, P. K. (2002). Anisotropic material properties of fused deposition modeling ABS. *Rapid Prototyping Journal*, *8*(4), 248–257. https://doi.org/10.1108/13552540210441166

Alafaghani, A., Ablat, M. A., Abedi, H., & Qattawi, A. (2021). Modeling the influence of fused filament fabrication processing parameters on the mechanical properties of ABS parts. *Journal of Manufacturing Processes*, *71*, 711–723.

Ali, Z., Yan, Y., Mei, H., Cheng, L., & Zhang, L. (2023). Effect of infill density, build direction and heat treatment on the tensile mechanical properties of 3D-printed carbon-fiber nylon composite. *Composite Structure, 304,* 116370.

Alsubari, S., Zuhri, M. Y. M., Sapuan, S. M., Ishak, M. R., Ilyas, R. A., & Asyraf, M. R. M. (2021). Potential of natural fiber reinforced polymer composites in sandwich structures: A review on its mechanical properties. *Polymers*, *13*(3), 1–20. https://doi.org/10.3390/polym13030423

Attoye, S., Malekipour, E., & El-mounayri, H. (2019). Correlation between process parameters and mechanical properties in parts printed by the fused deposition modeling process. In S. Kramer, J. L. Jordan, H. Jin, J. Carroll & A. M. Beese (Eds.), *Mechanics of Additive and Advanced Manufacturing*, Volume 8, Conference Proceedings of the Society for Experimental Mechanics Series (pp. 35–41). Springer. https://doi.org/10.1007/978-3-319-95083-9_8

Beg, D. A., & Hasan, M. F. (2020). Study of mechanical properties of polypropylene natural fiber composite. *International Journal for Research in Applied Science & Engineering Technology. 8*(9), 255-259. https://doi.org/10.22214/ijraset.2020.31453

Birosz, Tamas, M., Ledenyak, D., & Ando, M. (2022). Effect of FDM infill patterns on mechanical properties. *Polymer Testing*, *113*, 107654. https://doi.org/10.1016/j.polymertesting.2022.107654

Hamid, H. A., Omar, G., Muhammad, N., Azmmi, N., & Hasan, R. (2022). Proceedings optimization of natural polymer additives towards tribological behavioural of bio-oil extracted from peel waste of *musa aluminata balbisiana*. *Materials Today: Proceedings*, *51*, 1316–1322. https://doi.org/10.1016/j.matpr.2021.10.392

Hanon, M. M., Dobos, J., & Zsidai, L. (2021). The influence of 3D printing process parameters on the mechanical performance of PLA polymer and its correlation with hardness. *Procedia Manufacturing*, *54*, 244–249. https://doi.org/10.1016/j.promfg.2021.07.038

Hawary, O. El, Boccarusso, L., Ansell, M. P., Durante, M., & Pinto, F. (2023). An overview of natural fiber composites for marine applications. *Journal of Marine Science and Engineering*, *11*(1076), 1–52. https://doi.org/10.3390/jmse11051076

Ilyas, R. A., Zuhri, M. Y. M., Aisyah, H. A., Asyraf, M. R. M., Hassan, S. A., Zainudin, E. S., Sapuan, S. M., Sharma, S., Bangar, S. P., Jumaidin, R., Nawab, Y., Faudzi, A. A. M., Abral, H., Asrofi, M., Syafri, E., & Sari, N. H. (2022). Natural fiber-reinforced polylactic acid, polylactic acid blends and their composites for advance applications. *Polymers*, *14*(202), 1–39. https://doi.org/10.3390/polym14010202

Jeon, H., Park, J., Kim, S., Park, K., & Yoon, C. (2020). Effect of nozzle temperature on the emission rate of ultrafine particles during 3D printing. *Robotics and Computer-Integrated Manufacturing*, *30*, 306–314. https://doi.org/10.1111/ina.12624

Jumaidin, R., Sapuan, S. M., Jawaid, M., Ishak, M. R., & Sahari, J. (2017). Thermal, mechanical, and physical properties of seaweed/sugar palm fibre reinforced thermoplastic sugar palm Starch/Agar hybrid composites. *International Journal of Biological Macromolecules*, *97*, 606–615. https://doi.org/10.1016/j.ijbiomac.2017.01.079

Khan, M. S., & Mishra, S. B. (2020). Minimizing surface roughness of ABS-FDM build parts: An experimental approach. *Materials Today: Proceedings*, *26*, 1557–1566. https://doi.org/10.1016/j.matpr.2020.02.320

Kristiawan, R. B., Imaduddin, F., Ariawan, D., Ubaidillah, & Arifin, Z. (2021). A review on the fused deposition modeling (FDM) 3D printing: Filament processing, materials, and printing parameters. *Open Engineering*, *11*(1), 639–649. https://doi.org/10.1515/eng-2021-0063

Lalegani, D. M., & Mohd Ariffin, M. K. A. (2020). The effects of combined infill patterns on mechanical properties in FDM process. *Polymers*, *12*(12), 2792. https://doi.org/10.3390/polym12122792

Le Duigou, A., Correa, D., Ueda, M., Matsuzaki, R., & Castro, M. (2020). A review of 3D and 4D printing of natural fibre biocomposites. *Materials and Design*, *194*, 108911. https://doi.org/10.1016/j.matdes.2020.108911

Mastura, M. T., Noryani, M., Hazliza Aida, C. H., Nuzaimah, M., Shaharuzaman, M. A., Zakaria, N. H., & Loh, Y. F. (2022). Statistical analysis of the performance of young's modulus of natural fiber composites and synthetic fiber composites. *Jurnal Teknologi*, *84*(6–2), 151–162. https://doi.org/10.11113/jurnalteknologi.v84.19366

Muhammad, N., Shaharuzaman, M. A., Taha, M. M., & Buniamin, F. F. (2022). Prediction of mechanical and physical properties of hybrid composites using ROHM. *Proceedings of Mechanical Engineering Research Day 2022*, *August*, 95–96.

Müller, M., Jirků, P., Šleger, V., Mishra, R. K., Hromasová, M., & Novotný, J. (2022). Effect of infill density in FDM 3D printing on low-cycle stress of bamboo-filled PLA-based material. *Polymers*, *14*(22). https://doi.org/10.3390/polym14224930

Muthe, L. P., Pickering, K., & Gauss, C. (2022). A Review of 3D / 4D printing of poly-lactic acid composites with bio-derived reinforcements. *Composites Part C: Open Access*, *8*(April), 100271. https://doi.org/10.1016/j.jcomc.2022.100271

Płatek, P., Rajkowski, K., Cieplak, K., Sarzyński, M., Małachowski, J., Woźniak, R., & Janiszewski, J. (2020). Deformation process of 3D printed structures made from flexible material with different values of relative density. *Polymers*, *12*(9). https://doi.org/10.3390/POLYM12092120

Radzi, A. M., Sapuan, S. M., Jawaid, M., & Mansor, M. R. (2017). Influence of fibre contents on mechanical and thermal properties of roselle fibre reinforced polyurethane composites. *Fibers and Polymers*, *18*(7), 1353–1358. https://doi.org/10.1007/s12221-017-7311-8

Samykano, M., Selvamani, S. K., Kadirgama, K., Ngui, W. K., Kanagaraj, G., & Sudhakar, K. (2019). Mechanical property of FDM printed ABS: Influence of printing parameters. *International Journal of Advanced Manufacturing Technology*, *102*(9–12), 2779–2796. https://doi.org/10.1007/s00170-019-03313-0

Tanveer, M. Q., Mishra, G., Mishra. S., & Sharma., R. (2022). Effect of infill pattern and infill density on mechanical behaviour of FDM 3D printed Parts-a current review. *Materials Today: Proceedings, 62*, 100-108. https://doi.org/10.1016/j.matpr.2022.02.310

Pertanika J. Sci. & Technol. 32 (S3): 69 - 79 (2024)

PERTANIKA JOURNALS

SCIENCE & TECHNOLOGY

Journal homepage: http://www.pertanika.upm.edu.my/

Carrageenan-based Film Utilization for Eco-friendly Tea Bag

Yeni Pamita Sukmawati, Putri Alisya Oktavia Sarumaha, Nabila Fisa Sabrina, Reza Widyasaputra* and Ida Bagus Banyuro Partha

Department of Agricultural Product Technology, Faculty of Agriculture Technology, Institut Pertanian Stiper (INSTIPER), 55283, Yogyakarta, Indonesia

ABSTRACT

This study addresses concerns related to potential health risks associated with chlorine residues in traditional tea bags, which exhibit resistance to decomposition in soil. Consequently, the study utilized carrageenan, derived from *Eucheuma cottonii* seaweed, as a coating material for edible film. This research explores the impact of carrageenan concentration and drying temperature on the performance of tea bags. This study applied the randomized complete block design to analyze the impact of three carrageenan concentrations (1%, 3%, and 5%) at three different drying temperatures (80ºC, 85ºC, and 90ºC) on carrageenan-based film. The investigation comprehensively evaluates the compliance of the carrageenan-based film with commercial-grade quality standards through critical factors such as thickness, solubility, mechanical strength and hedonic analysis. The findings indicate that the most effective carrageenan-based edible film can be produced at a concentration of 3% and a drying temperature of 90°C, highlighting its potential as an eco-friendly alternative in tea bag production.

Keywords: Carrageenan concentration, carrageenan-based edible film, drying temperature, *Eucheuma cottonii*, tea bag

ARTICLE INFO

Article history:
Received: 22 February 2024
Accepted: 30 May 2024
Published: 30 July 2024

DOI: https://doi.org/10.47836/pjst.32.S3.06

E-mail addresses:
yenipamitas@gmail.com (Yeni Pamita Sukmawati)
putrisar28@gmail.com (Putri Alisya Oktavia Sarumaha)
nabilahfisa21@gmail.com (Nabila Fisa Sabrina)
rezaws@instiperjogja.ac.id (Reza Widyasaputra)
thp@instiperjogja.ac.id (Ida Bagus Banyuro Partha)
* Corresponding author

INTRODUCTION

Indonesia has many traditions that make it a country full of diversity and beauty. Each corner has special, interesting characteristics and cannot be replaced easily. Among the myriad fascinating traditions, one that stands out is the ritual of drinking tea, locally referred to as “Ngeteh” in the Javanese dialect (Fernandes & Kurniawan, 2014).

ISSN: 0128-7680
e-ISSN: 2231-8526

Tea is a frequently enjoyed beverage known for both its affordability and positive impact on health, owing to the beneficial compounds found within it. Over time, there has been a growing preference for tea bags due to their convenience and practicality. An emerging habit involves leaving the tea steeping for an extended duration to extract more of its benefits. However, it is important to note that prolonged steeping can dissolve chlorine, a paper-bleaching agent in the tea bag, without the consumer's awareness. (Wansi & Wael, 2014).

Apart from the chlorine content in tea bags, the POM Agency (2016) conveys several things related to the content of tea bags, namely, "Tea bags are generally made of paper and plastic." Polyethylene plastic in tea bags serves the purpose of heat sealing, and its notable characteristic is that it does not melt at the boiling point of water, which is evident when tea bags remain unopened. Including microplastics in tea bags raises concerns for health and the environment, as these particles are challenging to decompose. Furthermore, the persistence of microplastics in the environment can lead to potential ecological repercussions, emphasizing the need for sustainable alternatives in tea bag production (Afrin et al., 2022).

In this context, edible film packaging emerges as an alternative material with the potential to maintain the quality of food ingredients while being environmentally friendly. According to Siah et al. (2015), applying edible film packaging using seaweed as a viable raw material provides a novel approach to tea bag production. Through initial processing to obtain carrageenan flour derived from seaweed, this flour becomes a pivotal component in producing edible films for crafting tea bags.

Carrageenan is the sap of the seaweed *Eucheuma cottonii*, and this type belongs to the class of red algae *(Rhodophyceae*). Carrageenan can be obtained by extracting seaweed with water or alkaline solvents. Carrageenan is a linear polysaccharide with a large molecule consisting of more than 1000 galactose residues consisting of ester, potassium, sodium, and potassium sulfate with galactose and 3,6 anhydrogalactopolymer (Rusli et al., 2017). Based on cell bonds and gel properties, carrageenan can be divided into three types, namely kappa, iota, and lambda. Kappa carrageenan produces the strongest gel properties, while lambda carrageenan does not form a gel in water. Still, lambda carrageenan interacts well with protein, so this type is suitable for food production. *E. cottonii* produces kappa carrageenan that dissolves in hot water and forms a gel in water (Fardhyanti & Julianur, 2015).

Carrageenan derived from seaweed can be used as a thickener, superstitious, stabilizer, and emulsifier. Apart from that, carrageenan is also widely used in the industrial world, both in the food, cosmetics, and pharmaceutical industries. This research uses carrageenan as a food coating in edible film. Nonetheless, there is a significant gap in research on the factors that influence the production of biodegradable tea bags using edible seaweed films. This study aims to fill this gap by investigating crucial factors such as the ideal proportion of carrageenan flour and an appropriate drying temperature. This sustainable approach not

only introduces an eco-friendly packaging solution but also harnesses the natural properties of seaweed, potentially enhancing the overall health benefits of tea consumption.-

MATERIALS AND METHODS

This research used carrageenan flour from seaweed (*E. cottonii*) from Maluku's coastal area. Food-grade glycerin and distilled water were purchased from the chemical center shop. The Indonesian black tea (Poci brang) was purchased from the Maguwoharjo traditional market.

Production of Carrageenan Based Film (Rani & Kalsum, 2016)

According to Figure 1, the production of the edible film involved several key steps. A carrageenan solution was initially prepared at three concentration levels: 1%, 3%, and 5% (w/v). For each concentration, 1, 3, and 5 grams of carrageenan flour were placed into a 100 mL measuring cup, and distilled water was added to reach a volume of 100 mL. The mixture was then stirred using a magnetic stirrer and heated until it reached a temperature of 60°C. Once this temperature was attained, 10% (v/v) glycerol was introduced to the solution as a plasticizer, with continuous stirring and further heating to reach 80°C. The

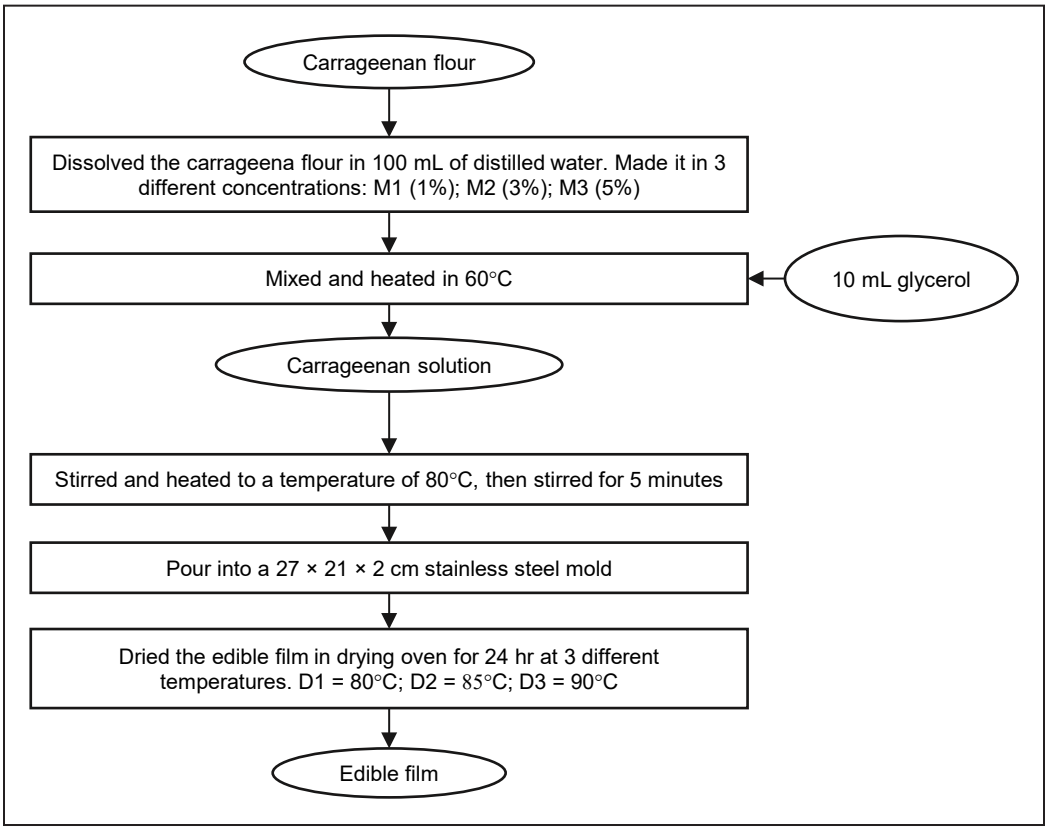

Figure 1. Carrageenan based edible film preparation

still-warm carrageenan solution was poured into a plastic mold or tray and left to stand for 10 minutes at room temperature. The sample was oven-dried for 10 hours at different temperatures (factor D parameters).

Production of Pouch

The pouch (tea bag) was produced according to Figure 2. The film sample was then cut into a 6 × 10 cm rectangular shape. It was started by folding the 10 cm edge to 1 cm and then folding the edible film in half until the bag was 5 cm long. The pocket was sealed on both the right and left sides. The bag was filled with ¾ of a tea bag's worth of tea powder, then sealed the top to ensure no part of the bag was open. Finally, a hole was made in the bag with a needle to allow proper tea extraction.

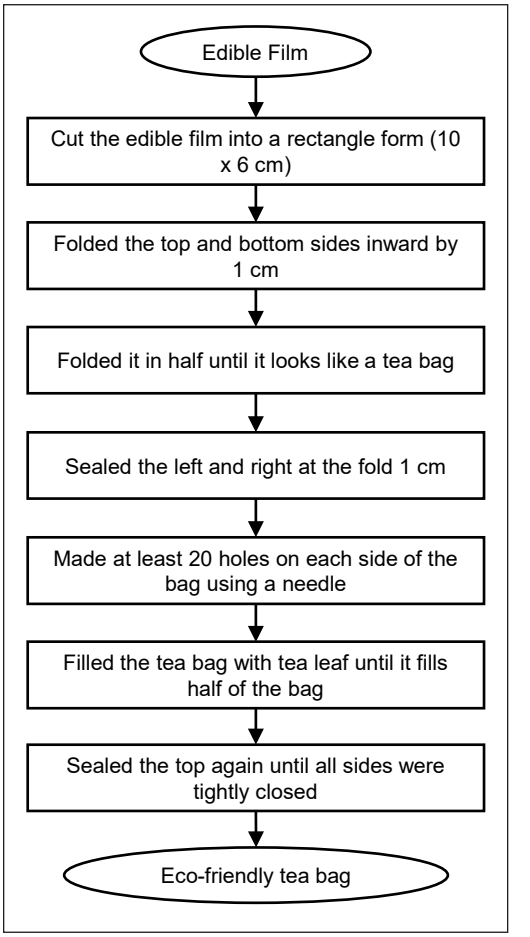

Figure 2. Eco-friendly tea bag preparation

Water Content and Solubility Analysis

The squares (2 × 2 cm) were cut from the films and weighed (W1), then the films were put in the Ecocell 55 (105°C) oven for 2 h and then weighed again (W2). The squares were put in the beaker containing 25 mL of distilled water, and after 24 h at laboratory temperature, the films were dried and weighed (W3). Water content and solubility were calculated according to Equations 1 and 2:

$$\text{Water content (\%)} = [(W1-W2)/W1] \times 100 \quad [1]$$

$$\text{Solubility (\%)} = [(W2-W3)/W2] \times 100 \quad [2]$$

Ash Content Analysis

TAPPI standard method, T211 om-85, was used to determine the ash content. The oven-dried sample (2 g) was burned (dry oxidation) in a muffle furnace model at 575 ± 25°C for 4 h. This standard test method was used to determine the volume of ash remaining after dry oxidation of the sample. The percentage of ash was calculated by Equation 3:

$$\text{Ash (\%)} = \frac{\text{Weight of solids remaining (g)}}{\text{Original weight of carbon (g)}} \times 100 \quad [3]$$

Tensile Strength and Elongation Analysis

Tensile strength and elongation were measured using a UTM (*Universal Testing Machine*). The squares (5 × 10 cm) were cut from the films and placed under the top plate. The working principle of UTM is that the plate will apply a pulling force to the object until it breaks. Later, the parameters in UTM will show the maximum value or data on the strength of the material (Tensile Strength). The elongation data was also shown by comparing the object's length before and after being tested.

Organoleptic Test

An organoleptic test was performed on 20 untrained panelists with two parameters (color and aroma). Seven sequential scales were used, starting from 1 (dislike very much), 2 (dislike), 3 (dislike slightly), 4 (neither like nor dislike), 5 (like slightly), 6 (like), and 7 (like very much).

Statistical Analysis

This research used a Completed Block Design (CBD) with two treatment factors and two repetitions. Factor I was the Percentage of Carrageenan Addition (M), with three concentrations, M1 (1%), M2 (3%), and M3 (5%), and Factor II was the Effect of Drying Temperature (D), with temperature variations D1 (80°C), D2 (85°C) D3 (90°C). The process was replicated twice to yield 18 experimental units (3 x 3 x 2 repetitions). The data obtained was analyzed with analysis of variance (ANOVA) at a 95% confidence level ($p \leq 0.05$).-

RESULTS AND DISCUSSION

The test results showed that carrageenan flour had an average water content of 5.3 ± 0.8 % and an ash content of 13.2 ± 0.9 %. The results indicated that the novel tea bag preparation method complied with commercial-grade quality standards, according to the Standard National Indonesia (SNI) specifications, which specified a maximum water content of 14% and an ash content of 18% for commercial carrageenan flour.

Figure 3 illustrates the thickness analysis, wherein measurements were taken from three sides. The depicted results represent the average value obtained from the thickness analysis.

As illustrated in Figure 3, it is evident that elevating the temperature results in a thinner formation of the edible film due to increased water evaporation, thereby reducing its thickness. Conversely, a higher percentage of carrageenan leads to a thicker edible film. It was attributed to the increased total solid content in the higher percentage of edible films. This observation aligns with findings from Supeni (2012). Notably, the Japanese

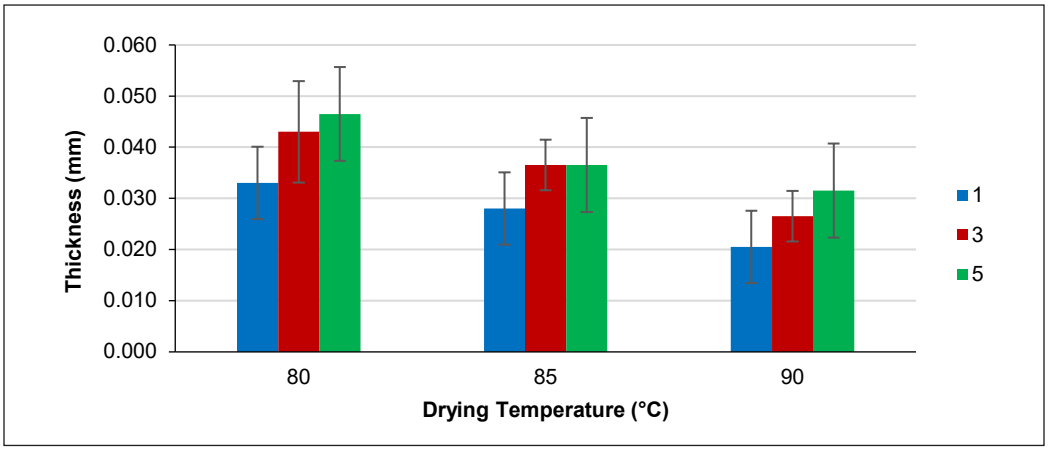

Figure 3. Effect of different percentages of carrageenan (1%, 3% and 5%) and drying temperature (80°C, 85°C and 90°C) against edible film thickness (mm).
Note. Values given are mean (SD)

Industry Standard stipulates a maximum allowable thickness for the edible film at 0.25 mm, confirming that the formed edible film complies with the standard (Dwimayasanti & Kumayanjati, 2019). Furthermore, the analysis of variance revealed no significant difference in the drying temperature and thickness factor, showing the stability and consistency of the results under varying conditions.

The data of solubility analysis in hot water can be obtained in Figure 4, which shows that the higher the percentage of carrageenan, the higher the solubility. This outcome is attributed to the increase in the dissolved solids content originating from the basic ingredients for making edible films as well as an increase in the number of intermolecular bonds in the edible film-making solution and the nature of carrageenan which is hydrophilic and can only dissolve in hot water solvents (Rusli et al., 2017). Examining Figure 4 reveals

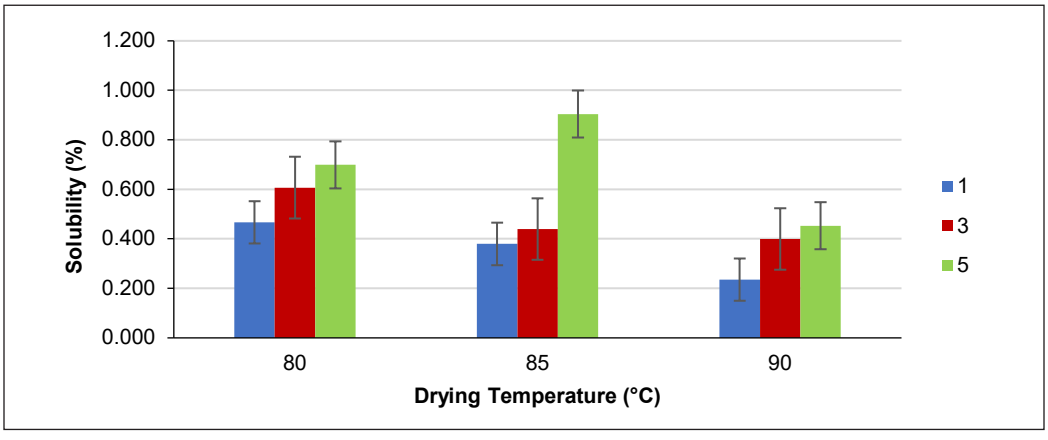

Figure 4. Effect of different percentages of carrageenan (1%, 3%, 5%) and drying temperature (80°C, 85°C and 90°C) against the solubility of edible film in hot water (%)

a direct proportionality between the percentage of carrageenan and solubility in each drying temperature treatment. This correlation may be influenced by the solvent temperature, causing a substantial dissolution of the edible film's solids in water, resulting in higher solubility for a higher percentage of carrageenan. Conversely, the drying temperature exhibits an inverse relationship, with higher temperatures leading to lower solubility of the edible film. Higher drying temperature reduces the water content of the film. Low water content would form a denser film structure (Sutharsan et al., 2023). The film would be less accessible to the water. The analysis of variance showed that there was no significant difference in drying temperature and solubility factor.

Consequently, the film prepared under elevated temperatures is preferable, as it would exhibit reduced susceptibility to water penetration. This feature emphasizes their improved water resistance and signifies their overall advantageous quality in terms of durability and potential for extended use in hot beverages.

Tensile strength is a crucial mechanical property of edible film, as it directly correlates with the film's capability to shield or encapsulate food ingredients and prevent the food products from experiencing physical or chemical changes (Rusli et al., 2017).

In Figure 5, it was seen that there was an increase in tensile strength for a higher percentage of carrageenan. In general, the higher the concentration of carrageenan given, the tensile strength or elongation of the edible itself increased. A higher percentage of carrageenan enhances the edible film's water-binding ability due to the inherent hygroscopic nature of carrageenan. This forms a gel matrix, increasing the bonds between constituent molecules and yielding a more compact edible film. Consequently, this leads to higher elongation percentages and tensile strength in the edible film. (Handito, 2011). However, the study results did not exhibit this phenomenon, which was potentially influenced by the higher drying temperature. The elevated temperature increased water evaporation,

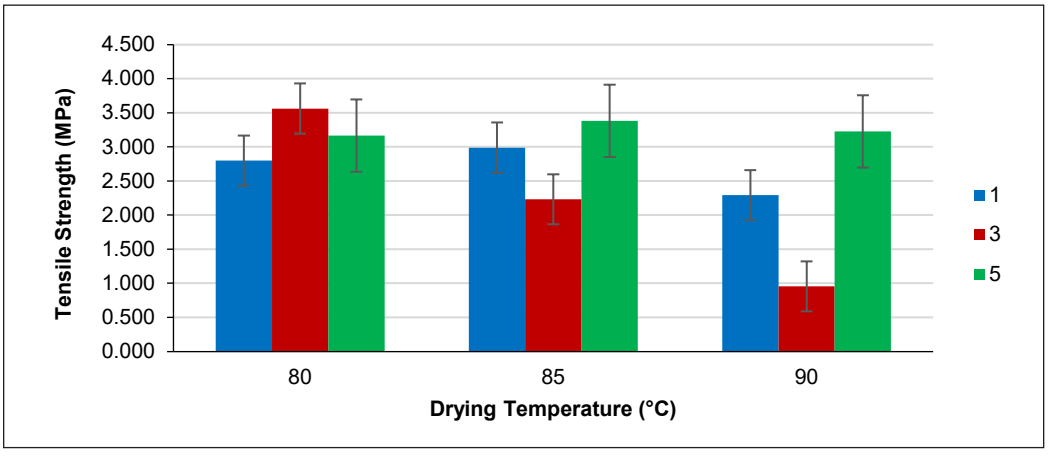

Figure 5. Effect of different percentages of carrageenan (1%, 3% and 5%) and drying temperature (80°C, 85°C and 90°C) on tensile strength of edible film (MPa)

diminishing carrageenan's gelling properties and reducing the edible film's tensile strength (Handito, 2011). In accordance with the Japanese Industrial Standard (1975), the edible film's tensile strength should be at least 0.39 MPa. This requirement is achieved by all edible films produced in this study via the novel process.

Based on Figure 6, it was observed that increasing the percentage of carrageenan increased the elongation of the edible film. Likewise, with tensile strength, a higher percentage of carrageenan made the carrageenan molecules that formed the film matrix stronger so that the film became more inelastic or brittle. Increasing the concentration of carrageenan could increase the bonding between polymeric materials (Rahmawati et al., 2019). As a result, the percentage of elongation decreased. The edible film with the smallest elongation value resulting from this research was at a carrageenan concentration of 3% at a drying temperature of 90ºC, which could be categorized as having the highest mechanical strength. Darawati and Pranoto (2010) supported this opinion that the stronger the film formed, the more difficult it was to elongate, thus reducing the extension percentage value.

From Figure 7, the organoleptic score of aromas was between 4–5 (neither like nor dislike to like slightly). The higher the drying temperature, the lower the favorability value of the aroma. The aroma was a volatile compound that was easy to evaporate during drying (Qu et al., 2019; Chen et al., 2020). Additionally, the analysis of variance indicated no significant difference in the organoleptic score of aromas based on varying carrageenan percentages. Considering the economic benefits, applying lower carrageenan concentrations as the edible film is preferable.

From Figure 8, it was observed that the higher the drying temperature and the increased percentage of carrageenan, the value of the color preference decreased because,

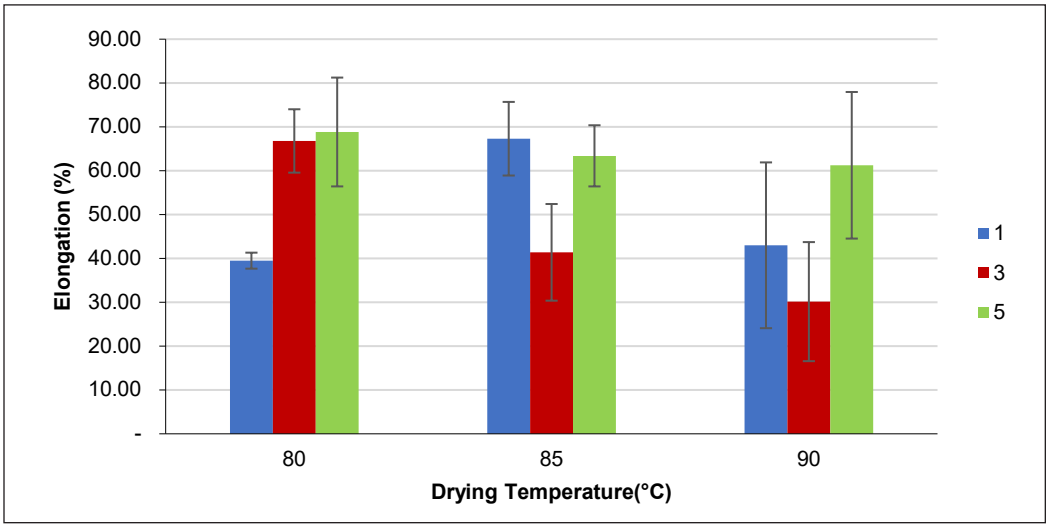

Figure 6. Effect of different percentages of carrageenan (1%, 3% and 5%) and drying temperature (80°C, 85°C and 90°C) against elongation of edible film (%)

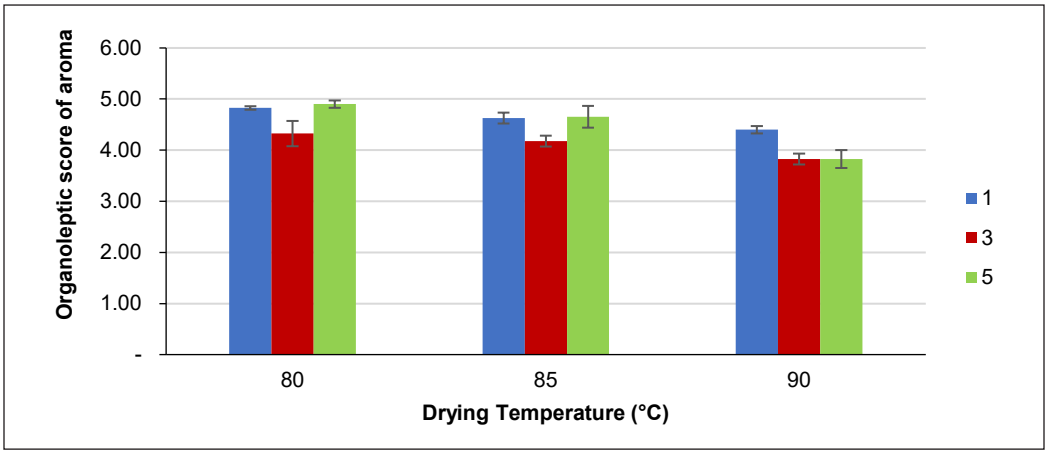

Figure 7. Effect of different percentages of carrageenan (1%, 3% and 5%) and drying temperatures (80°C, 85°C and 90°C) regarding the aroma of tea brewing

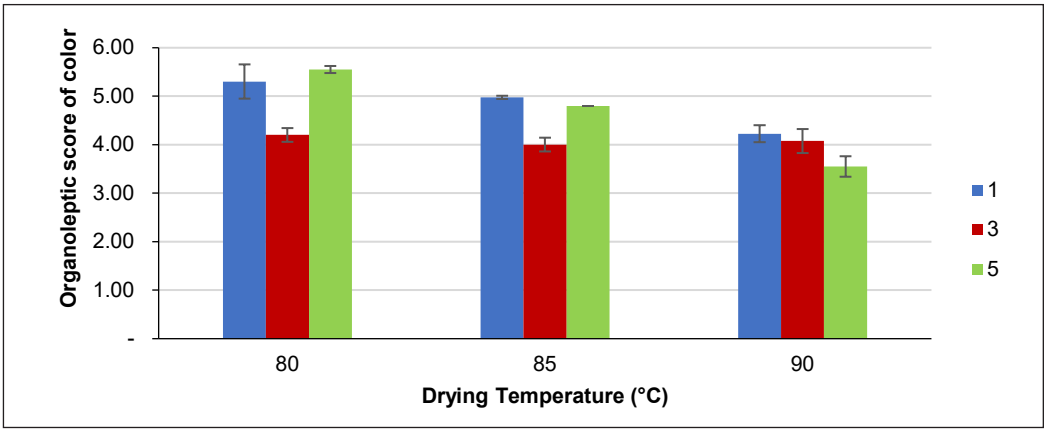

Figure 8. Effect of different percentages of carrageenan (1%, 3% and 5%) and drying temperatures (80°C, 85°C and 90°C) regarding the color of tea brewing

according to the panelists, the color faded when steeping the tea. Analysis of variance showed that there was a significant difference in drying temperature and color hedonic parameters. Variance analysis showed a significant difference in color hedonic parameters dependent on the drying temperature. According to Aluthgama et al. (2020), in black tea, the color is primarily attributed to the presence of theaflavins and thearubigins, responsible for the bright red color and dark-brown pigments, respectively. Referring to Figure 4, it is evident that solubility decreases with an increase in drying temperature. If the film is highly soluble, it may interact more readily with these compounds, resulting in a darker rather than faded appearance. Consequently, the relationship between solubility, drying temperature, and the interaction with these compounds can affect the final color outcome of the brewed tea.

CONCLUSION

Ultimately, this study investigates the feasibility of using carrageenan-based edible film derived from seaweed as an eco-friendly alternative to tea bag production. A novel finding that emerged in this study reveals a direct relationship between carrageenan percentage and solubility across different drying temperatures. This correlation, influenced by solvent temperature, leads to lower solubility for higher carrageenan percentages. The study also determined the ideal parameters for producing the edible film based on carrageenan, indicating a 3% carrageenan concentration and a 90°C drying temperature. This specific combination complies with commercial-grade quality standards. However, it also addresses critical factors such as the requirement for lower thickness and solubility, enhanced mechanical strength, and favorable aroma and color characteristics, as determined by hedonic evaluation. These parameters, which balance economic efficiency and desirable film characteristics, provide an environmentally conscious alternative material for producing high-quality tea bags. Overall, this investigation lays the groundwork for developing biodegradable and eco-friendly tea bags, presenting a sustainable solution to environmental concerns associated with conventional tea bag materials.

ACKNOWLEDGEMENT

Facilities and funds provided by The Directorate General of Higher Education, Research and Technology of Indonesia are gratefully acknowledged.

REFERENCES

Afrin, S., Rahman, M. M., Akbor, M. A., Siddique, M. A. B., Uddin, M. K., & Malafaia, G. (2022). Is there tea complemented with the appealing flavor of microplastics? A pioneering study on plastic pollution in commercially available tea bags in Bangladesh. *Science of The Total Environment*, *837*, 155833. https://doi.org/10.1016/j.scitotenv.2022.155833.

Aluthgama, A. G. S. R., Bandarab, N. P. S. N., Dissanayakeb, P. K., & Dissanayakec, R. M. B. B. B. (2020). Evaluation of physicochemical and organoleptic properties of wild tea (*Camellia sinensis*) compared to selected commercially grown tea cultivars in Sri Lanka. *Journal of Agriculture and Value Addition*, *3*(1), 1-10. https://doi.org/10.4038/java.v3i1.115

Chen, D., Xing, B., Yi, H., Li, Y., Zheng, B., Wang, Y., & Shao, Q. (2020). Effects of different drying methods on appearance, microstructure, bioactive compounds and aroma compounds of saffron (*Crocus sativus* L.). *LWT*, *120*, 108913.https://doi.org/10.1016/j.lwt.2019.108913

Darawati, M., & Pranoto, Y. (2010). Penyalutan kacang rendah lemak menggunakan selulosa eter dengan pencelupan untuk mengurangi penyerapan minyak selama penggorengan dan meningkatkan stabilitas oksidatif selama penyimpanan [Ether cellulose coatings by dipping on partially defatted peanuts]. *Jurnal Teknologi dan Industri Pangan, 21*(2), 20-26.

Dwimayasanti, R., & Kumayanjati, B. (2019). Karakterisasi edible film dari karagenan dan kitosan dengan metode layer by layer [Characterization of edible film from carrageenan and chitosan using the layer-by-layer method]. *Jurnal Pascapanen dan Bioteknologi Kelautan dan Perikanan*, *14*(2), 141-150.

Fardhyanti, D. S., & Julianur, S. S. (2015). Karakterisasi *edible film* berbahan dasar ekstrak karagenan dari rumput laut (*Eucheuma cottonii*) [Characterization of Edible Film Based on Carrageenan Extract from Seaweed (*Eucheuma Cottonii*)]. *Jurnal Bahan Alam Terbarukan, 4(2), 68-73*.

Fernandes, E., & Kurniawan, D. (2014). Perancangan media promosi menu afternoon tea Café Hare and Hatter Surabaya [Designing promotional media for the afternoon tea menu of Café Hare and Hatter Surabaya]. *Jurnal DKV Adiwarna*. *1*(4), 15-21.

Handito, D. (2011). Pengaruh konsentrasi karagenan terhadap sifat fisik dan mekanik edible film [The effect of carrageenan concentrations on mechanical and physical properties of edible films]. *Agroteksos*, *21*, 151-7.

Japanese Industrial Standard. (1975). *Japanese Standards Association* (Vol. 2: 1707).

POM Agency. (2016, December 7). Penjelasan BPOM terkait berita tentang kantong teh celup yang mengandung racun. *Badan BPOM*. https://www.pom.go.id/penjelasan-publik/penjelasan-bpom-terkait-berita-tentang-kantong-teh-celup-yang-mengandung-racun

Qu, F., Zhu, X., Ai, Z., Ai, Y., Qiu, F., & Ni, D. (2019). Effect of different drying methods on the sensory quality and chemical components of black tea. *LWT*, *99*, 112-118. https://doi.org/10.1016/j.lwt.2018.09.036

Rahmawati, M., Arief, M., & Satyantini, W. H. (2019, February). The effect of sorbitol addition on the characteristic of carrageenan edible film. In *IOP Conference Series: Earth and Environmental Science* (Vol. 236, No. 1, p. 012129). IOP Publishing. https://doi.org/10.1088/1755-1315/236/1/012129

Rani, H., & Kalsum, N. (2016). Kajian proses pembuatan *edible film* dari rumput laut *gracilaria* sp. dengan penambahan gliserol [Study of the process of making edible film from seaweed *gracilaria* sp. with the addition of glycerol]. In *Prosiding Seminar Nasional Pengembangan Teknologi Pertanian* (Vol. 1 No. 1 pp. 219-225).

Rusli, A., Metusalach, M., & Tahir, M. M. (2017). Karakterisasi *edible film* karagenan dengan pemlastis gliserol [Characterization of edible film carrageenan with glycerol plasticizer]. *Indonesian Journal of Fishery Product Processing, 20*(2), 219–229. https://doi.org/10.17844/jphpi.v20i2.17499.

Siah, W M., Aminah, A., & Ishak, A. (2015). Edible films from seaweed (*Kappaphycus alvarezii*). *International Food Research Journal*. *22*(6), 2230-2236.

Supeni, G. (2012). Pengaruh formulasi *edible film* dari karagenan terhadap sifat mekanik dan penghalang [Effect of edible film formulation from carrageenan to mechanical and barrier properties]. *Jurnal Kimia dan Kemasan. 34*(2), 282–286. https://doi.org/10.24817/jkk.v34i2.1864

Sutharsan, J., Boyer, C. A., & Zhao, J. (2023). Effect of molecular weight and drying temperature on the physicochemical properties of chitosan edible film. *JSFA Reports*, *3*(8), 387-396. https://doi.org/10.1002/jsf2.142

Wansi, S., & Wael, S. (2014). Analisis kadar klorin pada teh celup berdasarkan waktu seduhan [Analysis of chlorine levels in tea bags based on steeping time]. *BIOPENDIX: Journal of Biology, Education and Applications, 1*(1), 22–31. https://doi.org/10.30598/biopendixvol1issue1page22-31

Pertanika J. Sci. & Technol. 32 (S3): 80 - 95 (2024)

PERTANIKA JOURNALS

SCIENCE & TECHNOLOGY

Journal homepage: http://www.pertanika.upm.edu.my/

Enhancing the Mechanical Strength and Thermal Stability of Polylactic Acid (PLA) with the Addition of Epoxidized Waste Cooking Oil (EWCO)

Nur Batrisyia Norhazlin[1], Nurul Hanim Razak[1,2]*, Anis Ainaa Omar[2], Mohd Hafidzal Mohd Hanafi[1,2] and Asmah Mat Desa[3]

[1]Faculty of Mechanical Engineering and Technology (FTKM), Universiti Teknikal Malaysia Melaka, Hang Tuah Jaya, 76100, Durian Tunggal, Melaka, Malaysia
[2]Centre for Advanced Research on Energy (CARe), Universiti Teknikal Malaysia Melaka, Hang Tuah Jaya, 76100, Durian Tunggal, Melaka, Malaysia
[3]Jabatan Alam Sekitar Pulau Pinang, Zon-B, Aras Bawah, Wisma Persekutuan Seberang Perai Utara, 13200 Kepala Batas, Pulau Pinang, Malaysia

ABSTRACT

Polylactic Acid (PLA) comes from renewable resources, has a reasonable biodegradability rate, and is used in biomedical, food packaging, textiles, and agricultural applications. PLA offers high mechanical strength and the ability to compost, similar to polyethylene terephthalate (PET) and nylon. However, the brittleness of PLA has always limited its usage. Therefore, bio-based plasticizers in the biopolymer matrices can increase flexibility (elasticity), durability, and workability. This study aims to determine the optimal blending ratio for the PLA blended with epoxidized waste cooking oil (EWCO) to enhance the mechanical and thermal properties of PLA/EWCO. The mechanical strength test consists of the hardness test (N/mm^2), flexural strength (MPa), and impact energy (kJ/m^2) adopted to evaluate the plasticizing characteristics. The thermal stability analysis involves glass transition temperature (T_g) (°C), cold-crystallization temperature (T_{cc}) (°C) and melting temperature (T_m) (°C). The blending ratio is 97.5PLA/2.5EWCO, 95PLA/5EWCO, 92.5PLA/7.5EWCO and 90PLA/10EWCO. As a result, 97.5:2.5 of PLA/EWCO reduces intermolecular interactions by stimulating more free volume in biopolymer chains' mobility and

ARTICLE INFO

Article history:
Received: 22 February 2024
Accepted: 30 May 2024
Published: 30 July 2024

DOI: https://doi.org/10.47836/pjst.32.S3.07

E-mail addresses:
batrisyianorhazlin@gmail.com (Nur Batrisyia Norhazlin)
nurulhanim@utem.edu.my (Nurul Hanim Razak)
anisainaa82@gmail.com (Anis Ainaa Omar)
hafidzal@utem.edu.my (Mohd Hafidzal Mohd Hanafi)
asmahdesa@doe.gov.my (Asmah Mat Desa)
* Corresponding author

ISSN: 0128-7680
e-ISSN: 2231-8526

enhancing the flexibility and elasticity of the PLA blends. Ultimately, the brittleness of PLA decreased with increasing EWCO bio-based plasticizer.

Keywords: Bioplastics, epoxidized waste cooking oil, mechanical strength, Polylactic Acid (PLA), thermal stability

INTRODUCTION

Plastic does not break down very efficiently in natural environments, where it may take up to a thousand years to degrade. A lack of efficient disposal of plastic waste harms the environment, including air, water, and soil pollution. Thus, researchers focus on biodegradable and natural materials since they are concerned about plastic pollution and its environmental effects, especially in oceans and waterways (Haryono et al., 2017). Bio-based plasticizers from epoxidase vegetable oil can replace petroleum-based plasticizers to improve flexibility and stability (Hosney et al., 2018).

However, besides many other usages, vegetable oil is highly demanded for human consumption, which urges researchers to look for better alternatives for bio-based plasticizer production that will not compete with food production. Waste cooking oil (WCO) is considered one of the renewable wastes that can be converted into green products, costing two to three times less than virgin vegetable oil (Benti et al., 2023). It could be an excellent option for producing bio-based plasticizers.

Many excellent benefits are offered by WCO, including the fact that it is low-cost, more accessible for purchase, and environmentally friendly. In addition to recycling WCOs, it also prevents improper waste disposal, which poses a threat to the environment (Suzuki et al., 2018). There are numerous advantages to using epoxidized WCO (EWCO) as a bio-based plasticizer, especially regarding environmental protection. As a result of the epoxidation reaction, carbon-carbon double bonds are converted into oxiranes (epoxides) with the aid of reagents such as air oxidation, hypochlorous acid, hydrogen peroxide, and organic peroxides.

Additional epoxidized vegetable oil as bio-based plasticizers in thermoplastic monomers such as polylactic acid (PLA) are reported to affect the mechanical properties positively (Suzuki et al., 2018). PLA is a thermoplastic monomer made from organic and renewable sources, such as corn starch, vegetable oil, and sugar cane (Pellis et al., 2021). Even though PLA has many advantages, including excellent mechanical strength, transparency, composability, and safety, it also has poor properties, such as brittleness and toughness., which severely limit its applications (Thuy et al., 2018). For applications requiring more flexibility, the plasticity of (PLA) must be improved (Tan et al., 2019), especially in the blending formulation.

According to published research in Table 1, the studies proved that 1-10% of epoxidized vegetable oil (EVO) was confirmed to impact the PLA polymer significantly regarding thermal and mechanical properties (Garcia-Garcia et al., 2020). The proper selection of

epoxidized vegetable oil as a bio-based plasticizer for PLA needs to be evaluated on a case-by-case basis as it highly depends on the compatibility of different epoxidized vegetable oil with PLA, and the effect of the bio-based plasticizers percentage on the thermal and mechanical properties of the produced PLA.

Although many studies have explored the effects of different blending ratios on flexural strength, impact energy, and hardness, there is still a potential research gap in determining the ideal blending ratio for maximizing the mechanical strength and thermal stability of the PLA/EWCO simultaneously. Moreover, further exploring how varying processing parameters, such as the blending technique, temperature, and sequence of addition, can influence the final properties of PLA/EWCO blends may help enhance our understanding of attaining the desired mechanical and thermal properties in these bio-based composite materials.

As a result of the numerous tests of PLA /EWCO on mechanical properties and thermal properties above, several advantages, disadvantages, and optimal blending ratios have been identified based on the ratio value set on PLA/EWCO based on the comparison between those two properties. Based on the research done by the researcher before, it was found that the trend of the properties and enhancement is similar based on mechanical and thermal properties.

It is crucial to optimize the optimal blending formulation ratio using the Analytic Hierarchy Process (AHP). EWCO is a renewable bio-based plasticizer that can be produced from waste cooking oil. It is a non-toxic and biodegradable material that has been shown to improve the flexibility and toughness of PLA (Siracusa et al., 2008).

Compared to pure PLA, a blend of PLA/EWCO may offer some advantages. Due to its flexibility and toughness, it is more resistant to breaking than other materials. Moreover, it is also biodegradable and compostable, making it a more sustainable material (Lasprilla et al., 2012).

According to previous studies in Table 1, the optimal composition of EWCO can significantly enhance the mechanical and thermal properties of bio-based plasticizers. As Garcia-Garcia et al. (2020) reported, the impact energy increased with a higher bio-based plasticizer content of up to 2.5% of EKO. All these results clearly show that PLA-2.5% EKO bio-based plasticizer has good mechanical properties.

Thermal properties result from the study by Garcia-Garcia et al. (2020), incorporating 2.5% of EKO as a bio-based plasticizer into PLA produced a saturation of bio-based plasticizers in the polymeric matrix and only a modest increase of crystal orientation. However, in the study by Thuy et al. (2018), with the same amount of 5% addition of EeRSO into PLA, as the glass transition temperature decreased, the crystal content and melting temperature decreased, and the initial decomposition temperature increased, those properties improved. Also, a study by Chieng et al. (2014) claimed that 5 wt% epoxidized vegetable oil (EVO) produced better results in thermal properties than PLA.

Table 1
Effect of different blending formulations of PLA and epoxidized vegetable oils on the mechanical and thermal properties

Vegetable Oils	Blending Formulation Ratio		Thermal properties			Mechanical properties	Authors
	Polymer	Plasticizer	Glass Transition Temperature (°C)	Cold-crystallization temperature (°C)	Melting temperature (°C)	Impact Energy (kJ/m²)	
Epoxidized Keranja Oil (EKO)	PLA (100%)	0	61.2	98.8	173	34-38	Garcia-Garcia et al., 2020
	PLA (99%)	EKO (1%)	61.1	93.1	171.8	35-39	
	PLA (97.5%)	EKO (2.5%)	60.4	91.3	171.4	37-41	
	PLA (95%)	EKO (5%)	58.3	90.4	171	49-53	
	PLA (90%)	EKO (10%)	55	90.6	171.3	47-51	
Epoxidized Rubber Seed Oil (EeRSO)	PLA (100%)	0	65	115.5	167.5	0.0009-0.0095	Thuy et al., 2018
	PLA (95%)	EeRSO (5%)	60	112.5	165.5	0.0180-0.0184	
Epoxidized Palm Oil (EPO)	PLA (100%)	0	62.85	124.11	149.79	-	Chieng et al., 2014
	PLA (100%)	EPO (5%)	60.12	114.16	147.62	-	
	PLA (100%)	EPO (7%)	60.79	108.97	146.97	-	

MATERIALS AND METHODS

Bio-based Plasticizers Preparation

PLA 3001D poly (lactic acid) (270,000 g mol^{-1}) in the form of pellets was supplied by NatureWorksTM LLC (Omar et al., 2023). The PLA was first dried at 50°C for 2 hours (Giita Silverajah et al., 2012) to prevent the hydrolysis of PLA before being used in blend preparation. For the epoxidized process, 88% of Formic Acid, HCOOH, and 30% of Hydrogen Peroxide H_2O_2 were obtained from Systerm Chemicals Company in Malaysia. PLA and EWCO were manually mixed until they were well blended in the blending formulation ratio 97.5PLA/2.5EWCO (Garcia-Garcia et al., 2020), 95PLA/5EWCO (Thuy et al., 2018), 92.5PLA/7.5EWCO (Chieng et al., 2014) and 90PLA/10EWCO (Garcia-Garcia et al., 2020), as indicated in Table 2 and Figure 1. PLA can only accommodate about 10% plasticizer due to the potential migration of the plasticizer and the resulting negative impact on its mechanical properties (Marturano et al., 2023).

EWCO was prepared in a 3-necked round bottom flask with 40 g of WCO and 3.7 g of HCOOH stirred at 30°C for 30 minutes. Following that, 32 g of H_2O_2 was dropped into the flask within 30 minutes, and the solution was stirred using a magnetic stirrer for about 7 hours (Cai et al., 2020). EWCO is then washed and rinsed with distilled water.

EWCO was dried at ambient temperature for four hours, while pure PLA was dried at 80°C for four hours (Thuy & Lan, 2021). As hydrolysis produces large amounts of degradation products from monosaccharides, PLA was preheated before blending to prevent hydrolysis (Garcia-Garcia et al., 2020). The percentages in Table 2 indicate how PLA and EWCO were manually mixed. Once mixed, the mixtures were extruded in a twin-screw extruder at temperatures ranging from 165°C to 180°C. After extruding, samples were collected and crushed to produce pellets. As shown in Figure 1, the PLA blends were placed in a rectangular mold, which was then heated at 220°C for 30 seconds (Omar et al., 2023).

Table 2
Blending formulation ratio of PLA/ EWCO

Polymer (PLA %)	Plasticizer (EWCO %)
100	0
97.5	2.5
95	5
92.5	7.5
90	10

Source: Omar et al., 2023

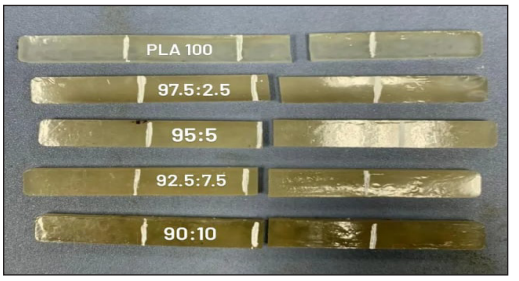

Figure 1. PLA/EWCO

Experimental Mechanical Properties

Rockwell Hardness

According to ASTM E18-22, the Rockwell hardness test can determine a material's hardness. The material sample is a standard size of 6.4 mm (0.25 inch) thickness while

the indenter is ball type. The sample types of PLA blended with EWCO were measured five times according to the blending formulation ratio, and the results were analyzed. Five measurements were replicated for each formulation of PLA/EWCO.

Flexural Strength

According to the ASTM D790 standard for plastics, flexural tests were conducted per the standard to determine flexural or bending properties. The size of the specimen is a cross-section of 3.2 mm x 12.7 mm and a length of 127 mm, which is suitable for plastic molding in a universal flexural test machine IBERTEST ELIB 30 (S.A.E. Ibertest, Madrid, Spain), using an operating mode in which it was subjected to three-point bending, as per the operation mode. Each sample related to the PLA blending formulation ratio mixed with EWCO was tested at least five times.

Impact Test

The Charpy impact test (ASTM D2794) was used in this experiment. The materials were evaluated for their ability to absorb/impact energy during fracture using a Charpy pendulum (6 J) from Metrotech S.A (San Sebastian, Spain), which complied with ISO 197:1993 guidelines (Garcia-Garcia et al., 2020). The size of the specimen is 64 x 12.7 x 3.2 mm. Each sample was drilled with a notch containing a depth of 2 mm and a radius of 0.25 mm in the center. Five samples of PLA/EWCO were tested according to the blending ratio, and the average value was calculated.

Experimental Thermal Properties

The thermal properties of polylactic acid (PLA) were analyzed using differential scanning calorimetry (DSC) after plasticizing with epoxidized waste cooking oil (EWCO). The DSC results for the treated and plasticized PLA samples were obtained by heating them in a nitrogen atmosphere at a flow rate of 50 mL/min^{-1}, from 30°C to 700°C under thermogravimetric analysis (TGA) dynamic mode at a heating rate of 10°C/min^{-1}. The plasticizers decreased the PLA's glass transition temperature (T_g), and the degree of crystallinity (Xc) was calculated using the melting and cold crystallization enthalpy from the DSC data.

The analysis conducted a DSC test under a nitrogen atmosphere using a Mettler-Toledo 821 calorimeter (Schwerzenbach, Switzerland) (flow rate 66 mL min^{-1}). As a procedure, the test involved two heating stages at 20°C for 10 minutes each, followed by a cooling stage at 20°C for 10 minutes, and a final heating stage at 250°C for 10 minutes. The sample weight ranged from 5 mg to 20 mg, and the second heating scan aimed to determine the glass transition temperature (T_g), crystallization temperature (T_{cc}), and melting temperature (T_m) of the sample.

Optimization Process

The Analytic Hierarchy Process (AHP) has been used to optimize the best percentage value. This model-based verification AHP optimization aims to identify the optimal blend PLA/EWCO to achieve mechanical properties (Flexural, tensile, and impact energy) and thermal stability (glass transition temperature, cold-crystalization temperature, and melting temperature). A series of pairwise comparisons may produce some inconsistencies.

The Consistency Ratio (CR) is an essential part of the hierarchical framework of AHP since it can determine the consistency of pairwise comparison judgments. For each of the criteria, all comparisons between criteria and alternatives were analyzed for consistency (Razak et al., 2022). The overall AHP analysis has been presented in Figure 2. The reason for adopting AHP is that AHP provides reciprocal pairwise comparisons and has a multi-level hierarchical structure analysis to propose the best alternatives from a discrete set of feasible alternatives

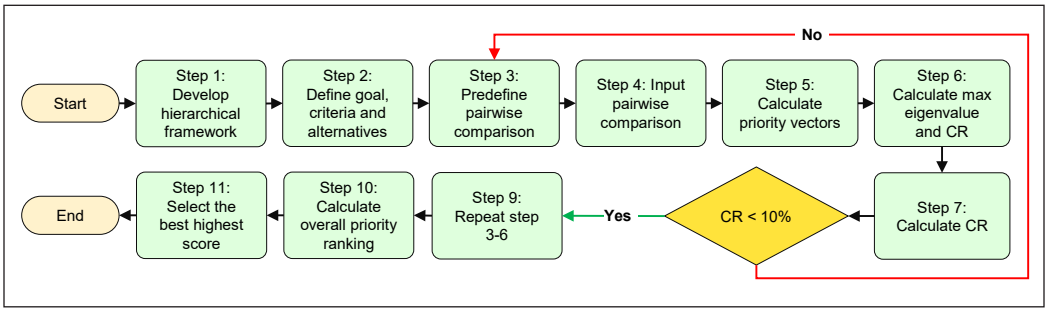

Figure 2. AHP method

RESULTS AND DISCUSSION

Effect on Mechanical Strength

Figure 3 shows the results on the mechanical properties of the PLA/EWCO plasticizers.

According to the process, PLA becomes less rigid when plasticized with EWCO because epoxidized palm oil reduces tensile strength. There is a possibility that the plasticizer interacts with the PLA matrix, decreasing the intermolecular forces and increasing the mobility of the polymer chains, which results in a decrease in rigidity for the material.

A hardness test can be used to evaluate a material's properties, such as strength, elasticity, and wear resistance, and therefore aid in selecting the appropriate material or treatment for other applications. PLA caused an increase in Rockwell hardness before it became static at 5 EWCO% to 7.5 EWCO%. However, a further increase to 10 EWCO% has caused a reduction in Rockwell hardness. Incorporating EWCO plasticizer into PLA makes the material more flexible and less indentation-resistant than pure PLA. However, extensive addition of EWCO will lead to a more brittle product, as the higher the EWCO is added, the more complex the material becomes.

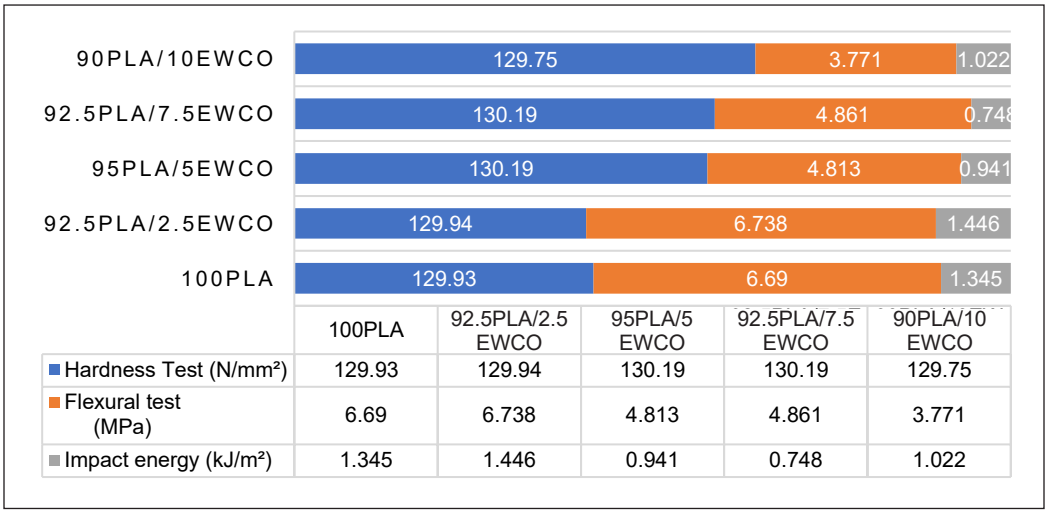

	100PLA	92.5PLA/2.5 EWCO	95PLA/5 EWCO	92.5PLA/7.5 EWCO	90PLA/10 EWCO
Hardness Test (N/mm²)	129.93	129.94	130.19	130.19	129.75
Flexural test (MPa)	6.69	6.738	4.813	4.861	3.771
Impact energy (kJ/m²)	1.345	1.446	0.941	0.748	1.022

Figure 3. Mechanical properties of PLA/EWCO

According to ASTM D790, the flexural test shows that the more EWCO is added to the PLA, the more the load data increases until the specimen breaks (Rostamiyan et al., 2015). As a result, the strength of the material decreases when EWCO is added, resulting in a weak material when the ratio of EWCO and PLA is 92.5:7.5. Increases in flexural strength can result in higher hardness values, indicating that the material is more resilient and can maintain its shape under load. In contrast, decreased flexural properties can reduce hardness, make it more brittle, and indicate that the material is more susceptible to external forces causing deformation.

The impact energy of PLA/EWCO blends is higher than that of pure PLA. In other words, PLA/EWCO resists sudden breakage under an impact load. Figure 3, results on mechanical properties, shows that the force value decreases when more EWCO values are added to the PLA. This result is similar to Thuy et al. (2018). By adding more EWCO, the PLA will become soft and weak. The lower load transfer capacity of the material is also the reason for the reduced impact strength of the composites during the test (Girimurugan et al., 2020).

The results of two out of three tests in Figure 3 indicated that 97.5PLA/2.5EWCO was the best based on mechanical properties (flexural and impact energy). As a result, the hardness value results of 97.5PLA/2.5EWCO can be considered optimal. Based on the results demonstrated in Figure 3, 97.5PLA/2.5EWCO has the best mechanical strength, such as optimal hardness, higher flexibility, and higher energy impact.

Effect on Thermal Stability

In addition to providing valuable information regarding the thermal stability of materials, DSC can be used to determine their thermal decomposition and degradation behavior

by measuring various parameters related to their thermal behavior (Liu et al., 2013). Information such as this is essential for assessing the safety of handling, processing, and storing materials, especially in chemical manufacturing, pharmaceutical manufacturing, and polymer manufacturing.

Thermal stability is significant for this study because the PLA may decompose when heated due to high temperatures. In addition, the time and temperature at which physical changes occur when PLA is heated or cooled when blended with EWCO. According to the data obtained from the DSC Thermal Analysis test and analyzed, Figure 4 summarizes the test results. Adding EWCO to PLA does not result in significant differences from pure PLA according to the ratio set. However, small changes in value can have a significant impact, even if the difference in weight is only minimal.

Heat is applied to a sample at a constant rate, and heat flow is measured to maintain a constant temperature difference between the sample and the reference material. As a result of the DSC curve, information can be obtained about the thermal transitions of the material, including their peak temperatures and enthalpy changes. A DSC test is usually conducted in three stages, such as heating, cooling, and reheating, to determine the thermal properties of a polymer PLA. During the first heating stage, the thermal history of the sample is erased, while the cooling and reheating stages provide information regarding the cold-crystallization and melting of the polymer. Reheating determines the glass transition temperature (T_g) while cooling and reheating determine the cold-crystallization temperature (T_{cc}) and melting temperature (T_m).

As shown in Figure 4, The glass transition temperature (T_g) of pure PLA is around 60°C, but when EWCO plasticizer is added, it lowers the T_g of PLA to below 53.77°C,

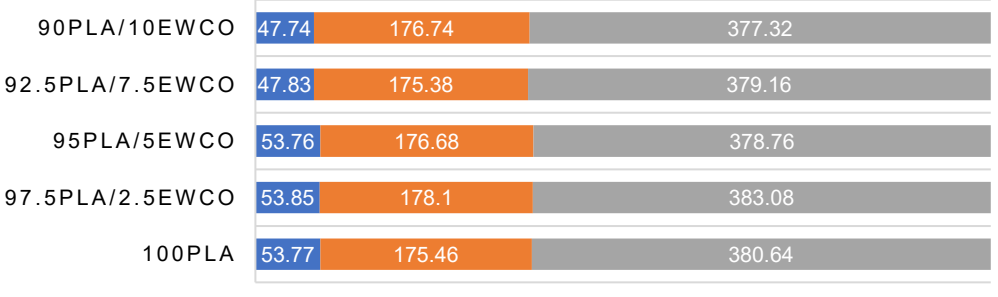

	100PLA	97.5PLA/2.5 EWCO	95PLA/5 EWCO	92.5PLA/7.5 EWCO	90PLA/10 EWCO
Glass transition temperature (°C)	53.77	53.85	53.76	47.83	47.74
Cold-Crystallization temperature (°C)	175.46	178.1	176.68	175.38	176.74
Melting temperature (°C)	380.64	383.08	378.76	379.16	377.32

Figure 4. Thermal properties of PLA/EWCO

making it more flexible and less rigid (Turco et al., 2019). However, adding too much EWCO can produce a weak and soft material. PLA's cold-crystallization temperature (T_{cc}) is between 170°C and 180°C, but when EWCO plasticizer is added, it disrupts the crystal structure, making it harder for the material to crystallize. The T_{cc} increases with EWCO but decreases when more than 5% is added. PLA's melting temperature (T_m) is around 290°C–380°C (Carrasco et al.). However, when EWCO plasticizer is added, it decreases, and the melting temperature value becomes unstable when the addition of EWCO exceeds 5%. This instability in Tm may be caused by changes in the PLA crystal structure brought about by EWCO plasticizers.

During crystallization, the temperature affected the degree of crystallinity of the polymer, which, as a result, affected the melting temperature (Scoti et al., 2024). As the degree of crystallinity in polymers increases, various material properties, such as hardness, strength, and barrier properties, improve. Techniques such as Differential Scanning Calorimetry (DSC) determine the degree of crystallinity. Due to thermodynamic regulation, the crystallization temperature is always lower than the temperature at which the melting occurs. As a result of their chemical modifications and crystallization abilities, 2.5 EWCO can alter the crystallization and melting behavior of polymers, impacting their thermal properties. Based on the results in Figure 4, 97.5PLA/2.5EWCO has the best thermal stability, such as higher glass transition temperature, cold crystallization temperature, and melting temperature.

Figure 5a) PLA/EWCO (97.5:2.5) indicates the DSC curve suggests a shift in the baseline around 53.85°C, which means the occurrence of a "glass transition." In addition, a chemical reaction of a mix of reagents generates an exothermic peak of around 178.1°C, indicating an exothermic reaction caused by crystallization. Observing an endothermic peak around 383.08°C indicates an endothermic reaction by melting. It can be seen in Figure 4 that no significant differences exist between graphs a,b,c, and d. in Figure 5.

Optimum Blending Formulation of EWCO for Enhancing Thermal and Mechanical Properties of PLA

The mechanical and thermal properties results have been optimized using the Analytic Hierarchy Process (AHP) to get an average calculated value of PLA/EWCO. In the AHP, model-based formulations were evaluated for their ability to achieve the trade-off between mechanical strength (hardness, flexural strength, impact energy) and thermal stability (glass transition temperature, cold crystallization temperature, melting temperature).

Figure 6 shows that flexural strength is the high-priority attribute and characteristic for selecting the optimal blending of PLA/EWCO, followed by hardness and impact, while for thermal stability, glass transition temperature is the main factor, followed by cold-crystallization temperature and melting temperature. According to Figure 7,

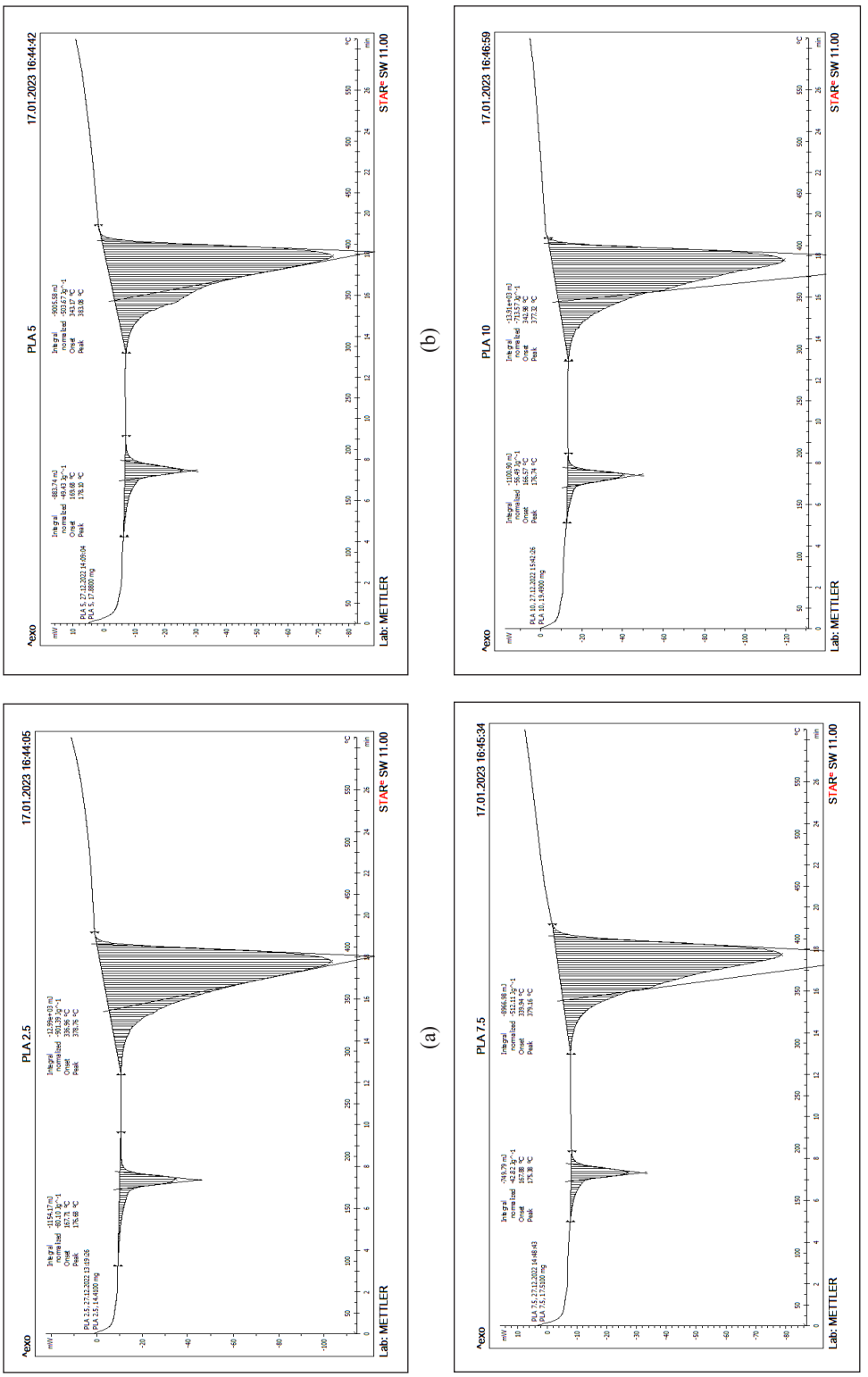

Figure 5. (a) PLA/EWCO (97.5:2.5); (b) PLA/EWCO (95:5); (c) PLA/EWCO (92.5:7.5); and (d) PLA /EWCO (90:10)

100PLA has the highest percentage followed by 97.5PLA/2.5EWCO, 95.5PLA/5EWCO, 92.5PLA/7.5EWCO and 90PLA/10EWCO. As shown in Figure 7, AHP has generated a combination of weight criteria based on mechanical and thermal properties.

Blending the formulation of PLA/EWCO with the ratio of 97.5PLA/2.5EWCO resulted in the highest mechanical and thermal properties. When PLA is combined with the EWCO plasticizer, it disrupts the crystal structure of PLA, hindering crystallization and promoting an amorphous structure. This disruption may occur due to the bulky epoxidized oil molecules interfering with the close packing of PLA chains, thus inhibiting the formation of highly ordered crystals. The addition of 2.5% EWCO enhances the interfacial interaction between PLA and EWCO, thereby enhancing mechanical strength through Van der Waals force and acid-base interactions (Sumesh et al., 2022) and optimizing the properties of PLA in terms of plasticity, mechanical properties, and thermal stability. This enhanced performance is attributed to the plasticizing effect of EWCO, which reduces intermolecular forces between PLA chains, allowing increased mobility and deformation of the chains under stress.

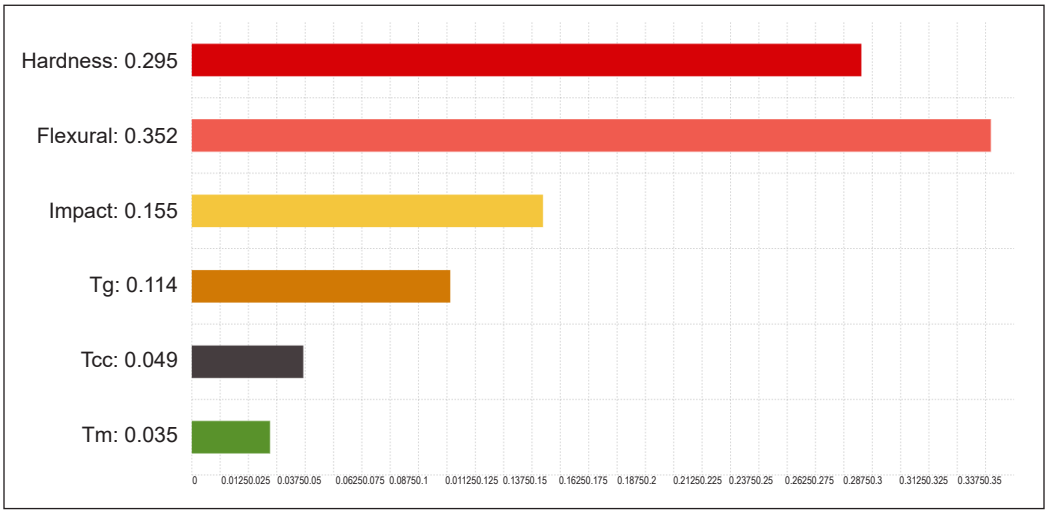

Figure 6. Weight criteria for mechanical and thermal properties

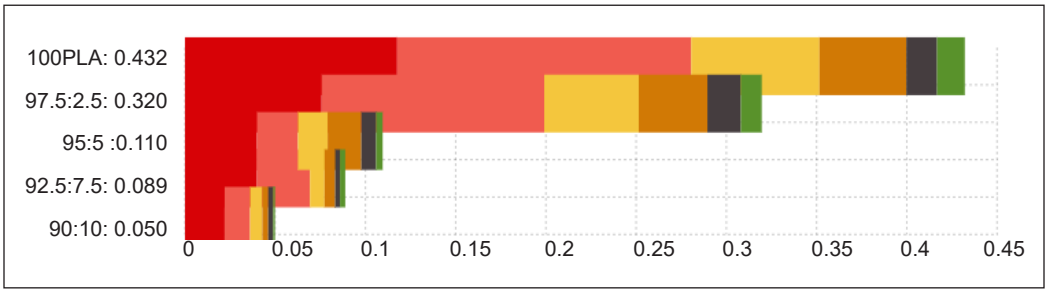

Figure 7. Scored alternatives for optimal blending formulation PLA/EWCObio-based plasticizers

CONCLUSION

This paper has the potential of EWCO in enhancing PLA's mechanical properties and thermal stability. The results indicate that 97.5:2.5 of PLA/EWCO reduces intermolecular interactions by stimulating more free volume in biopolymer chains' mobility and enhancing flexibility in mechanical properties. Meanwhile, the thermal stability increased with increasing bio-based plasticizers up to 2.5% of EWCO based on the AHP analysis that has been done on all properties, from glass transition temperature to cold crystallization temperature and melting temperature.

CREDIT AUTHORSHIP CONTRIBUTION STATEMENT

Nur Batrisyia Norhazlin: Writing the original draft, methodology, software, and investigation; Nurul Hanim Razak: Conceptualization, methodology, validation, proofreading; Anis Ainaa Omar: Data curation, formal analysis; Mohd Hafidzal Mohd Hanafi: Methodology, writing-review and editing; Asmah Mat Desa: Investigation and proofreading.

DECLARATION OF COMPETING INTEREST

The authors declare that they have no known competing financial interests or personal relationships that could have appeared to influence the work reported in this paper.

ACKNOWLEDGEMENTS

The authors gratefully acknowledge the Universiti Teknikal Malaysia Melaka (UTeM) for funding the research work with grant number JURNAL/2021/FKM/Q00063. This research has been supported by the Kesidang Scholarship, Universiti Teknikal Malaysia Melaka (UTeM).

REFERENCES

Benti, N. E., Aneseyee, A. B., Geffe, C. A., Woldegiyorgis, T. A., Gurmesa, G. S., Bibiso, M., Asfaw, A. A., Milki, A. W., & Mekonnen, Y. S. (2023). Biodiesel production in Ethiopia: Current status and future prospects. *Scientific African, 19,* e01531. https://doi.org/10.1016/j.sciaf.2022.e01531

Cai, D. L., Yue, X., Hao, B., & Ma, P. C. (2020). A sustainable poly (vinyl chloride) plasticizer derivated from waste cooking oil. *Journal of Cleaner Production*, *274,* 122781. https://doi.org/10.1016/j.jclepro.2020.122781

Carrasco, F., Pérez, O. S., & Maspoch, M. L. (2021). Kinetics of the thermal degradation of poly (lactic acid) and polyamide bio blends. *Polymers*, *13*(22), 3996. https://doi.org/10.3390/polym13223996

Chieng, B. W., Ibrahim, N. A., Then, Y. Y., & Loo, Y. Y. (2014). Epoxidized vegetable oils plasticized poly(lactic acid) biocomposites: Mechanical, thermal and morphology properties. *Molecules*, *19*(10), 16024–16038. https://doi.org/10.3390/molecules191016024

Garcia-Garcia, D., Carbonell-Verdu, A., Arrieta, M. P., López-Martínez, J., & Samper, M. D. (2020). Improvement of PLA film ductility by plasticization with epoxidized Karanja oil. *Polymer Degradation and Stability*, *179*, 109259. https://doi.org/10.1016/j.polymdegradstab.2020.109259

Giita Silverajah, V. S., Ibrahim, N. A., Zainuddin, N., Wan Yunus, W. M. Z., & Hassan, H. A. (2012). Mechanical, thermal and morphological properties of poly(lactic acid)/epoxidized palm olein blend. *Molecules*, *17*(10), 11729–11747. https://doi.org/10.3390/molecules171011729

Girimurugan, R., Pugazhenthi, R., Maheskumar, P., Suresh, T., & Vairavel, M. (2020). Impact and hardness behaviour of epoxy resin matrix composites reinforced with banana fiber/camellia sinensis particles. *Materials Today: Proceedings*, *39*, 373–377. https://doi.org/10.1016/j.matpr.2020.07.597

Haryono, A., Triwulandari, E., & Jiang, P. (2017). Interaction between vegetable oil based plasticizer molecules and polyvinyl chloride, and their plasticization effect. In *AIP Conference Proceedings* (Vol. 1803, No. 1). AIP Publishing. https://doi.org/10.1063/1.4973172

Hosney, H., Nadiem, B., Ashour, I., Mustafa, I., & El-Shibiny, A. (2018). Epoxidized vegetable oil and bio-based materials as PVC plasticizer. *Journal of Applied Polymer Science, 135*(20). 46270. https://doi.org/10.1002/app.46270

Lasprilla, A. J. R., Martinez, G. A. R., Lunelli, B. H., Jardini, A. L., & Filho, R. M. (2012). Poly-lactic acid synthesis for application in biomedical devices - A review. *Biotechnology Advances*, *30*(1), 321–328. https://doi.org/10.1016/j.biotechadv.2011.06.019

Liu, X., Wang, Y., Yu, L., Tong, Z., Chen, L., Liu, H., & Li, X. (2013). Thermal degradation and stability of starch under different processing conditions. *Starch/Staerke*, *65*(1–2), 48–60. https://doi.org/10.1002/star.201200198

Marturano, V., Marotta, A., Salazar, S. A., Ambrogi, V., & Cerruti, P. (2023). Recent advances in bio-based functional additives for polymers. *Progress in Materials Science*, *139*, 101186. https://doi.org/10.1016/j.pmatsci.2023.101186

Omar, A. A., Hanafi, M. H. M., Razak, N. H., Razak, N. A. A., & Grasianto. (2023). Effect of epoxidized waste cooking oil plasticizer in improving the mechanical properties of Polylactic Acid (PLA). *Chemical Engineering Transactions*, *106*, 319–324. https://doi.org/10.3303/CET23106054

Pellis, A., Malinconico, M., Guarneri, A., & Gardossi, L. (2021). Renewable polymers and plastics: Performance beyond the green. *New Biotechnology*, *60*, 146–158. https://doi.org/10.1016/j.nbt.2020.10.003

Razak, N. H., Hashim, H., Yunus, N. A., & Klemeš, J. J. (2022). Integrated linear programming and analytical hierarchy process method for diesel/biodiesel/butanol in reducing diesel emissions. *Journal of Cleaner Production*, *337*, 130297. https://doi.org/10.1016/j.jclepro.2021.130297

Rostamiyan, Y., Fereidoon, A., Rezaeiashtiyani, M., Mashhadzadeh, A. H., & Salmankhani, A. (2015). Experimental and optimizing flexural strength of epoxy-based nanocomposite: Effect of using nano silica and nano clay by using response surface design methodology. *Materials and Design*, *69*, 96–104. https://doi.org/10.1016/j.matdes.2014.11.062

Scoti, M., De Stefano, F., Talarico, G., & De Rosa, C. (2024). The genetics in polymers: Crystallization as a fingerprint of the molecular microstructure. *Polymer*, *293*, 126637. https://doi.org/10.1016/j.polymer.2023.126637

Siracusa, V., Rocculi, P., Romani, S., & Rosa, M. D. (2008). Biodegradable polymers for food packaging: A review. *Trends in Food Science and Technology*, *19*(12), 634–643. https://doi.org/10.1016/j.tifs.2008.07.003

Sumesh, K. R., Anton, J., Spatenka, P., & Sourkova, H. J. (2022). *Experimental studies on the influence of plasma treatment of polyethylene in carbon fiber composites: Mechanical and morphological studies. Polymers*, *14*(6), 1095.

Suzuki, A. H., Botelho, B. G., Oliveira, L. S., & Franca, A. S. (2018). Sustainable synthesis of epoxidized waste cooking oil and its application as a plasticizer for polyvinyl chloride films. *European Polymer Journal*, *99*, 142–149. https://doi.org/10.1016/j.eurpolymj.2017.12.014

Tan, J., Lu, T., Li, R., Zhang, S., Liu, W., Zhu, X., Zhang, J., & Xin, J. (2019). Biodegradable waste frying oil-based ethoxylated esters as highly efficient plasticizers for poly(lactic acid). *ACS Sustainable Chemistry and Engineering*, *7*(19), 15957–15965. https://doi.org/10.1021/acssuschemeng.9b02312

Thuy, N. T., & Lan, P. N. (2021). Investigation of the impact of two types of epoxidized vietnam rubber seed oils on the properties of polylactic acid. *Advances in Polymer Technology*, *2021*(1), 6698918. https://doi.org/10.1155/2021/6698918

Thuy, N. T., Duc, V. M., & Liem, N. T. (2018). Properties of poly (lactic acid) plasticized by epoxidized rubber seed oil. *Vietnam Journal of Chemistry*, *56*(2), 181–186. https://doi.org/10.1002/vjch.201800010

Turco, R., Ortega-Toro, R., Tesser, R., Mallardo, S., Collazo-Bigliardi, S., Boix, A. C., Malinconico, M., Rippa, M., Di Serio, M., & Santagata, G. (2019). Poly (lactic acid)/thermoplastic starch films: Effect of cardoon seed epoxidized oil on their chemicophysical, mechanical, and barrier properties. *Coatings*, *9*(9). https://doi.org/10.3390/coatings9090574

REFEREES FOR THE PERTANIKA
JOURNAL OF SCIENCE AND TECHNOLOGY

VOL. 32 (S3) 2024

The Editorial Board of the Pertanika Journal of Science and Technology wishes to thank the following:

Ahmad Ilyas Rushdan
(UTM, Malaysia)

Boon Jia Geng
(UMK, Malaysia)

Ezyana Kamal Bahrin
(UPM, Malaysia)

Fatimah A'thiyah Sabaruddin
(UPM, Malaysia)

Goh Kheng Lim
(NUiS, Singapore)

Khairiah Badri
(UKM, Malaysia)

Khoo Pui San
(UTM, Malaysia)

Latifah Jasmani
(FRIM, Malaysia)

Loh Yueh Feng
(MTIB, Malaysia)

Mariusz Mamiński
(SGGW, Poland)

Maya Ismayati
(BRIN, Indonesia)

Mohd Nor Faiz Norrrahim
(UPNM, Malaysia)

Norhayani Othman
(UTM, Malaysia)

Rafidah Jalil
(FRIM, Malaysia)

Ren Jun Li
(SCUT, China)

Suriani Sani
(UTM, Malaysia)

Widya Fatriasari
(BRIN, Indonesia)

Zhang Chun Hui
(SCUT, China)

BRIN - Nasional Research and Innovation Agency
FRIM - Forest Research Institute Malaysia
MTIB - Malaysian Timber Industry Board
NUiS - Newcastle University in Singapore
UKM - Universiti Kebangsaan Malaysia
UMK - Universiti Malaysia Kelantan
UPM - Universiti Putra Malaysia
UPNM - Universiti Pertahanan Nasional Malaysia
UTM - Universiti Teknologi Malaysia
SCUT - South China University of Technology
SGGW - Warsaw University of Life Sciences

While every effort has been made to include a complete list of referees for the period stated above, however if any name(s) have been omitted unintentionally or spelt incorrectly, please notify the Chief Executive Editor, *Pertanika* Journals at executive_editor.pertanika@upm.edu.my

Pertanika Journal of Science & Technology
Vol. 32 (S3) 2024

Natural Polymers and Derivatives: Composition, Uses and Application

Preface i
Lee Chuan Li, Chin Kit Ling and Ainun Zuriyati Mohamed @ Asa'ari

UV-absorption Capacity of Selected Crude and Functionalized Lignin for Use in Sunscreens 1
Jeanette O. Grande-Flores and Biljana M. Bujanovic

Preparation of Pulp, Microfibrillated Cellulose, and Paper Hand Sheets from Bakong (*Hanguana malayana* (Jack) Merr.) 15
Glenn Christian P. Acaso, Ramon A. Razal, Veronica P. Migo, Catalino G. Alfafara and Adela S. Torres

The Effects of Autohydrolysis Pretreatment on the Properties of OPT Pulps for the Production of Dissolving Pulp 27
Natra Joseph, Mohamad Haafiz Mohamad Kassim, Mazlan Ibrahim, Nurul Fazita Mohammad Rawi, Kumar Sudesh, Takamitsu Arai, Akihiko Kosugi and Leh Cheu Peng

The Effect of Spinning Parameters and Fiber Blending Ratio on the Physical Properties of Pineapple Leaf Fiber (PALF)-Cotton Yarns 41
Nurul Husna Zolkifflee, Mohd Nazrul Roslan, Juliana Abdul Halip, Khairu Kamarudin, Muhammad Farid Shaari and Asna Nabilah Aziz

Comprehensive Evaluation of Printing Process Parameters and Tensile Properties of Coconut Polypropylene Filament Composites in Additive Manufacturing 57
Noryani Muhammad, Mohd Aiman Jamaludin, Nuzaimah Mustafa, Yuzliza Yusuf, Mohd Adrinata Sharuzaman and Nurul Hanim Razak

Carrageenan-based Film Utilization for Eco-friendly Tea Bag 69
Yeni Pamita Sukmawati, Putri Alisya Oktavia Sarumaha, Nabila Fisa Sabrina, Reza Widyasaputra and Ida Bagus Banyuro Partha

Enhancing the Mechanical Strength and Thermal Stability of Polylactic Acid (PLA) with the Addition of Epoxidized Waste Cooking Oil (EWCO) 80
Nur Batrisyia Norhazlin, Nurul Hanim Razak, Anis Ainaa Omar, Mohd Hafidzal Mohd Hanafi and Asmah Mat Desa

Pertanika Editorial Office, Journal Division
Putra Science Park,
1st Floor, IDEA Tower II,
UPM-MTDC Technology Centre
Universiti Putra Malaysia
43400 UPM Serdang
Selangor Darul Ehsan
Malaysia

http://www.pertanika.upm.edu.my/
E-mail: executive_editor.pertanika@upm.edu.my
Tel: +603 9769 1622

PENERBIT UPM PRESS
http://penerbit.upm.edu.my
E-mail : penerbit@upm.edu.my
Tel : +603 9769 8855

ISSN 0128-7680
e-ISSN 2231-8526